Insect Systematics and Diversity, (2022) 6(1): 4; 1–31
https://doi.org/10.1093/isd/ixab025
Research

ENTOMOLOGICAL SOCIETY OF AMERICA
SHARING INSECT SCIENCE GLOBALLY

OXFORD

Molecular Phylogenetics, Phylogenomics, and Phylogeography

Species Paraphyly and Social Parasitism: Phylogenomics, Morphology, and Geography Clarify the Evolution of the *Pseudomyrmex elongatulus* Group (Hymenoptera: Formicidae), a Mesoamerican Ant Clade

Philip S. Ward[1,3,] and Michael G. Branstetter[2]

[1]Department of Entomology and Nematology, University of California, Davis, CA 95616, USA, [2]U.S. Department of Agriculture, Agricultural Research Service, Pollinating Insects Research Unit, Utah State University, Logan, UT 84322, USA, and [3]Corresponding author, e-mail: psward@ucdavis.edu

Subject Editor: Jeffrey Sosa-Calvo

Received 29 June 2021; Editorial decision 25 October 2021

Abstract

Using genetic, morphological, and geographical evidence, we investigate the species-level taxonomy and evolutionary history of the *Pseudomyrmex elongatulus* group, a clade of ants distributed from southwestern United States to Costa Rica. Through targeted enrichment of 2,524 UCE (ultraconserved element) loci we generate a phylogenomic data set and clarify the phylogenetic relationships and biogeographic history of these ants. The crown group is estimated to have originated ~8 Ma, in Mexico and/or northern Central America, and subsequently expanded into southern Central America and the southwestern Nearctic. The *P. elongatulus* group contains a mix of low- and high-elevation species, and there were apparently multiple transitions between these habitat types. We uncover three examples of one species—of restricted or marginal geographical distribution—being embedded phylogenetically in another species, rendering the latter paraphyletic. One of these cases involves an apparent workerless social parasite that occurs sympatrically with its parent species, with the latter serving as host. This suggests a sympatric origin of the parasite species within the distribution range of its host. Species boundaries are tested using three molecular delimitation approaches (SODA, bPTP, BPP) but these methods generate inflated species estimates (26–46 species), evidently because of a failure to distinguish population structure from species differences. In a formal taxonomic revision of the *P. elongatulus* group, based on almost 3,000 specimens from ~625 localities, we allow for geographic variation within species and we employ distinctness-in-sympatry criteria for testing hypotheses about species limits. Under these guidelines we recognize 13 species, of which nine are new: *P. arcanus*, **sp. nov.** (western Mexico); *P. capillatus*, **sp. nov.** (western Mexico); *P. cognatus*, **sp. nov.** (Chiapas, Mexico to Nicaragua); *P. comitator*, **sp. nov.** (Chiapas, Mexico); *P. ereptor*, **sp. nov.** (Veracruz, Mexico); *P. exoratus*, **sp. nov.** (southeastern Mexico, Honduras); *P. fasciatus*, **sp. nov.** (Chiapas, Mexico to Costa Rica); *P. nimbus*, **sp. nov.** (Costa Rica); and *P. veracruzensis*, **sp. nov.** (Veracruz, Mexico). Our study highlights the value of combining phylogenomic, phenotypic, and geographical data to resolve taxonomic and evolutionary questions.

Key words: taxonomy, phylogenetics, ultraconserved elements, biogeography, species delimitation

A comprehensive taxonomic accounting of species, including delimitation of their phenotypic and geographic boundaries, and placement within a phylogenetic framework, remains an unfinished task for most insect groups (Footit and Adler 2017), including ants (Ward 2014). This research is all the more urgent because of ongoing habitat destruction and degradation (Hansen et al. 2013, Edwards et al. 2019, Wolf et al. 2021), particularly in tropical regions where species diversity is highest (Lomolino et al. 2017) and where many species have yet to be discovered and described. In recent years, phylogenomic approaches have enabled great progress in clarifying the evolutionary history of major lineages of insects (e.g., Misof et al. 2014), but such methods have seen less application to species-level

© The Author(s) 2022. Published by Oxford University Press on behalf of Entomological Society of America. All rights reserved. For permissions, please e-mail: journals.permissions@oup.com.

Version of Record, first published online January 25, 2022 with fixed content and layout in compliance with Art. 8.1.3.2 ICZN

Downloaded from https://academic.oup.com/isd/article/6/1/4/6514767 by ThULB Jena user on 27 January 2022

taxonomy. There has been extensive debate about the best way to rejuvenate and modernize alpha-taxonomy, but most observers agree that integrating multiple lines of evidence—both phenotypic and genetic—leads to more robust hypotheses about species boundaries (Yeates et al. 2011, Fujita et al. 2012, Pante et al. 2015).

The current study uses a combination of morphological, geographical, and phylogenomic data to delimit species and investigate phylogenetic relationships in a clade of ants that has evolved across the Mesoamerican landscape. This region supports a diverse biota, derived from both Nearctic and Neotropical source lineages and containing high numbers of endemic species (Savage 1966, Halffter 1987, Marshall and Liebherr 2001, Sánchez-González et al. 2008, Halffter and Morrone 2017, Beza-Beza et al. 2021). Diversification of taxa has been influenced by a varied topography and complex geological history (Graham 2010, Gutiérrez-García and Vázquez-Domínguez 2013, Fitz-Díaz et al. 2018, Davison et al. 2021).

The focal taxon in this study, the *Pseudomyrmex elongatulus* group (Ward 2017), is a clade of ants distributed from southwestern United States to Costa Rica, with a center of diversity in southern Mexico. The genus *Pseudomyrmex* itself contains more than 200 species, found throughout tropical and warm temperate regions of the New World (Ward 2019). Whereas most species of *Pseudomyrmex* inhabit lowland habitats, the members of the *P. elongatulus* group have a propensity to occupy higher-elevation sites. The group is one of several Mesoamerican clades of *Pseudomyrmex* (Chomicki et al. 2015) that require taxonomic attention.

Our goals in this study are 1) revision of the species-level taxonomy of the *P. elongatulus* group, based on morphological and molecular evidence; 2) estimation of phylogenetic relationships, using UCE (ultra conserved element) phylogenomic data; 3) inference of historical changes in geographical distribution and elevation; and 4) evaluation of three molecular species delimitation methods that can be feasibly applied to genome-scale data sets. We also document three examples of 'species paraphyly' and two apparent cases of workerless social parasites, and consider the implication of these findings for modes of speciation in these ants.

Materials and Methods

Taxonomy

Approximately 2,930 ant specimens (mostly workers) of the *P. elongatulus* group were examined, from ~625 localities in the United States, Mexico, and Central America. This material came from, or has been deposited in, the following collections:

AMNH American Museum of Natural History, New York, NY, USA
ANIC Australian National Insect Collection, CSIRO, Canberra, Australia
ANSP Academy of Natural Sciences, Philadelphia, PA, USA
BMNH Natural History Museum, London, United Kingdom
CASC California Academy of Sciences, San Francisco, CA, USA
CEET Colección de Insectos Asociados a Plantas Cultivadas en la Frontera Sur, El Colegio de la Frontera Sur, Tapachula, Mexico
CHAH Henry A. Hespenheide Collection, University of California at Los Angeles, CA, USA
CMNH Carnegie Museum of Natural History, Pittsburgh, PA, USA
CNCC Canadian National Collection of Insects, Arachnids and Nematodes, Ottawa Research and Development Centre, Ottawa, Canada
CSCA California State Collection of Arthropods, California Department of Food and Agriculture, Sacramento, CA, USA (previously CDAE)
CUIC Cornell University Insect Collection, Ithaca, NY, USA
CZUG Colección Entomológica, Centro de Estudios en Zoología, CUCBA, Universidad de Guadalajara, Mexico
EBCC Estación de Biología Chamela, Jalisco, Mexico
EMEC Essig Museum of Entomology, University of California at Berkeley, CA, USA (previously CISC)
FSCA Florida State Collection of Arthropods, Gainesville, FL, USA
GCSC Gordon C. Snelling Collection, Los Angeles, CA, USA
GKMC G. K. Mosser Collection, Antioch College, Yellow Springs, OH, USA
IEXA Colección Entomológica del Instituto de Ecología, A.C., Xalapa, Mexico
INBC Instituto Nacional de Biodiversidad, San José, Costa Rica
JTLC J. T. Longino Collection, University of Utah, UT, USA
KWJC Klaus W. Jaffé Collection, Caracas, Venezuela
LACM Los Angeles County Museum of Natural History, Los Angeles, CA, USA
MCZC Museum of Comparative Zoology, Harvard University, Cambridge, MA, USA
MHNG Muséum d'Histoire Naturelle, Geneva, Switzerland
MIZA Instituto de Zoología Agrícola, Universidad Central de Venezuela, Maracay, Venezuela (previously IZAV)
MNHN Muséum National d'Histoire Naturelle, Paris, France
MSNG Museo Civico di Storia Naturale, Genoa, Italy (previously MCSN)
MUCR Museo de Insectos, Universidad de Costa Rica, Costa Rica
MZLU Museum of Zoology, Lund University, Lund, Sweden
MZSP Museu de Zoologia da Universidade de São Paulo, Brazil
NHMW Naturhistorisches Museum, Vienna, Austria
OSAC Oregon State Arthropod Collection, Oregon State University, Corvallis, OR, USA
PSWC P. S. Ward Collection, University of California at Davis, CA, USA
RAJC R. A. Johnson Collection, Tempe, AZ, USA
SEAN Museo Entomológico, Asociación Nicaragüense de Entomología, León, Nicaragua
SEMC Snow Entomological Museum, University of Kansas, Lawrence, KS, USA
SMPC Stacy M. Philpott Collection, University of California at Santa Cruz, CA, USA
STDC ShawnT. Dash Collection, Hampton University, Hampton, VA, USA
UCDC Bohart Museum of Entomology, University of California at Davis, CA, USA
UCRC Entomology Research Museum, University of California at Riverside, CA, USA
UNAM Colección Nacional de Insectos, Instituto de Biología, Universidad Nacional Autónoma de México, Coyoacán, Mexico (=CNIN)
USNM National Museum of Natural History, Washington, DC, USA

Downloaded from https://academic.oup.com/isd/article/6/1/4/6514767 by ThULB Jena user on 27 January 2022

UTEP UTEP-BC Entomology Collection, University of Texas at El Paso, TX, USA (William P. Mackay Collection, previously cited as WPMC)
UTIC Entomology Collection, University of Texas at Austin, TX, USA
UVGC Colección de Artrópodos, Universidad del Valle de Guatemala, Guatemala City, Guatemala
UWEM Entomology Museum, University of Wisconsin, Madison, USA
ZMHB Museum für Naturkunde der Humboldt Universität, Berlin, Germany

The following metric measurements and indices were employed (for additional details see Ward 2019). All measurements are given in millimeters, to two decimal places.

HW Head width: maximum width of head, including the eyes.
HL Head length: midline length of the head capsule, measured in full-face (dorsal) view, from the anterior clypeal margin to the midpoint of a line tangential to the posterior margin of the head
EL Eye length: length of the compound eye, measured with the head in full-face view.
MFC Minimum frontal carinal distance: minimum distance between the frontal carinae, posterior to their fusion with, or approximation to, the antennal sclerites.
FL Profemur length: length of the profemur, measured along its long axis in posterior view.
FW Profemur width: maximum measurable width of profemur, measured in the same view as FL, perpendicular to FL.
PL Petiole length: length of the petiole, measured in lateral view, from the lateral flanges at the anterior end of the petiole to the posterior extremity of the petiole.
PH Petiole height: maximum height of the petiole, measured in lateral view perpendicular to PL, but excluding any protruding anteroventral or posteroventral processes.
DPW Dorsal petiole width: maximum width of the petiole, measured in dorsal view.
PPW Dorsal postpetiole width: maximum width of the postpetiole, measured in dorsal view.
LHT Metatibia length: length of the metatibia, measured in dorsal view, orthogonal to the plane of tibial flexion and excluding the proximomedial portion of the articulation with the metafemur.
CI Cephalic index: HW/HL
REL Relative eye length: EL/HL
REL2 Relative eye length, using head width: EL/HW
FCI Frontal carinal index: MFC/HW
FI Profemur index: FW/FL
PLI Petiole length index: PH/PL
PWI Petiole width index: DPW/PL
MSC Mesosomal setal count: number of standing hairs, i.e., those forming an angle of 45° or more with the cuticular surface (Wilson 1955), visible in outline on the dorsal surface of the mesosoma.
HTC Metatibial setal count: number of standing hairs visible in outline on the outer (extensor) surface of the metatibia.
MTC Mesotibial setal count: equivalent setal count for mesotibia.

Very short (<0.04 mm long) standing hairs were excluded from setal counts. Terminology for surface sculpture follows Harris (1979). Observation of integument sculpture was made under diffuse (fluorescent) light.

Specimens lacking coordinates on the locality label were georeferenced with the use of Google Earth (https://www.google.com/earth), GEOnet Names Server (https://geonames.nga.mil/gns/html), regional topographic maps, and the following literature sources: Caudell (1907), Fairchild (1912), García Cubas (1891), Janzen (1967), Goodrich and van der Schalie (1937), Palacios Roji García and Palacios Roji García (2006), Petrunkevitch (1909), Schultze-Jena (1938), Selander and Vaurie (1962), Skwarra (1934), Slevin (1923), Smith (1899), and Wheeler (1936).

For the sake of brevity, the section of each species account listing 'Other material examined' (i.e., material other than type specimens) has been limited to citation of the locality, elevation, and collector. Elevations were converted to meters if given in feet. The expression 'c.u.' signifies collector unknown. More complete collection data for all examined specimens is available in Supp Table S1 (online only). When referring to type specimens of described taxa, 'examined' indicates that the specimen was directly examined by one of us (P.S.W.).

Like most ants, those in the genus *Pseudomyrmex* reproduce sexually, and this underpins our adherence to Mayr's biological species concept (Mayr 1942, Coyne and Orr 2004) when attempting to delimit species. We searched for phenotypic or genetic gaps that would indicate reproductive isolation between populations or sets of populations. We allowed for geographical variation within species, i.e., we did not assume species-wide panmixia. When examining phylogenies we expected assemblages of conspecific populations to be monophyletic or, in some instances after recent speciation events, paraphyletic (Ross 2014). The challenge of determining the status of closely related but partly differentiated, allopatric populations was addressed using a rough 'sympatry yardstick': such populations were treated as different species if they showed as much phenotypic differentiation as closely related sympatric species (Tobias et al. 2010). In addition to this integrative approach to determining to species boundaries, based on taxonomic expertise and the principles enunciated above, we also subjected a subset of sequenced specimens to three molecular species delimitation methods, as detailed below under Molecular Species Delimitation.

Molecular Data Generation

For sequencing, we attempted to choose a geographically representative set of specimens. Four of the species in the *P. elongatulus* group were represented by singletons, while the other nine species were represented by 2–8 individuals. We also included three individuals from the *P. fervidus* group, the sister group of the *P. elongatulus* group (Chomicki et al. 2015), for a grand total of 49 terminals (Supp Table S2 [online only]).

DNA was extracted from single ants, either adults or pupae, using the DNeasy Blood and Tissue Kit (Qiagen, Valencia, CA), and quantified with a Qubit fluorometer (HS Assay Kit, Life Technologies Inc., Carlsbad, CA). We sheared 5–50 ng input DNA to a target size of ~600 bp using either a Diagenode BioRuptor (Diagenode Inc., Denville, NJ) or QSonica Q800R3-110 (Qsonica Inc., Newtown, CT). Sheared DNA was input into a modified library prep procedure utilizing Kapa Hyper Prep kits (Roche Sequencing, Kapa Biosystems, Wilmington, MA) and custom dual-indexing adapters (Glenn et al. 2019). All library preparation steps were performed at quarter volume except for PCR, which was done at full volume. We cleaned libraries using 1.0× SPRI beads and quantified the cleaned products with Qubit. Enrichment of UCE loci was carried out using taxon-specific versions of the Hymenoptera v2 UCE probeset (Branstetter et al. 2017), which targets up to 2,590 UCE loci in Hymenoptera. Most taxa were enriched using the ant-specific version of the probe

Downloaded from https://academic.oup.com/isd/article/6/1/4/6514767 by ThULB Jena user on 27 January 2022

set, but three samples were enriched using a bee-ant-specific version (Grab et al. 2019). The probes and enrichment kit were purchased from Arbor Biosciences (Ann Arbor, MI). Enrichment was performed following either a standard UCE protocol (enrichment protocol v1.5 available at ultraconserved.org), based on Blumenstiel et al. (2010), or by using a modified protocol in which we followed Arbor Biosciences v3.02 protocol for enrichment day 1, and the standard UCE protocol for day 2. For the procedure we combined up to 10 samples into equimolar enrichment pools and used 500 ng of DNA for the hybridization reaction, which was carried out over 24 h at 65°C. Following enrichment, each pool was quantified via qPCR and then pooled into a final sequencing pool of 100–110 samples. Sequencing pools were sent to either the University of Utah Genomics Core for sequencing on an Illumina HiSeq 2500 or Novogene (Novogene Inc., Sacramento, CA) for sequencing on an Illumina HiSeq X.

Molecular Data Processing

To produce a variety of results on which to base phylogenetic and taxonomic conclusions, we processed the raw sequence data following three slightly different pathways, producing a standard UCE data set, a phased UCE data set, and a mitogenome data set. Phased data sets were generated because recent evidence suggests that phased data can outperform unphased data in phylogeny inference, divergence dating, and species delimitation, particularly at shallow phylogenetic depths (Andermann et al. 2019). The mitogenome data set was generated and analyzed because mitochondrial DNA (mtDNA) is often present as bycatch in UCE data (Ströher et al. 2016) and mtDNA can provide an independent assessment of evolutionary history since it evolves separately from the nuclear genome. Additionally, given that the mitogenome is maternally inherited, it is likely to show reciprocal monophyly between species more rapidly than nuclear markers—assuming that this is not offset by a tendency to introgress across species boundaries.

Raw sequence data were demultiplexed either by the University of Utah Bioinformatics Core or manually using BBTools (Bushnell 2014). Most subsequent data processing steps were carried out using the Phyluce v1.6 package (Faircloth 2016) and associated programs. The raw sequence reads were cleaned using Illumiprocessor (Faircloth 2013), which incorporates Trimmomatic (Bolger et al. 2014), and then assembled using SPAdes (Bankevich et al. 2012). To identify and extract UCE contigs from the bulk set of contig sequences we used the ant-specific probe set file and the *match_contigs_to_probes* Phyluce script which calls the program LASTZ v1.0 (Harris 2007).

For the unphased UCE data set, we aligned UCE contigs using MAFFT v7.130b (Katoh and Standley 2013), with the L-INS-i algorithm, and we trimmed the resulting alignments using Gblocks (Talavera and Castresana 2007) and Spruceup (Borowiec 2019). For Gblocks, which trims entire columns, we used reduced stringency parameter settings (b1: 0.5, b2: 0.5, b3: 12, b4: 7). For Spruceup, which trims poorly aligned windows of outlier sequence data from individual samples based on a distribution of pairwise distances, we used the Jukes–Cantor distance method and the lognormal criterion. We tested cutoff values from 0.8 to 0.9999 and ultimately selected a value of 0.98 based on careful examination of branch lengths and support values in preliminary phylogenetic trees. After alignment trimming, we created a final locus set for analysis by filtering loci to have 95% taxon completeness. This resulted in a final locus set consisting of 2,006 UCE loci and 1.98 Mb of sequence data, of which 92,163 sites were informative (see Supp Table S5 [online only] for more information).

To create the phased UCE data set, we followed the phasing tutorial implemented in Phyluce v1.6 (https://phyluce.readthedocs.io/en/latest/tutorials/tutorial-2.html). Briefly, we aligned and edge-trimmed the uce contigs using the *seqcap_align* Phyluce script with default settings. We then mapped cleaned sequence reads to the edge-trimmed alignments for each sample and phased the alignments into separate '0' and '1' alleles. We used default settings for phasing, except we used the 'conservative' flag to make the program discard all base calls with limited certainty (covered by <3 reads). After phasing, we realigned the data using MAFFT with the L-INS-i algorithm, and then trimmed the data with Gblocks and Spruceup as described above for the unphased data. We then filtered the loci to have 95% taxon completeness for the final locus set. This resulted in a final locus set consisting of 1,862 UCE loci and 1.26 Mb of sequence data, of which 86,127 sites were informative (see Supp Table S5 [online only] for more information).

To extract mitogenomic data from assembled contigs we used a combination of the program MitoFinder (Allio et al. 2020) and a Phyluce script (*match_contigs_to_barcodes*). MitoFinder was developed to extract and annotate mtDNA genes from assemblies based on a reference. For this analysis, we used the previously generated SPAdes contigs as the input assemblies and a mitogenome of *Pseudomyrmex flavicornis*, downloaded from GenBank (Accession# BK010381), as the annotated reference. This approach worked well at extracting most mtDNA genes from most samples. At least one sample, however, did not work as well, and had a lot of missing data (*Pseudomyrmex_cognatus*_D1983). To ensure more complete data for the *cytochrome oxidase I* (COI) barcode gene, we used the Phyluce script *match_contigs_to_barcodes* and a complete reference sequence from *Pseudomyrmex_cognatus*_D1223 to slice out matching DNA from the assemblies. This approach successfully recovered missing sequence data for sample D1983 and three other samples. After extracting the mtDNA genes, all sequence data were combined and aligned using MAFFT. The ribosomal genes were trimmed using reduced stringency parameters and the coding genes were evaluated by eye using Mesquite. We translated the data to amino acids and examined all genes for evidence of mitochondrial pseudogenes. We then partitioned the matrix by gene and codon position for phylogenetic analysis. The full mitogenome data set included 15 loci, 12,581 bp of sequence data, 5,154 informative sites, and only 4.9% missing data. For just the barcode region of the COI gene, the data set included 658 bp of sequence data, 230 informative sites, and 0% missing data.

Phylogenetic Analyses

Tree Inference

For both UCE datasets (phased and unphased), we conducted concatenated and gene tree-species tree analyses. For the concatenated analysis, we partitioned the datasets using the Sliding Window Site Characteristics based on entropy approach (SWSC-EN) designed specifically for UCE data (Tagliacollo and Lanfear 2018). We first separated UCE loci into core and flank regions using the SWSC-EN program and then merged the data subsets using ModelFinder2 (Kalyaanamoorthy et al. 2017) within IQ-Tree v2.1.1 (Minh et al. 2020). The merging analysis was done using the *rclusterf* algorithm (set to check only the top 10% of merging schemes), the AICc criterion, and the GTR+G model of sequence evolution. After merging subsets, we ran phylogenetic analyses in IQ-Tree using the SWSC-EN partitioning scheme and the GTR+F+G4 model of sequence evolution. For branch support, we performed 1,000 Ultrafast Bootstrap replicates (UFB; Hoang et al. 2018) and 1,000 SH-like approximate likelihood ratio test replicates (SH-aLRT; Guindon et al. 2010).

To infer species trees, we estimated gene trees for all loci using IQ-Tree. We used the '-m MFP' option for model selection and performed 1,000 UFB replicates per search. Following tree inference, we combined all trees into a single file and collapsed branches with

Downloaded from https://academic.oup.com/isd/article/6/1/4/6514767 by ThULB Jena user on 27 January 2022

less than or equal to 30% UFB support using the program Newick Utilities (Junier and Zdobnov 2010). We then input the trees into the summary species tree program ASTRAL-III v5.7.3 (Zhang et al. 2017). For the unphased data, all terminals were left as separate samples. However, for the phased data, we input a species file that assigned the two alleles for each species to a single species. We did not combine separate populations of the same putative species into single species. Branch support was assessed using the default local posterior probability metric.

The mitogenome dataset was analyzed with IQ-Tree v2.1.1. The dataset was partitioned by gene and codon position and merged using the '-m TESTMERGE -merit AICc' options. Branch support was assessed based on 1,000 UFB and SH-aLRT replicates. In addition to the full mitogenome dataset, we also performed a reduced analysis using just the 658 bp region of the DNA barcode gene *cytochrome oxidase I* (COI). The analysis was performed with partitioning by position, and using the GTR+F+G4 model of sequence evolution.

Divergence Dating

There is no fossil record for the *P. elongatulus* group. We assigned the root node (the most recent common ancestor, or MRCA, of the *P. elongatulus* group and its sister taxon, the *P. fervidus* group) a normal prior distribution, with mean 15.6 ± 3.4 Ma, based on the molecular clock of Chomicki et al. (2015, Supp Fig. S4 [online only]) which involved comprehensive sampling of the entire subfamily Pseudomyrmecinae and the use of several fossil calibrations. Based on the same source we employed a prior of 9.2 ± 2.4 Ma on the MRCA of the *P. elongatulus* group. By calibrating these two nodes (root and crown *elongatulus* group), we aimed to better constrain the analysis to match the results of Chomicki et al. (2015).

We inferred a dated tree for both the phased and unphased data sets using BEAST v2.6.3 (Bouckaert et al. 2014). For the sequence data, we filtered the UCE loci to have 100% taxon occupancy and then randomly selected and concatenated 500 loci. We used a fixed tree topology based on the result of the concatenated analyses and made the trees ultrametric by performing a strict clock analysis using the *chronos* function in the R (R Core Team 2021) package APE v5.4 (Paradis et al. 2004). This function implements a penalized likelihood divergence dating method that computes efficiently (Kim and Sanderson 2008, Paradis 2013). For the BEAST analysis, we did not partition the data set, in order to speed up run convergence and performance. We used an uncorrelated lognormal clock model, the GTR+G4 model of sequence evolution, and a birth–death tree prior. The birth–death model was selected because it has been shown to produce accurate ages when intraspecific samples are included, as is the case here (Ritchie et al. 2017). For each data set we conducted five independent analyses, each run for 2×10^8 generations, sampling every 5×10^3 generations. The resulting run data were examined for convergence and adequate ESS values in Tracer v1.7 (Rambaut et al. 2018). Burnin was set appropriately and the tree files were combined using LogCombiner and summarized with TreeAnnotator. Node heights were set to mean ages.

Biogeographic Analysis

We assigned each species to one or more of five coarse biogeographic regions: 1) southwestern Nearctic: southwestern United States and immediately adjacent northern Mexico; 2) western Mexico: central and southern Baja California, adjacent western mainland Mexico, south to Oaxaca, and east to the eastern margin of the Mexican Plateau; 3), eastern Mexico: from Tamaulipas to the Isthmus of Tehuantepec; 4) northern Central America: south of the Isthmus of Tehuantepec to the Nicaraguan Depression; and 5) southern Central America: south of the Nicaraguan Depression to Panama (the two species in this region are known so far only from Costa Rica). We input the distribution information and the dated, phased phylogeny (pruned to one sample per species), into the program BioGeoBEARS (Matzke 2013). We set the analysis to have three max areas and we removed areas that were nonadjacent ('AD','AE','BE','CE','ABE','ACE','ADE','BCE'). We tested each of the available models: dispersal, extinction, cladogenesis (DEC; Ree et al. 2005, Ree and Smith 2008), an ML version of the dispersal–vicariance model (DIVA-like; Ronquist 1997), and an ML version of the Bayesian Analysis of Biogeography model (BayArea-like; Landis et al. 2013). Because of recent criticisms of the +j model, we excluded this option from the analysis (Ree and Sanmartín 2018). All other settings were left at default values.

Trait Evolution: Elevation

All but one member of the *P. elongatulus* group can be unambiguously identified as being either a low-elevation species (mean elevation across all locality records <500 m, and most populations occurring below 800 m) or high-elevation species (mean elevation across all locality records >950 m, and most populations above 800 m). *Pseudomyrmex apache* is an exception: it has a much greater elevation range than any other species (20–2,020 m; mean 905 m, and median 790 m, based on 145 locality records). We reconstructed elevation as a discrete trait using the *ace* function in the R package APE v5.4. This function implements a maximum likelihood-based reconstruction of ancestral states and allows for the testing of alternative models. We coded species as 1) low elevation, 2) high elevation, and 3) low and high elevation. We tested the equal rates (ER), symmetrical rates (SYM), and all rates different (ARD) models and selected the best model based on the results of likelihood ratio tests.

Molecular Species Delimitation

We tested our integratively delimited species by implementing three molecular species delimitation approaches. We tested two quick methods that do not require reducing the size of the data set and one full Bayesian approach that usually does require data set reduction. First, we tried the recently developed multilocus method SODA (Rabiee and Mirarab 2021), which uses gene trees, quartet-based inference methods, and the multispecies coalescent model to infer species boundaries. The program is a summary method that relies on the same analytical machinery as ASTRAL. It is very fast, can be used on large data sets, and is nearly as accurate as the full Bayesian program BPP (Flouri et al. 2018). We tested the method using gene trees estimated from the phased and unphased data sets. Like the ASTRAL analyses, we collapsed nodes with less than or equal to 30% UFB support. We ran each analysis using the SWSC-EN concatenated tree as a guide tree and we input a species file for the phased data, telling the program how to combine the phased samples. For the second approach, we used the program bPTP (Zhang et al. 2013), which delimits species based on single tree files and a model of speciation that is based on number of substitutions. We ran the analysis using trees generated from the concatenated phased and unphased UCE data, from the mitogenome analysis, and from the DNA barcode only analysis. In each case, we used the bPTP server (https://species.h-its.org) and input rooted trees with outgroups pruned and we performed 500,000 MCMC generations.

Lastly, Bayesian delimitation of species was conducted using the program BPP v4.4 (Yang and Rannala 2010, Rannala and Yang 2013, Flouri et al. 2018), which employs the multispecies

Downloaded from https://academic.oup.com/isd/article/6/1/4/6514767 by ThULB Jena user on 27 January 2022

coalescent model to compare different species delimitation models. We ran the analysis on phased and unphased sequence alignments. Using the full 49-taxon data set, we encountered poor mixing and convergence among replicate runs. To improve convergence and reduce analysis time, we extracted subsets of taxa from the full data set and we used only the 500 most informative loci for each analysis. Using a Phyluce script (*extract_taxa_from_alignments*), we extracted taxon sets corresponding to the *Pseudomyrmex championi*, *cognatus*, and *elongatulus* species complexes, and for each we included the three samples of *P. salvini* as outgroups. We employed the same set of alignments used for the other phylogenetic and delimitation analyses to keep the data sets comparable. However, we filtered the alignments to have 100% complete taxon occupancy and we removed gap-only columns after extracting the taxon subsets. We also calculated the number of informative sites for each taxon set separately before selecting the 500 most informative loci. Using the SWSC-EN concatenated tree, pruned to match the taxon subset, as a guide tree, we performed multiple runs of the species delimitation only method (A10). We used delimitation algorithm 1 and treated the data as phased haplotype data with either 1 (unphased) or 2 (phased) sequences. We allowed for rate variation among loci and used default settings for the model and clock parameters. For thetaprior and tauprior we used diffuse values to define the inverse gamma distribution, using 3 and 0.002 for theta and 3 and 0.015 for tau. For each data set we performed five independent runs with 1×10^4 burnin generations and 1×10^5 postburnin generations, sampling every 5 generations. We examined individual runs for convergence and then combined runs to generate the final delimitation. We inspected the final output tree and identified nodes having ≥95% posterior probability as being supported.

Nomenclature

This paper and the nomenclatural act(s) it contains have been registered in Zoobank (www.zoobank.org), the official register of the International Commission on Zoological Nomenclature. The LSID (Life Science Identifier) number of the publication is: urn:lsid:zoobank.org:pub:C6D0780E-90ED-42D1-8A60-72D1E03607AC.

Results

Phylogeny and Divergence Dating

The phylogenetic results based on UCE data provide robust resolution of relationships among species in the *P. elongatulus* group (Fig. 1; Supp Figs. 1-3 [online only]). Relationships are mostly concordant among analyses (phased, unphased, concatenated, species

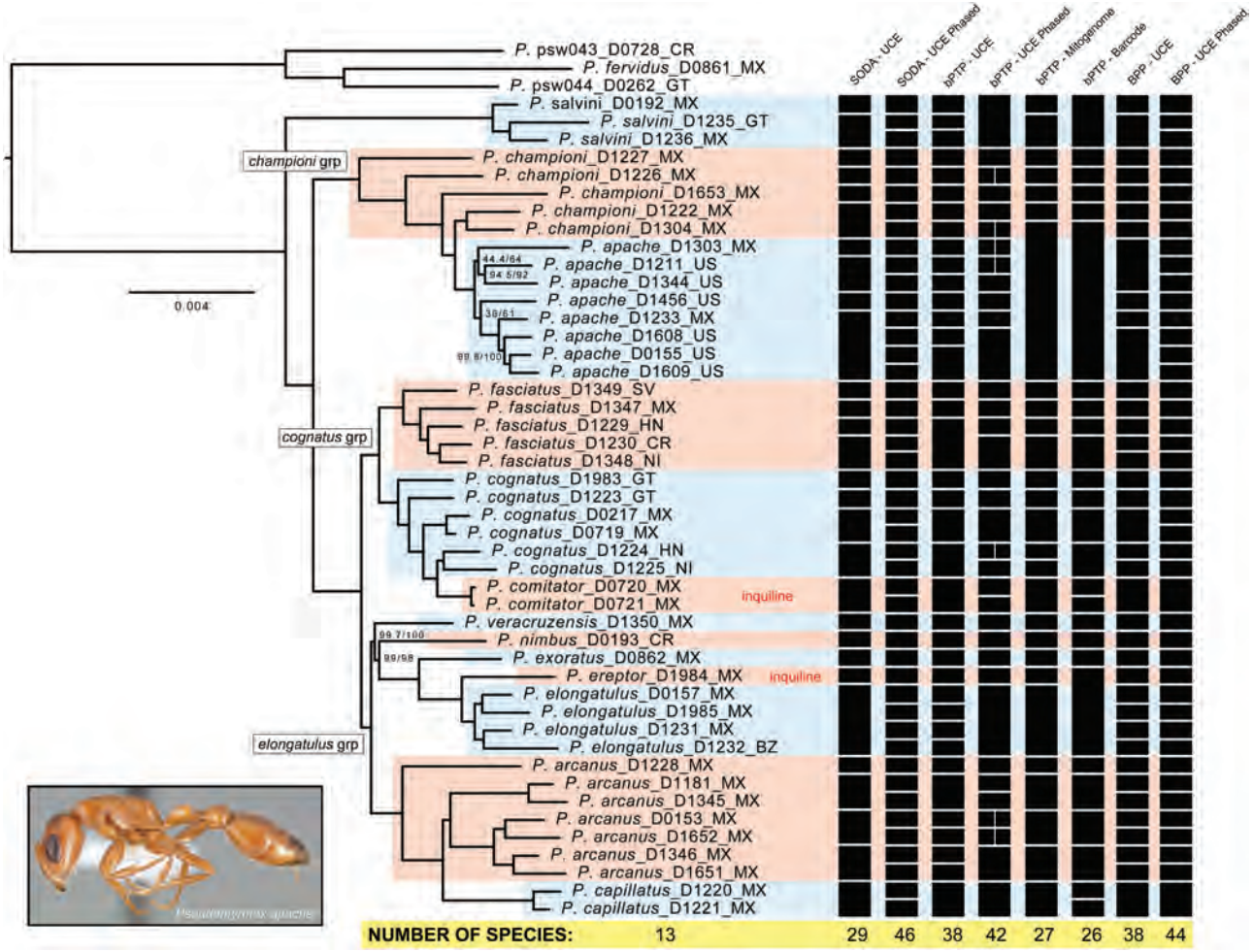

Fig. 1. Phylogeny and molecular species delimitation results for the *P. elongatulus* species group. The presented phylogram was inferred from 2,006 unphased UCE loci using the SWSC-EN partitioning scheme and the program IQ-Tree v2.1.1. Support values are ultrafast bootstrap (UFB) and SH-like approximate likelihood ratio test (SH-aLRT) percentages; nodes without support values have maximum support (100/100). Clades are colored by the final species delimitation. Results from the molecular species delimitation methods SODA, bPTP, and BPP are presented to the right of the phylogeny, with each black box indicating one species.

Downloaded from https://academic.oup.com/isd/article/6/1/4/6514767 by ThULB Jena user on 27 January 2022

tree), with only a few differences at the population level within the species *P. apache* and *P. cognatus*. *Pseudomyrmex salvini* is recovered as sister to all other species, with strong support. The *P. championi* complex (*P. championi*, *P. apache*) is sister to the remaining species, and the latter is comprised of two major clades: the *P. cognatus* complex (*P. cognatus*, *P. comitator*, *P. fasciatus*) and the *P. elongatulus* complex (*P. arcanus*, *P. capillatus*, *P. elongatulus*, *P. ereptor*, *P. exoratus*, *P. nimbus*, *P. veracruzensis*). Relationships within the *P. elongatulus* complex are also well resolved. *Pseudomyrmex arcanus* and its embedded species, *P. capillatus* (see below under Species Paraphyly), are sister to the other species, which resolve as: (*P. veracruzensis*, (*P. nimbus*, (*P. exoratus*, (*P. ereptor*, *P. elongatulus*)))). These results are mostly concordant with the mitogenome phylogeny (Supp Fig. S6 [online only]) except in deeper and more poorly supported parts of the mitochondrial tree, where this marker has less resolving power. The results are less congruent overall for the DNA barcode (COI) phylogeny, which shows multiple discrepancies with both the mitogenome tree and the UCE tree (Supp Fig. S7 [online only]), with intermingling of species samples and poor recovery of phylogenetic relationships. In both mitochondrial trees (mitogenome and COI), one divergent sample of *P. cognatus* (D1983) grouped more closely with samples of its sister species *P. fasciatus* than with other *P. cognatus*, although with only modest support.

Divergence dating with the phased data set (Fig. 2; Supp Fig. S5 [online only]) returned slightly younger ages than the unphased data (Supp Fig. S4 [online only]), matching the trend reported by Andermann et al. (2019), where it was shown that allele phasing leads to more accurate estimates of divergence dates. Focusing on the phased results, we recovered a crown group age for the *P. elongatulus* group of 7.8 million years ago (Ma) (5.4–10.2 Ma 95% Highest Posterior Density [HPD]) during the Miocene epoch. The *P. championi* complex evolved 5.1 Ma (3.5–6.7 Ma 95% HPD), but *P. apache*, which is nested inside *P. championi* did not diverge from *P. championi* until 2.3 Ma (1.5–3.0 Ma 95% HPD). The *P. cognatus* complex evolved 3.4 Ma (2.3–4.5 Ma 95% HPD)

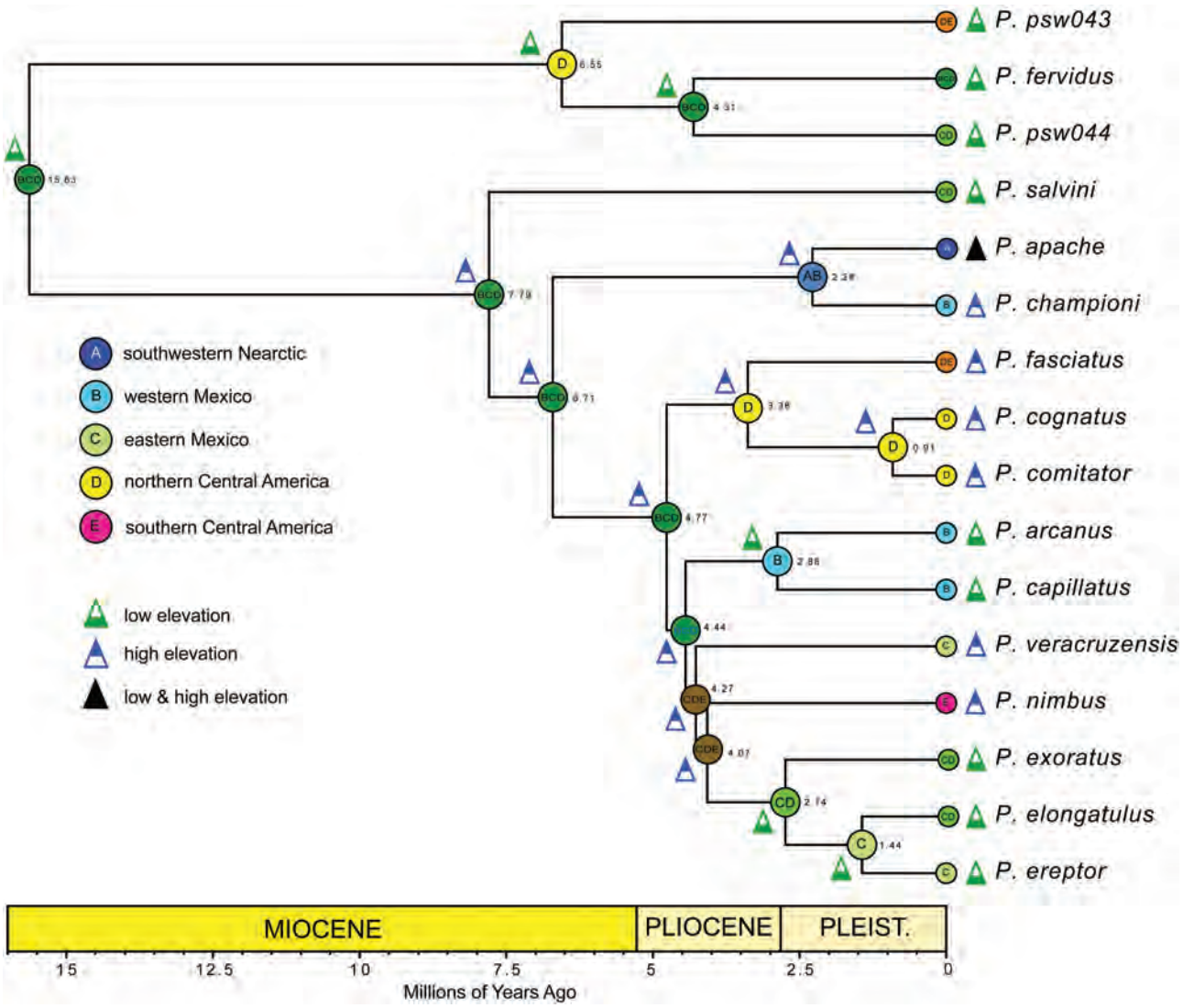

Fig. 2. Chronogram, biogeographic history, and ancestral state reconstruction of elevation range for the *P. elongatulus* species group. The chronogram is based on analysis of 500 phased UCE loci using the program BEAST2 and terminals are pruned to show only one terminal per species (see Supp Fig. 5 [online only] for the full result). Node numbers are mean ages in millions of years ago (Ma). Circles on nodes indicate most likely ancestral areas as indicated by BioGeoBEARS and the best performing DEC model. Mountain symbols on nodes depict most likely trait reconstructions for elevation range inferred using the best performing ER model and the *ace* function in the R package APE.

Downloaded from https://academic.oup.com/isd/article/6/1/4/6514767 by ThULB Jena user on 27 January 2022

and the *P. elongatulus* complex emerged 4.4 Ma (3.1–5.9 Ma 95% HPD). The embedded socially parasitic species *P. comitator* diverged from its sister species *P. cognatus* most recently 0.9 Ma (0.6–1.3 Ma 95% HPD). The crown age of *P. cognatus*, however, is much older, dating to 2.5 Ma (1.6–3.3 Ma 95% HPD). The other social parasite, *P. ereptor*, is estimated to have diverged from its host species 1.4 Ma (0.9–2.0 Ma 95% HPD).

Biogeography

The DEC model conferred the highest likelihood on the data but performed only slightly better than the next best DIVA-like model (AICc 88.4 vs 90.6). The BayAREA-like model was significantly worse (AICc 94.9). All model results are presented in Supp Table S6 (online only), and Supp Figs S8–S13 (online only). Under the DEC model reconstruction (Fig. 2; Supp Figs. S8–S9 [online only]), stem and crown *P. elongatulus* group evolved in the combined region of western and eastern Mexico and northern Central America (areas B, C, and D), being absent from the southwestern Nearctic and southern Central America regions (areas A and E). A stem-group origin in northern Central America received only a slightly lower probability (Supp Fig. S9 [online only]). The *P. championi* complex is estimated to have originated in the southwest Nearctic plus western Mexico (areas A and B), with the two daughter species diverging due to vicariance. Taking into account the paraphyly of *P. championi* relative to *P. apache* (see Species Paraphyly below), an origin of this complex in western Mexico is arguably more plausible. The remaining species, minus *P. salvini*, also had a widespread ancestral distribution in areas B, C, and D. The *P. cognatus* complex originated in northern Central America (area D), with *P. fasciatus* later expanding its range farther south (area E). The *P. elongatulus* complex had a widespread origin in areas B, C, and D, and a more complex subsequent history. The species pair *P. arcanus* + *P. capillatus* evolved in western Mexico (area B). The remaining species are inferred to have originated and diversified in the wetter regions of eastern Mexico and northern Central America (areas C and D), with dispersal into southern Mesoamerica by *P. nimbus*.

Trait Reconstruction

The simplest ER model was favored over the alternative SYM and ARD models based on likelihood-ratio testing (Supp Table 7 [online only]). Under the ER model, the stem group ancestor of the *P. elongatulus* group had a high probability of being low elevation, but the ancestor of the crown group had a slightly elevated probability of being high elevation (Fig. 2; Supp Fig. 14 [online only]). Most nodes within the group were reconstructed to be high elevation, with three switches to low elevation and one expansion to include low and high elevation. A lowland ancestral state for crown *P. elongatulus* group is almost equally supported, however, making plausible the occurrence of multiple retreats to high elevation. Trait reconstructions inferred from all models are presented in Supp Figs. 14–16 (online only).

Species Paraphyly

We uncovered three cases in which one nominal species was nested within a set of populations of a second nominal species, rendering the latter paraphyletic (Fig. 1). This is not an uncommon pattern in nature (Funk and Omland 2003, Syring et al. 2007, Ross 2014). Taking into account the geographic distributions of these *Pseudomyrmex* taxa, each of these three situations can be reasonably interpreted as an outcome of speciation involving two lineages with different effective population sizes. The resulting delay in time to allelic monophyly (coalescence) of the larger, 'parental' population compared to the smaller, 'daughter' population creates a paraphyletic/monophyletic relationship (Avise 2000).

One case involves an apparent workerless social parasite (inquiline). *Pseudomyrmex cognatus* is a widespread species, with typical workers, queens, and males, occurring from southern Mexico to Nicaragua. Its embedded sister species, *P. comitator*, is known only from two highly modified queens, one of which was found in a *P. cognatus* nest. *Pseudomyrmex comitator* is so far recorded only from two adjacent sites in Chiapas, but in the UCE (and mitochondrial) phylogeny it is not sister to the Chiapas population of *P. cognatus*; rather it is more closely related to *P. cognatus* samples from Honduras and Nicaragua (Fig. 1; Supp Figs. 1–3 [online only]). This supports the idea that the speciation event generating *P. comitator* occurred sufficiently long ago for the process of coalescence in *P. cognatus* to have proceeded some distance—but not to completion.

A second case of social parasitism, involving *P. elongatulus* and *P. ereptor*, arguably represents a later stage in this process. *Pseudomyrmex elongatulus* is distributed from northeastern Mexico to Guatemala and Belize, whereas *P. ereptor* is known from a single alate queen located in a nest of *P. elongatulus* in Veracruz. *Pseudomyrmex ereptor* has several hallmarks of social parasitism, including miniaturization, modified mandibles, and a very broad postpetiole. In the UCE phylogeny, however, it is sister to the entire assemblage of *P. elongatulus* samples (Fig. 1), rather than being nested phylogenetically within the latter. The samples of *P. elongatulus* in this phylogeny include an individual, D1985, from the same nest in which *P. ereptor* was collected. This finding implies a greater age of the divergence between these two species, such that the parent taxon, *P. elongatulus*, has achieved monophyly at all or most loci.

The two other cases of species paraphyly do not appear to involve social parasitism. *P. arcanus* occurs widely in western Mexico. Its embedded relative, *P. capillatus*, is a free-living, twig-nesting species known from tropical dry forest at Estación Biología Chamela, Jalisco (and one other location in Colima). The two species are sympatric at Chamela, yet our two sequenced samples of *P. capillatus* are not closely related to the sympatric sample of *P. arcanus*. Instead, they are sister to a broader set of samples representing all but one of the *P. arcanus* populations (Fig. 1), indicating that *P. arcanus*, like *P. cognatus*, is in the process of achieving allelic coalescence.

In contrast to these three examples, the last case of a monophyletic/paraphyletic relationship involves two species, *P. apache* and *P. championi*, that are both widespread and can be expected to have large effective population sizes. *Pseudomyrmex apache* has a more geographically marginal distribution, however, relative to the *P. elongatulus* group as a whole (Fig. 19). *Pseudomyrmex apache* occurs in southwestern United States and adjacent northern Mexico, while *P. championi* is widespread in western Mexico. This suggests a scenario in which *P. apache* originated from northern populations of *P. championi*, and then subsequently expanded to colonize much of the arid Southwest.

Molecular Species Delimitation

For the *P. elongatulus* group the molecular species delimitation analyses inferred substantially more species than our final integrative delimitation of 13 species (see Taxonomy section below). The number of delimited species ranged from 26 to 46 species (Fig. 1). For species represented in our tree by multiple samples, the increase in estimated numbers of 'species' was as much as eight-fold (see *P. apache*, where all eight populations were designated as different species in two of the analyses). Counter to expectations, analyses based on the phased UCE data produced the highest estimates of species diversity. The SODA

Downloaded from https://academic.oup.com/isd/article/6/1/4/6514767 by ThULB Jena user on 27 January 2022

analysis of the phased data delimited all terminals as separate species, resulting in 46 ingroup species. In contrast, the SODA analysis of the unphased data delimited just 29 species. The bPTP analysis of the phased UCE data delimited 42 species, whereas the unphased data resulted in 38 species. The bPTP analyses of the mitogenome and DNA barcode data delimited 27 and 26 species respectively. The BPP analyses of UCE data produced comparable results, delimiting 38 species with unphased data and 44 species with phased data.

Taxonomy

Pseudomyrmex elongatulus Group

Worker Diagnosis. Moderate in size (HW 0.82–1.21, LHT 0.68–1.12), with a variably elongate head (CI 0.67–0.96), and medium to large eyes (REL 0.38–0.59, REL2 0.46–0.66). Masticatory margin of mandible with 5–6 teeth; mesial tooth on basal margin closer to apicobasal angle than to proximal tooth. Palp formula 6,4. Median clypeal lobe laterally rounded. Frontal carinae separated by basal scape width or less (FCI 0.02–0.07). Profemur relatively slender in most species (FI 0.37–0.49). Pronotal humeri and lateral margins of pronotum rounded. Metanotal groove varying from moderately impressed to absent. Basal and declivitous faces of propodeum weakly to moderately differentiated and usually subequal in length, in profile the juncture between the two gently rounded. Petiole relatively long and slender (PL/HL 0.48–0.69; EL/PL 0.72–0.90), much longer than high or wide (PLI 0.43–0.61, PWI 0.41–0.58); petiole with small anteroventral tooth; anterior peduncle of petiole weakly to moderately differentiated. Postpetiole broader than long, with small anteroventral tooth. Body sculpture punctulate-coriarious to coriarious-imbricate, the integument sublucid to opaque; dorsum of head never with extensive smooth, shiny interspaces; punctulae usually separated by their diameters or less. Standing pilosity generally sparse, nearly always absent from the extensor faces of tibiae, and usually present as 1–2 pairs on the pronotum, petiole, and postpetiole, while being absent from mesonotum and propodeum (MSC 2–8); one exceptional species with greater amounts of pilosity (MSC 23–28, HTC 0, MTC 1–2) including on the mesonotum and propodeum. Appressed pubescence dense but short on most of body, including head and abdominal tergite IV. Color varying from light yellow- or orange-brown to dark brownish-black, often variously bicolored.

Comments. In an earlier synopsis of *Pseudomyrmex* species groups (Ward 1989), the *P. elongatulus* group was subsumed under the *P. pallens* group. The two groups share a number of similar worker characteristics (6,4 palp formula, 5–6 teeth on the masticatory margin of the mandibles, and laterally rounded median clypeal lobe) but molecular studies have demonstrated that they are not closely related (Ward and Downie 2005, Chomicki et al. 2015). A recent worker-based key to *Pseudomyrmex* species groups (Ward 2017) separated the *P. elongatulus* group and *P. pallens* group primarily by geography: the species in the *P. pallens* group are almost wholly confined to South America, with just one species, *P. pallens*, extending north of Colombia as far as Costa Rica, while the *P. elongatulus* group occurs from southwestern United States to Costa Rica. Workers of the one overlapping species, *P. pallens*, can be distinguished from those of the *P. elongatulus* group by the combination of dense standing pilosity (MSC 13–28) and long eyes relative to petiole length (EL/PL 0.91–1.20).

List of Included *Pseudomyrmex* Species

P. apache Creighton 1953; southwestern United States, northern Mexico
P. arcanus, **sp. nov.**; western Mexico
P. capillatus, **sp. nov.**; Jalisco and Colima, Mexico
P. championi (Forel 1899); western Mexico
= *P. leonhardi* (Stitz 1937) (synonymy: Kempf 1961)
P. cognatus, **sp. nov.**; Chiapas, Mexico to Nicaragua
P. comitator, **sp. nov.**; Chiapas, Mexico
P. elongatulus (Dalle Torre 1892); northeastern Mexico to Guatemala and Belize
=*P. elongatus* (F. Smith 1877) (preoccupied)
=*P. decipiens* (Forel 1899) (synonymy: Kempf 1967)
P. ereptor, **sp. nov.**; Veracruz, Mexico
P. exoratus, **sp. nov.**; southeastern Mexico, Honduras
P. fasciatus, **sp. nov.**; Chiapas, Mexico to Costa Rica
P. nimbus, **sp. nov.**; Costa Rica
P. salvini (Forel 1899); southeastern Mexico to Honduras
P. veracruzensis, **sp. nov.**; Veracruz, Mexico

Key to Species, Based on the Workers and Queens

This key is based primarily on characteristics of workers but we have attempted to incorporate queen features as far as possible. Because queens are less well known, sample sizes are included for all queen measurements. Unless otherwise noted, sample sizes are the same for all measurements cited within a given lug of a couplet. For two species (*Pseudomyrmex capillatus*, *P. veracruzensis*) queens are unknown. Two other species (*P. comitator*, *P. ereptor*) are known only from queens and are assumed to be workerless social parasites; they are treated at the beginning of the key.

1. Queens only; small (HL 1.00–1.01, LHT 0.69–0.70; *n* = 2) with short, high petiole (PLI 0.67–0.83) (Fig. 9); dark brownish-black; apparent workerless inquiline, known only from Chiapas, Mexico ..... *comitator* sp. nov.

   - Workers and queens, or queens only; queens larger (HL 1.19–1.49, LHT 0.76–1.12; *n* = 41), with more slender petiole (PLI 0.42–0.61); color variable 2

2. Queens only; mandibles smooth and shiny, with scattered punctures; postpetiole very broad, appearing ovorectangular in dorsal view (PPW/LHT 1.01; *n* = 1) (Fig. 12); light orange-brown; apparent workerless inquiline, known only from Veracruz, Mexico ..... *ereptor* sp. nov.

   - Workers and queens; mandibles usually striate; queen and worker postpetiole more slender, pyriform in dorsal view (queen PPW/LHT 0.66–0.91; *n* = 40); color variable 3

3. Head relatively broad (worker CI 0.90–0.96; queen CI 0.81–0.84 (*n* = 5)), with large eyes, whose length exceeds 0.5× head length (worker REL 0.54–0.59; queen REL 0.53–0.54) (Fig. 17); large species (worker HW 1.12–1.21; queen HW 1.18–1.24); southern Mexico to Honduras ..... *salvini*

   - Head more elongate (worker CI 0.67–0.90; queen CI 0.55–0.80 (*n* = 35)); eyes proportionately smaller, eye length subequal to, or less than, head length (worker REL 0.38–0.53; queen REL 0.38–0.48); smaller in size (worker HW 0.82–1.09; queen HW 0.76–1.11 (*n* = 33)), except for one uncommon Costa Rican species with worker HW 1.03–1.20 and queen HW 1.15–1.18 (*n* = 2) 4

4. Standing pilosity common on most of body, present on mesonotum and propodeum as well as pronotum (worker

Downloaded from https://academic.oup.com/isd/article/6/1/4/6514767 by ThULB Jena user on 27 January 2022

MSC 25-39; queen unknown but expected to have MSC ~35) (Fig. 13); body dark-brown, the scapes, mandibles, anterior quarter of head capsule, protibia and protarsus a contrasting light yellowish-brown; western Mexico .. *capillatus* sp. nov.

- Standing pilosity sparse, absent from worker and queen propodeum, and almost always absent from worker mesonotum (worker MSC 2–8, queen MSC 11–23 (n = 35)); color variable, not matching the above pattern 5

5. In profile, worker with pronounced metanotal groove and with dorsal face of propodeum convex and rounding insensibly into the declivitous face (Fig. 16); large species (worker HW 1.03–1.20; queen HW 1.15–1.18 (n = 2), with proportionately longer legs (worker FL 0.84–0.99, worker LHT 0.96–1.09; queen FL 0.97–0.99, queen LHT 1.03–1.07) and elongate eyes (worker REL 0.48–0.51; queen REL 0.48); head, propodeum, and gaster dark brown, other parts of body with variably lighter coloration (medium brown to yellow-brown); known only from Costa Rican cloud forest ..... *nimbus*

- Worker metanonotal groove usually weakly impressed or absent, but if conspicuously developed then propodeum more flattened, and dorsal face better differentiated from declivitous face (Fig. 10); disagreeing with one or more other characters: either smaller and/or with shorter legs and eyes and/or different color pattern; queen REL 0.38–0.46 (n = 33); occurring from southern United States to Costa Rica 6

6. Head very elongate (worker CI 0.67–0.69; queen CI 0.55–0.59 (n = 2)) (Fig. 14); profemur short and robust (worker FI 0.46–0.49, worker FW/HW 0.41–0.44; queen FI 0.47–0.49, queen FW/HW 0.45–0.46); southern Mexico to Honduras .... *exoratus*

- Head less elongate (worker CI 0.79–0.90; queen CI 0.68–0.76 (n = 20)); profemur generally more slender (worker FI 0.38–0.47, worker FW/HW 0.30–0.38; queen FI 0.42–0.49, queen FW/HW 0.34–0.41) 7

7. Worker with well-developed metanotal groove, conspicuous in profile (Fig. 10); in full-face view, head with rounded posterolateral corners and elongate eyes (worker REL 0.47–0.53; queen REL 0.44–0.46 (n = 5)) (Figs. 10 and 11); petiole slender, elongate-triangular in profile (worker PLI 0.44–0.52; queen PLI 0.45–0.51) (Figs. 10 and 11); leg moderately long, worker LHT/HL 0.74–0.79, queen LHT/HL 0.64–0.67; typically light yellow- to orange-brown with transverse infuscation on gaster, but head and mesosoma more infuscated in southern parts of range; eastern Mexico to Guatemala and Belize .... *elongatulus*

- Worker metanotal groove moderately developed to absent; not matching the combination of other features 8

8. Body unicolorous yellow-orange to ferrugineus-brown (gaster may have transverse fuscous patches) 9

- Body *either* bicolored (dark gaster contrasting with lighter colored mesosoma) *or* predominantly brown to brownish-black, the mesosoma either concolorous with head and gaster or moderately lighter 12

9 Body ferrugineus-brown (Fig. 18); relatively large species (worker HW 0.97–1.07; queen unknown) with rather elongate petiole (worker PL 0.65–0.77, worker PLI 0.44–0.49); higher elevations, Veracruz, Mexico ..... *veracruzensis*

- Body light yellow- to orange-brown; size variable, usually smaller (worker HW 0.82–1.00; queen HW 0.86–1.04 (n = 15)) and with less elongate petiole (worker PL 0.49–0.66, worker PLI 0.46–0.61; queen PL 0.71–0.84, queen PLI 0.47–0.58) 10

10. Worker metanotal groove very weakly impressed, scarcely discernable in profile (Fig. 15); eyes elongate (worker REL 0.45–0.48; queen REL 0.45–0.46 (n = 6)); yellow-orange, with conspicuous anterolateral patches on fourth abdominal (first gastric) tergite and dark transverse bands on abdominal tergites 5–6 (gastric tergites 2–3); Chiapas to Costa Rica ..... *fasciatus*

- Worker metanotal groove somewhat better developed, more obvious in profile (Figs. 4 and 5); eyes less elongate, on average (worker REL 0.40–0.47; queen REL 0.38–0.44 (n = 9)); yellow-orange, with at most anterolateral fuscous patches on fourth abdominal (first gastric) tergite, but without transverse bands on succeeding segments (tip of gaster may be infuscated) 11

11. In profile, worker propodeum and petiole more rounded (Fig. 5); eye relatively elongate (worker REL2 0.52–0.58; queen REL2 0.56–0.58 (n = 3)); worker petiole more slender (worker PLI 0.49–0.57); northwestern Mexico to Oaxaca ..... *arcanus*

- In profile, worker propodeum and petiole more angular (Fig. 4); eye shorter (worker REL2 0.48–0.53; queen REL2 0.53–0.55 (n = 6)); worker petiole more robust (worker PLI 0.55–0.61) (Fig. 3 [bivariate plots]); southwestern United States and adjacent northern Mexico ..... *apache*

12. Bicolored: dark brownish-black gaster contrasting with light orange-brown mesosoma (head may be dark or light); worker metanotal groove present and clearly discernable in profile (Fig. 6); eye shorter (worker REL 0.38–0.44; queen REL 0.40–0.42 (n = 3)); western Mexico ..... *championi*

- Body more uniformly dark brownish-black, at most mesosoma moderately lighter; worker metanotal groove very weakly impressed, barely discernable in profile (Fig. 7); eye usually longer (worker REL 0.45–0.48; queen REL 0.42–0.46 (n = 8)) but eye shorter in one divergent sample from Guatemala where worker REL 0.43–0.45 (see discussion in text); Chiapas, Mexico to Nicaragua ..... *cognatus*

Species Accounts

***Pseudomyrmex apache* Creighton**

Figs. 4 and 19

Pseudomyrmex apache Creighton 1953: 134. Syntype workers, queens, males, Brown Canyon, Baboquivari Mtns., Arizona, 4400 ft., 2 Sept 1951, in *Quercus oblongifolia* (W. S. Creighton) (AMNH, BMNH, LACM, MCZC, MZSP) [examined].

Pseudomyrmex apache Creighton; Creighton 1954. Biology and distribution.

Downloaded from https://academic.oup.com/isd/article/6/1/4/6514767 by ThULB Jena user on 27 January 2022

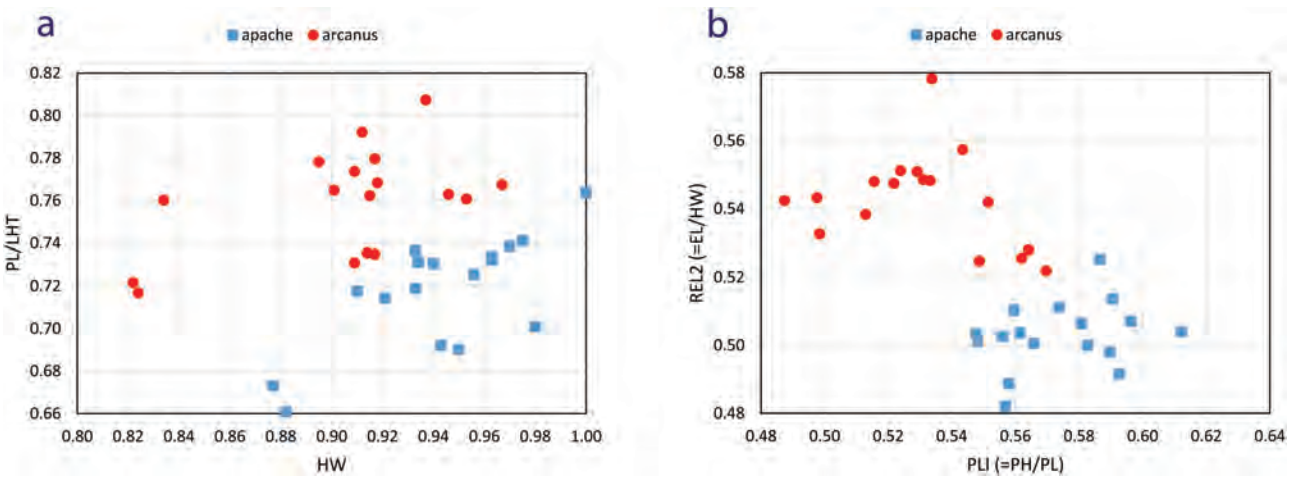

Fig. 3. Bivariate plots of measurements and indices concerned with eye size and petiole shape, in workers of *P. apache* (n = 17) and *P. arcanus* (n = 17). (a) PL/LHT (petiole length/metatibia length) by HW (head width); (b) REL2 (eye length/head width) by PLI (petiole height/petiole length).

Pseudomyrmex apache Creighton; Wheeler and Wheeler 1956: 380. Description of larva.

Pseudomyrmex apache Creighton; Ward 1985. Taxonomy and distribution.

Pseudomyrmex apache Creighton; Ward and Downie 2005: 314, 316. Placement in morphological and molecular phylogenies.

Pseudomyrmex apache Creighton; Chomicki et al. 2015: 4. Placement in molecular phylogeny.

Other material examined (AMNH, ANIC, BMNH, CASC, CHAH, CMNH, CNCC, CSCA, CUIC, EMEC, JTLC, LACM, MCZC, MNHN, MSNG, MZSP, PSWC, RAJC, SEMC, UCDC, UCRC, USNM, UTEP, UTIC).

Mexico, *Baja California*: 10 km W Mexicali (Snelling, R. R.); 10 mi E Bahia San Quintín (Williams, F. X.); 19 mi S Ensenada (Timberlake); 28 km E Ensenada, 750 m (Ward, P. S.); 3.5 mi Arroyo Santo Tomas (Sleeper, E. L.); 5 km S San Quintin (Heydon, S. L.); La Rumorosa, 1,200 m (Ward, P. S.); Mexicali (Snelling, R. R.); ***Chihuahua***: 16 mi W Gral. Trias, 1,770 m (Creighton, W. S.); 23 mi S Parral, 1,675 m (Creighton, W. S.); 3 mi S Encinillas, 1495 m (Creighton, W. S.); 34 mi S Parral, 1,770 m (Creighton, W. S.); 6 mi S Villa Matamoros (Gardner, R. C.; Kovacic, C. R.; Lorenzen, K.); Nogales Ranch, Sierra de en Medio, 1,525 m (Creighton, W. S.); Nogales Ranch, Sierra de en Medio, 1,585 m (Creighton, W. S.); Ojo del Cerro Chilicote (Townsend); ***Durango***: 9 mi E Palmito (Alpert, G.); Villa Ocampo, 1,735 m (Creighton, W. S.); ***Nuevo León***: China, 185 m (Creighton, W. S.); ***Sonora***: 3 mi E Punta Cirios, 60 m (Johnson, R. A.); 30 mi SE Agua Prieta (Roth, V.); 4.8 mi S Cananea (Roth, V.); Nogales (Perkins, R. C. L.); **United States, *Arizona***: *Cochise Co.*: 13 mi SW Apache (Rozen; Pavreau); 3 km SW Portal, 1,510 m (Ward, P. S.); 3 mi N Paradise, 1,525 m (Creighton, W. S.); 5 mi W Portal (Linsdale, D. D.); 7 km SE Sunnyside, 1670 m (Ward, P. S.); 9.5 km SW Portal, 1,775 m (Ward, P. S.); Carr Canyon, Huachuca Mtns., 1,645 m (Creighton, W. S.); Carr Canyon, Huachuca Mtns., 1,890 m (Obrien, C. W.); Cave Ck. Cyn., Chiricahua Mts., Herb Martyr Dam, 1,768 m (Hespenheide, H. A.); Cave Ck. Cyn., Chiricahua Mts., Sunny Flat, 1,554 m (Hespenheide, H. A.); Cave Creek Ranch, Chiricahua Mtns., 1,525 m (Wallace, G. E.); Cave Creek, Chiricahua Mts., 1,675 m (Kusche, J. A.); Chiricahua Mtns. (Knull, D. J.; Knull, J. N.); Chiricahua Mtns., 6 mi SE Camp Rucker (MacKay, W.); Chiricahua Mtns., Portal, 1,450 m (c.u.); Chiricahua Mtns., SWRS, 8 km W Portal, 1,650 m (Fisher, B. L.); Chiricahua Mtns., Tex Canyon, 14 km W Jct. Rt. 80 on FSR74, 1,615 m (Ward, P. S.); Chiricahua Mtns., Tex Canyon, 8.6 mi W Jct. Rt. 80 on FSR 74, 1615 m (Saux, C.); Chiricahua National Monument Cpgrd., 1,645 m (Creighton, W. S.); Cochise Stronghold, Dragoon [as 'Dragon'] Mtns. (O'Brien, C. W.); Cochise Stronghold, Dragoon Mtns., 1,585 m (Creighton, W. S.); Coronado Peak, 2,020 m (Ward, P. S.); Cottonwood Canyon, Peloncillo Mtns., 1,465 m (Creighton, W. S.); Garden Canyon, Huachuca Mtns., 1,770 m (Creighton, W. S.); Garden Canyon, Huachuca Mtns., 1,770 m (Creighton, W. S.); Huachuca Mtns. (c.u.); Huachuca Mtns. [as 'Huachuca M.'] (Knull, J. N.); Miller Canyon, Huachuca Mtns. (Creighton, W. S.); Paradise, Chiricahua Mts., 1,675 m (Kusche, J. A.); Portal (Alpert, G.); Portal (Raske, A. G.); Portal Mtn. (Nelson, J. W.); Portal, Cave Creek Ranch (Forister, G. W.); Ramsey Canyon [based on coordinates; no locality name cited], 1,700 m (Irwin; et al.); San Simon Rd., 4 mi NNW Portal, 1,400 m (Hespenheide, H. A.); Southwest Research Station, 8 km W Portal, 1,800 m (Alpert, G. D.); Southwestern Research Station, 1,680 m (Ward, P. S.); SW Res. Sta., Portal (Ewart, W. H.); *Gila Co.*: 18 km NNE Globe, 1,500 m (Ward, P. S.); Globe (Nutting); Jones Water Recr. Area, 17.3 mi N Globe (Schlinger, E. I.); Parker Ranch, Sixshooter Cyn. (Leech, H. B.; Green, J. W.); *Graham Co.*: Noon Creek, Pinaleña Mtns. (O'Brien, C. W.); Pinaleno Mts. (c.u.); Pinaleno Mts. [as 'Graham Mts., 3500 to 4500 ft.'], 1,220 m (Bohart, R. M.); Post Canon, Pinaleno Mtns., 1,675 m (Wheeler, W. M.); *La Paz*: Colorado R., 1 mi S Ehrenberg (Smith, N. J.); Maricopa Co.: 0.5 mi N Pinnacle Peak, 745 m (Johnson, R. A.); *Mohave Co.*: Hualapai Mtns., s. of Kingman, 1,450 m (Schlinger, E.); *Pima Co.*: 3 km ESE Schuchuli (Aalbu, R. L.); Abra Wash, Growler Mtns., OCNM, 395 m (Creighton, W. S.); Alamo Cañon, Ajo Mtns., 670 m (Creighton, W. S.); Alamo Cañon, Ajo Mtns., 700 m (Creighton, W. S.); Alamo Cañon, Ajo Mtns., 760 m (Creighton, W. S.); Alamo Cañon, Ajo Mtns., 790 m (Creighton, W. S.); Brown Canyon, Baboquivari Mtns., 1,340 m (Creighton, W. S.); Forestry Cabin, Baboquivari Mtns., 1,065 m (Creighton, W. S.); Gates Pass, Tucson Mountain Park, 960 m (Ward, P. S.); Madera Canyon, Santa Rita Mts., 1,060 m (Schlinger, E. I.); Madera Cyn. (Nelson, G. H.); Organpipe (Melander, A. L.); Organpipe Cactus National Monument (Tinkham, E. R.); Sabino Basin, Sta. Catalina Mts. (c.u.); Sabino Cyn. (Vesterby, V. L.); San Miguel (Algert, E. D.); San Miguel (c.u.); Santa Rita Exp. Range (Rudgers, J. A.); Santa Rita Exp. Stn., nr. Green Valley, 1,360 m (Karban, R.); Sasabe (Oman); Tucson (Dietrich, A.; Dietrich, H.); Tucson (Knull, J.); *Pima Co. or Pinal Co.*: Santa Catalina Mts. (Crandall, R. H.); Sta Catalina Mts.

Downloaded from https://academic.oup.com/isd/article/6/1/4/6514767 by ThULB Jena user on 27 January 2022

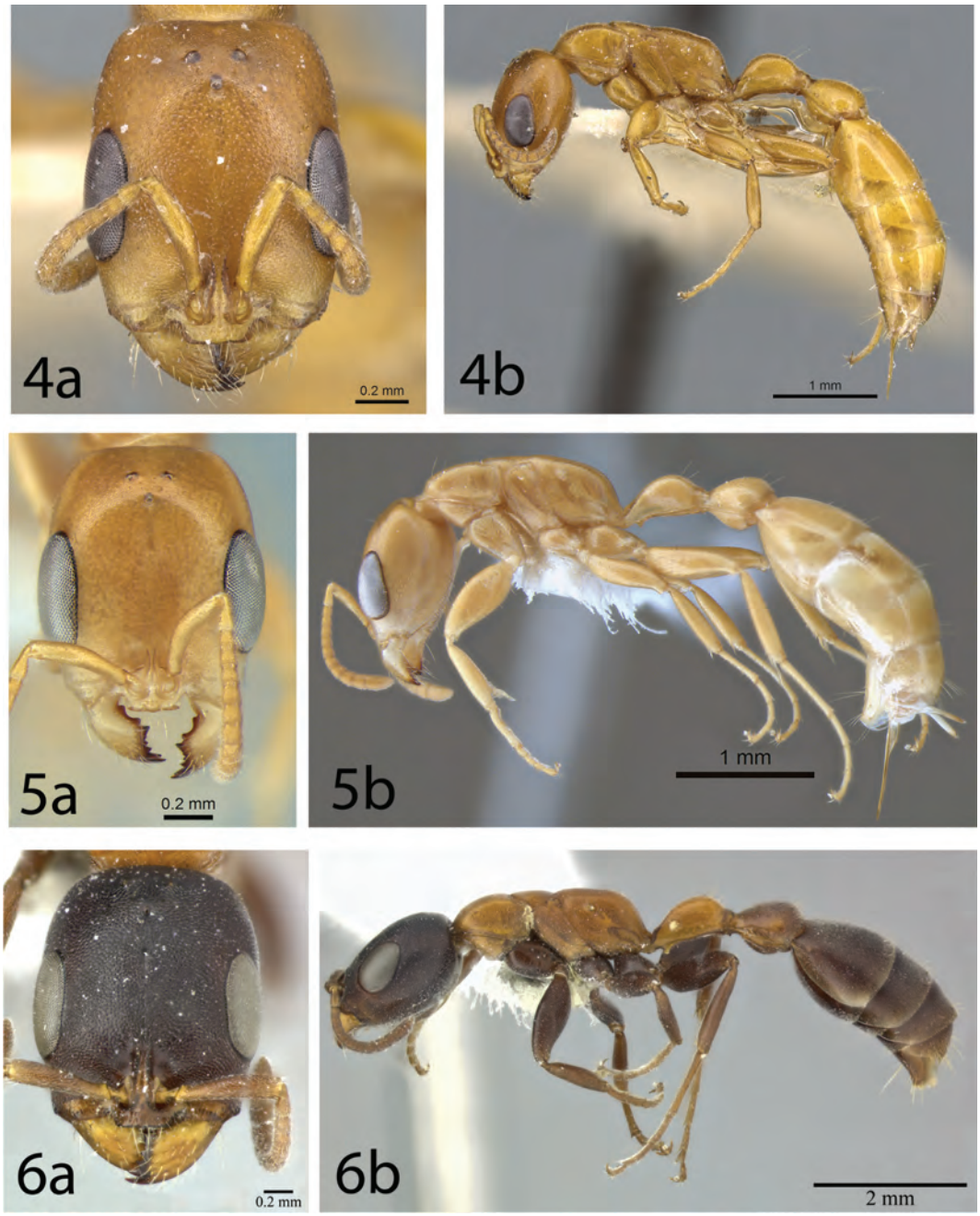

Fig. 4–6. *Pseudomyrmex elongatulus* group, workers, full-face dorsal view of head (a), and lateral profile of body (b). 4, *P. apache*, syntype, United States (CASENT0902872); 5, *P. arcanus*, holotype, Mexico (CASENT0863536); 6, *P. championi*, Mexico (CASENT0246349). Images from AntWeb (www.antweb.org); photographers Zach (Ziv) Lieberman (4), Phil Ward (5), Leah Benuska (6).

(Chrisman, M.); *Pima Co. or Santa Cruz Co.*: Catal Springs (Hubbard; Schwarz); Santa Rita Mtns. (Knull, J.); Santa Rita Mts. (Beamer, R. H.); Santa Rita Mts. (Bohart, R. M.); Santa Rita Mts. (Hubbard; Schwarz); *Pinal Co.*: 1.5 mi N Oak Flat Cpgrd., 1,235 m (Johnson, R. A.); 5 km NE Superior, 1,320 m (Ward, P. S.); *Santa Cruz Co.*: Canelo Pass, 1,615 m (Creighton, W. S.); Gooding Research Natural Area, Sycamore Canyon, 1,200 m (Ward, P. S.); Madera Canyon, Santa Rita Mtns. (Creighton, W. S.); Madera Cyn., 1,485 m (Kovac, C. R.); Madera Cyn., 1,485 m (Vesterby, V. L.); Madera Cyn. (Gilbert, A. J.; Smith, N. J.); Nogales (Burdine); Nogales (Knull, D. J.; Knull, J. N.); Pajarito Mtns., Sycamore Canyon, 1,220 m (Johnson, R. A.); Patagonia (Timberlake); Patagonia Mts., 2.6 mi W Harshaw (Leech, H. B.; Green, J. W.); Peña Blanca Springs, 1,130 m (Creighton, W. S.); Peña Blanca Springs (Byars, L. F.); Sweetwater, Santa Rita Mtns., 1,770 m (Creighton, W. S.); Sweetwater, Santa Rita Mtns., 1,830 m (Creighton, W. S.); Tumacacori Mtns. [as 'Tumacacori M.'] (Knull, D. J.; Knull, J. N.); Walker Canyon, vic. Pena Blanca (Gilbert, A. J.; Smith, N. J.); Washington Camp [as 'Camp Washington, Patagonia Mts.'] (c.u.); *Yavapai Co.*: Montezuma Castle, 977 m (Gadau, J. R.); *Yuma Co.*: Palm Cañon, Kofa Mtns., 670 m (Creighton, W. S.); Tacna (Hubbard, H. G.); ***California***: *Alameda Co.*: Cedar Mtn. Rancho, Los Mochos Scout Cmp. (Gagne, W. C.); *Butte Co.*: 6 km N Feather Falls (town), 600 m (Ward, P. S.); Magalia, 730 m (Ward, P. S.); *Colusa Co.*: 1 km W Fouts Springs, 600 m (Ward, P. S.); 3 km W Fouts Springs,

Downloaded from https://academic.oup.com/isd/article/6/1/4/6514767 by ThULB Jena user on 27 January 2022

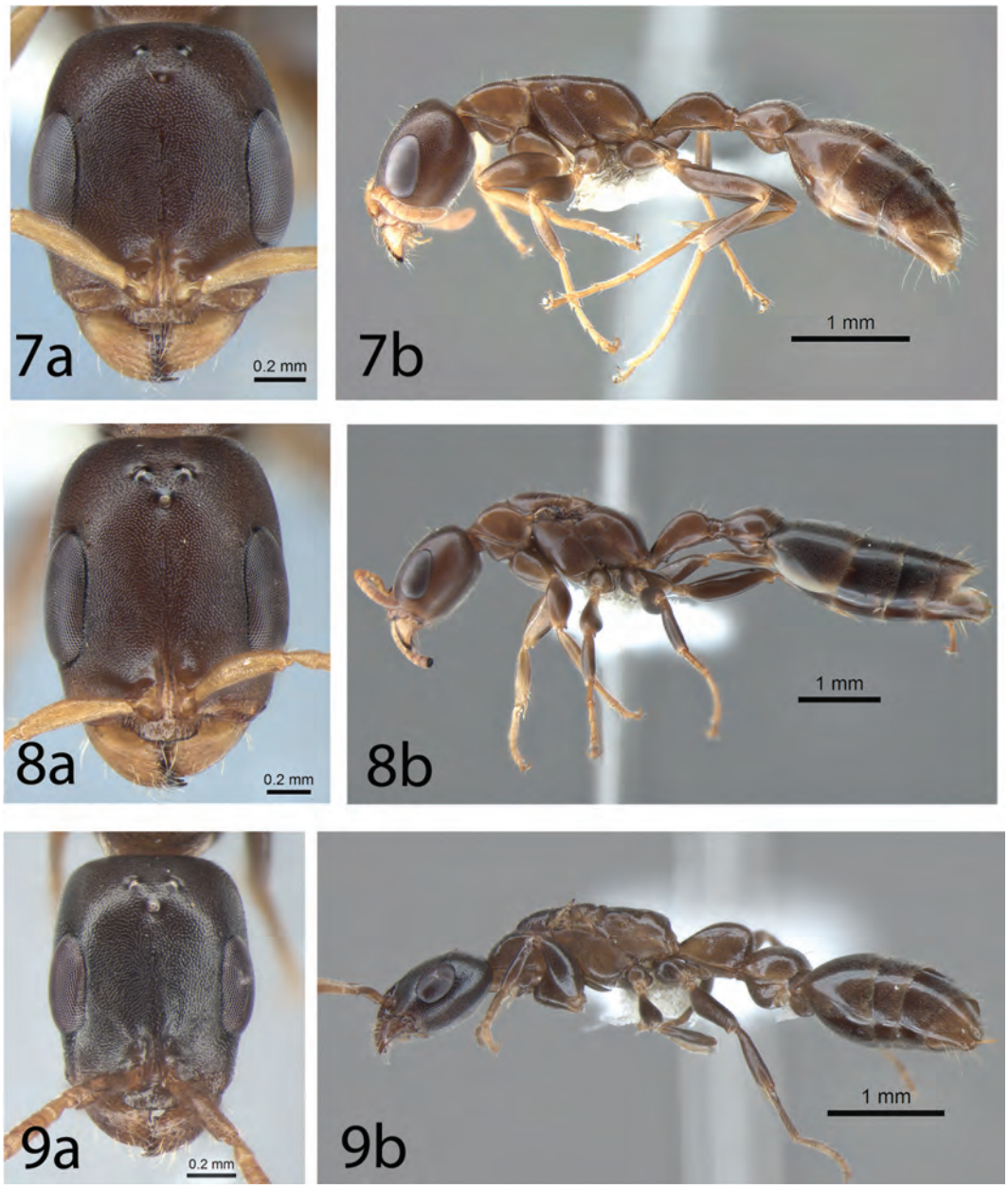

Fig. 7–9. *Pseudomyrmex elongatulus* group, workers and queens, full-face dorsal view of head (a), and lateral profile of body (b). 7, *P. cognatus*, holotype worker, Mexico (CASENT0863537); 8, *P. cognatus*, dealate queen, Mexico (CASENT0762787); 9, *P. comitator*, holotype queen, Mexico (JTLC000010310). Images from AntWeb (www.antweb.org); photographer Phil Ward.

1,125 m (Ward, P. S.); 4 mi E Leesville (Levin, D. P.); *Contra Costa Co.*: 2 km NW Mount Diablo, 650 m (Ward, P. S.); Arroyo del Cerro, Mount Diablo, 375 m (Ward, P. S.); Knobcone Point, Mt. Diablo SP, 550 m (Ward, P. S.); Long Ridge, Mount Diablo State Park, 560 m (Ward, P. S.); *El Dorado Co.*: 14 km NW Shingle Springs, 340 m (Ward, P. S.); 15 km ENE Georgetown, 960 m (Ward, P. S.); 2 km ENE Georgetown, 880 m (Ward, P. S.); 9 km SW Pilot Hill, 340 m (Ward, P. S.); *Fresno Co.*: Prather, 470 m (Clark, J.); *Glenn Co.*: Open Ridge, 4 km N St. John Mountain, 990 m (Ward, P. S.); S end, Black Butte Lake, 150 m (Ward, P. S.); S end, Black Butte Lake, 150 m (Wild, A. L.); *Imperial Co.*: Andrade (Johnson, B.); El Centro (Paddock); Holtville (Snelling, R. R.); Seeley (Pineda, L.); Winterhaven (c.u.); Winterhaven (Westcott, R. L.); *Lake Co.*: 14 km ESE Middletown, 240 m (Ward, P. S.); 20 km ESE Lower Lake, 575 m (Fisher, B. L.); 20 km ESE Lower Lake, 575 m (Ward, P. S.); Borax Lake (Westcott, E. L.); *Los Angeles Co.*: 1.8 km ENE Topanga, 370 m (Ward, P. S.); 3 mi N Mt. Baldy, San Gabriel Mtns., 1,585 m (Weidert, E.); Altadena (c.u.); Eaton Canyon Park (Thompson, M. E.); Foothill, Pasadena (Sturtevant, A. H.); Glendale (Schlinger, E. I.); Griffith Park (Nisson); Los Angeles [as 'Ls Angls'] (Coquillett); Pasadena (c.u.); Pasadena (Hamsher, C. A.); S. Gabriel Mtns., 7 mi N Mt. Baldy, 1,585 m (Weidert, E.); San Gabriel Canyon (Flock, R. A.); San Pedro (Peterson, D. L.); Sister Elsie Peak (c.u.); SW of Valyermo, San Gabriel Mtns., 1,435 m (Henné, C. A.); Tanbark Flat (Bechtel, R. C.); Tanbark Flat (Bohart, R. M.); Tanbark Flat (Lawrence, T.); Tanbark Flat (MacSwain, J. W.); Tanbark Flat (Williams, F. X.); *Los Angeles Co. or San Bernardino Co.*: Mtns. near Claremont (Baker); *Mariposa Co.*: Mariposa (c.u.); *Monterey Co.*: 15 km SW Jolon, Fort Hunter Liggett

Downloaded from https://academic.oup.com/isd/article/6/1/4/6514767 by ThULB Jena user on 27 January 2022

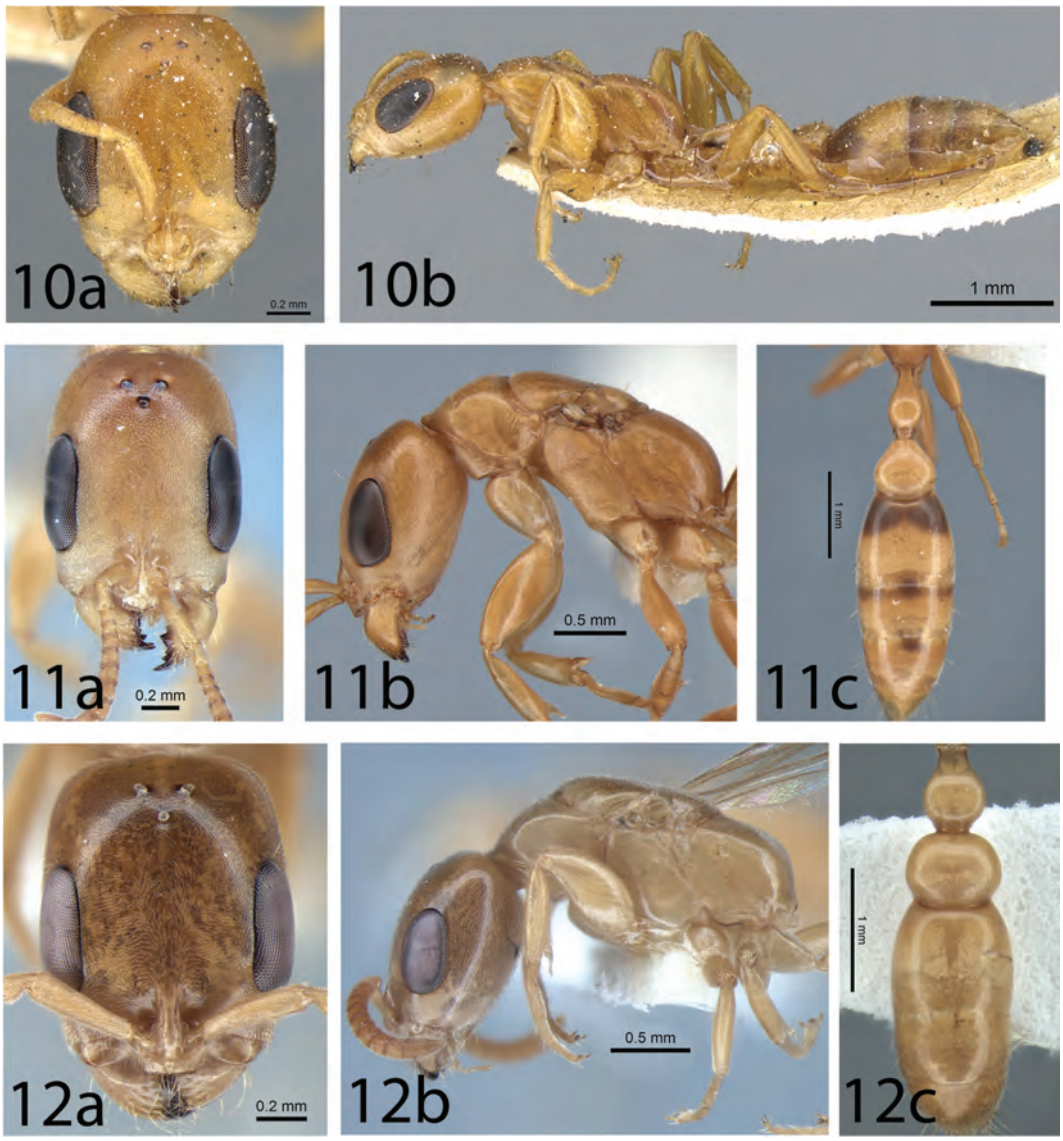

Fig. 10–12. *Pseudomyrmex elongatulus* group, workers and queens, full-face dorsal view of head (a), lateral profile of body (b), and dorsal view of petiole, postpetiole and gaster (c). 10, *P. elongatulus*, syntype worker, Mexico (CASENT0902874); 11, *P. elongatulus*, queen, Mexico (CASENT0762874); 12, *P. ereptor*, holotype queen, Mexico (CASENT0863524). Images from AntWeb (www.antweb.org); photographers Zach (Ziv) Lieberman (10), Phil Ward (11, 12).

MR, 490 m (Ward, P. S.); Hastings Res. (Shelford, V. E.); Indians Rd., Los Padres Natl. Forest, 720 m (Ward, P. S.); *Napa Co.*: 4 km E summit Mt. St. Helena, 450 m (Ward, P. S.); 5 km W Oakville, 560 m (Ward, P. S.); Bothe-Napa Valley St. Pk., 270 m (Ward, P. S.); Cedar Roughs, 10 km ESE Pope Valley, 610 m (Ward, P. S.); Mt. George, 8 km NE Napa, 320 m (Ward, P. S.); Mt. St. Helena (Buckett, J. S.); *Nevada Co.*: Empire Mine SHP, 780 m (Ward, P. S.); *Orange Co.*: Cleveland Nat. For., Chiguto Trail, below Blue Jay, 838 m (Strawn, A. J.); Irvine Park (Brown, K.); Laguna Beach (Culbertson); Limestone Canyon, El Toro Rd., 1.8 mi E Cooks Corner (Suarez, A. V.); Orange (Shanafelt, J. G.); Ortega Hwy, 4.3 mi NE Hwy 5 (Andersen, H.); San Clemente (Melander, A. L.); Santa Ana (McDonald, W.); Starr Ranch, 520 m (Ward, P. S.); Tonner Cyn. (MacKay, W. P.); Trabuco Cyn (Irwin, M. E.); Trabuco east (Eidert, E.); *Riverside Co.*: 6 mi S Valle Vista, Sec. 9, T.6S, R.1E, 716 m (Pinto, J.; Frommer, S.); Ag Ops citrus orchard, Riverside (c.u.); Blythe (Hardman, R. M.); Blythe (Van Duzee, E. P.); Cactus Spring Trail, between Hwy. 74 & Horsethief Cr., Deep Canyon area (Frommer, S.); Deep Canyon (MacKay, W. P.); Dripping Springs, Agua Tibia Mtns., 455 m (Creighton, W. S.); Hwy. 243, San Jacinto Mts., 915 m (Burnett, J.; Wasbauer, M.); Keen Camp, San Jacinto Mtns. (Shanafelt, J. G.); Palms to Pines Hwy. (Ross, E. S.); Pinyon Flat [as 'Pinon Flat'], San Jacinto Mts (Macdonald, R. L.); Pinyon Flat [as 'Pinon Flat'], San Jacinto Mts (Ross, E. S.); Poppet Flats (Clark, G.); Riverside (Clancy, D.); Riverside (Hokke, Z.); Riverside (Schlinger, E. I.); Riverside (Timberlake); Santa Rosa Plat. Res. (PEET survey); The Gavilan (Timberlake); White Water [as 'Whitewater'] (Melander, A. L.); Winchester (Icenogle, W.); *San Benito Co.*: San Benito Mtn., 1,320 m (Ward, P. S.); *San Bernardino Co.*: 2 mi N Yucaipa (Smith, N.; Smith, E.); Deep Canyon ('E. D. W.'); Deep Canyon (Niilns, T. W.); Mtn. Home Canyon (Timberlake); nr. Cajon Pass (c.u.); Oak Glenn, 1,065 m (Smith, N.); Yucaipa (Harp, G.; Cronk, W.); Yucaipa (Harper, G.); *San Diego Co.*: 'San Diego Co.' (Van Duzee, E. P.); 5.2 mi NW Ramona, Hwy. 78 (Frommer, S.; et al.); 5.9 mi NE Ramona, Hwy. 78 (Frommer, S.; et al.); 7 mi S Jct. 76 & 395 (Musgrove, C. H.); Campo (c.u.); Chula Vista (Bonita Long), 90 m (Suarez, A. V.); Chula Vista (Terranova), 78 m (Suarez, A. V.); Elliott

Downloaded from https://academic.oup.com/isd/article/6/1/4/6514767 by ThULB Jena user on 27 January 2022

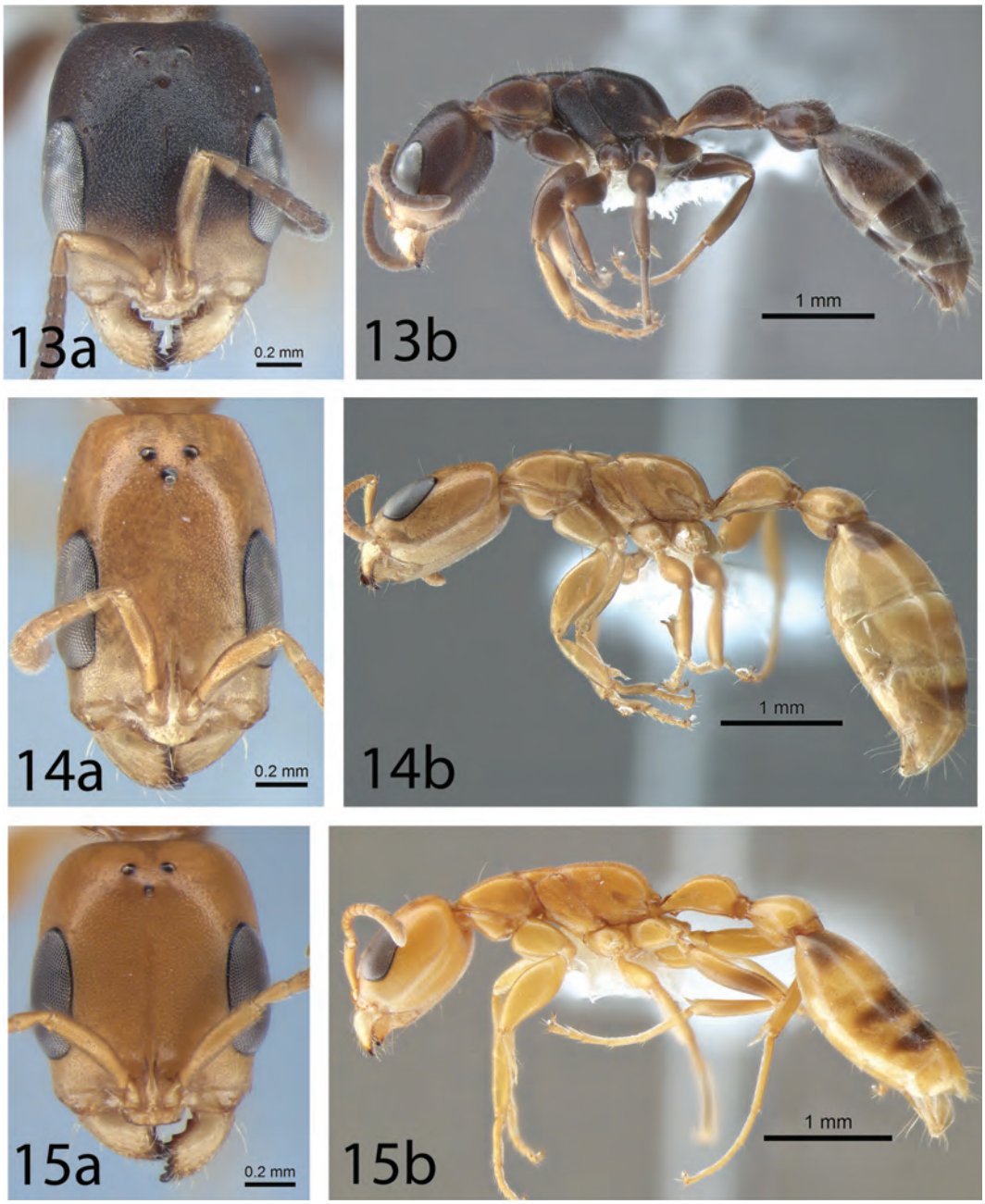

Fig. 13–15. *Pseudomyrmex elongatulus* group, workers, full-face dorsal view of head (a), and lateral profile of body (b). 13, *P. capillatus*, holotype, Mexico (CASENT0863535); 14, *P. exoratus*, holotype worker, Mexico (CASENT0863539); 15, *P. fasciatus*, holotype, Costa Rica (CASENT0863540). Images from AntWeb (www.antweb.org); photographer Phil Ward.

Reserve, 150 m (Suarez, A. V.); Elliott Reserve, 1 km E Miramar, 180 m (Ward, P. S.); Jacumba (Knull, D. J.; Knull, J. N.); La Jolla (Todd, E. L.); La Mesa (Mathers, R.); no specific locality (c.u. [Cook Colln.]); Pine Hills Lodge, 1,300 m (Wild, A. L.); Point Loma Naval Res. (Hawks; Bruyea); Poway (Sixtus; Bowers); San Diego (Blaisdell, F. E.); San Diego (Van Duzee, E. P.); Scripps Beach, La Jolla (Trepanier, M.); Torrey Pines S.P. (Trepanier, M.); Torrey Pines State Pk. (Faulkner; Brown); Torrey Pines State Reserve, 75 m (Carney, S. E.); Vista (Metcalf, H.); Witch Creek (Rude, P. A.); *San Luis Obispo Co.*: Cuesta Ridge, San Luis Obispo (Ball; Gilbert); La Panza Cp., 12 mi NE Pozo (Toschi, C. A.); Santa Lucia Range, 2 mi NW Cuesta Pass (Toschi, C. A.); Selby Campground, Carrizo Plain NM, 800 m (Ward, P. S.); *San Mateo Co.*: Jasper Ridge, 150 m (Ward, P. S.); *Santa Barbara Co.*: 1 km W Field Stn., Santa Cruz I., 240 m (Ward, P. S.); Can. del Medio, Santa Cruz I. (Schuster, R. O.; Toftner, E. C.); Cascada, Santa Cruz I., 110 m (Ward, P. S.); El Tigre Ridge, Santa Cruz I. (Waugaman, R. D.); N end Sedgwick Ranch, 610 m (Ward, P. S.); Ranger Peak, Los Padres N.F., 1,110 m (Ward, P. S.); Santa Cruz Island, Upper Maripro (Wetterer, J. K.); Santa Ynez Superstar Ranch (Schlinger, E. I.); Sedgwick Ranch, 740 m (Schlinger, E.); *Santa Clara Co.*: 'Santa Clara Co.' (c.u.); *Shasta Co.*: 1 km WNW Lamoine, 630 m (Ward, P. S.); *Solano Co.*: Cold Canyon, 300 m (Ward, P. S.); Cold Canyon, 420 m (Ward, P. S.); Cold Canyon, 600 m (Ward, P. S.); Cold Canyon, 19 km NNW Vacaville, 120 m (Ward, P. S.); Cold Canyon, 19 km NNW Vacaville, 95 m (Ward, P. S.); G. L. Stebbins Cold Canyon Reserve (French, L. D.); Pleasants Ridge, 18 km NNW Vacaville, 240 m (Ward,

Downloaded from https://academic.oup.com/isd/article/6/1/4/6514767 by ThULB Jena user on 27 January 2022

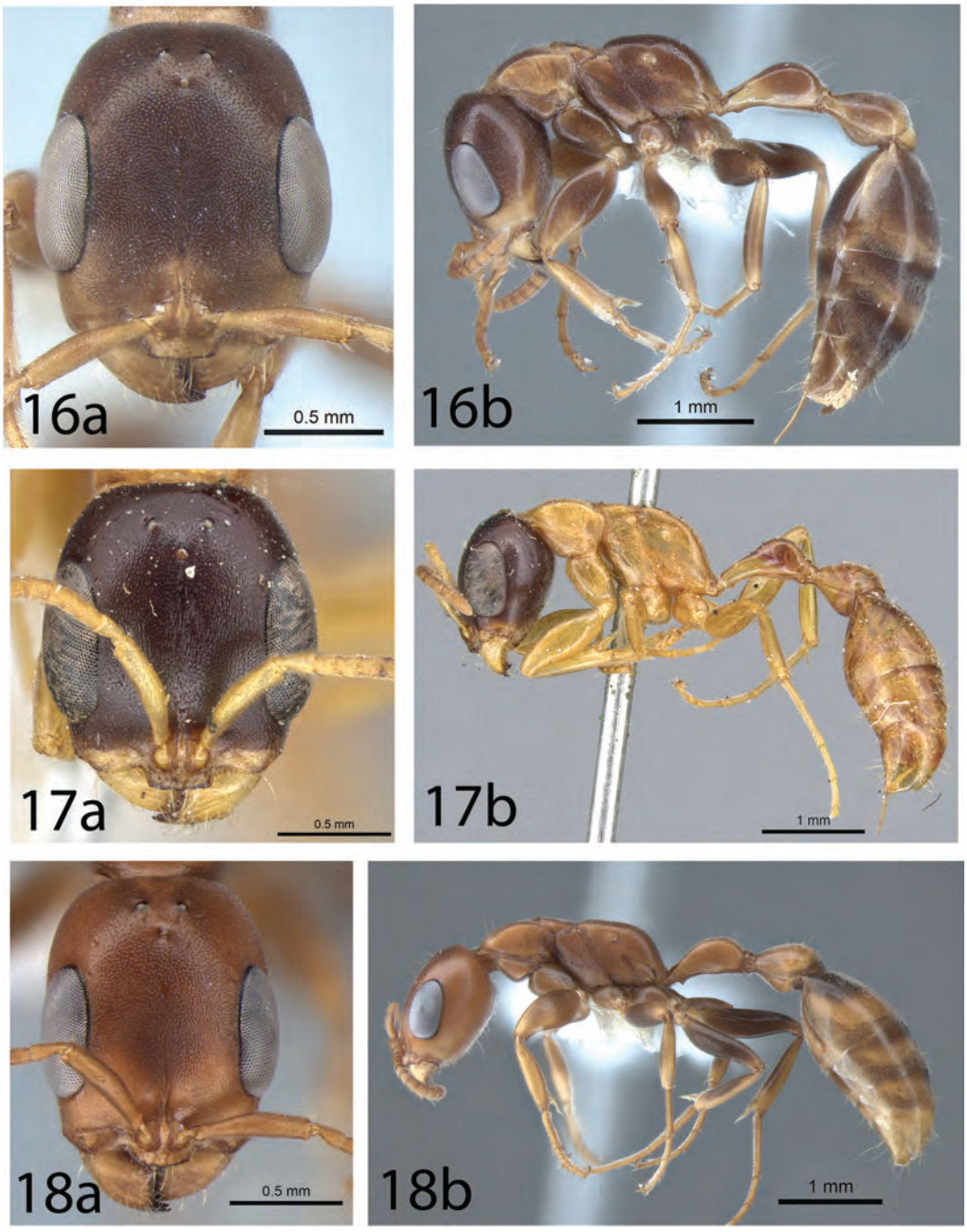

Fig. 16–18. *Pseudomyrmex elongatulus* group, workers, full-face dorsal view of head (a) and lateral profile of body (b). 16, *P. nimbus,* holotype, Costa Rica (CASENT0863541); 17, *P. salvini,* syntype, Mexico (CASENT0902879); 18, *P. veracruzensis,* holotype, Mexico (CASENT0863542). Images from AntWeb (www.antweb.org); photographers Phil Ward (16, 18), Zach (Ziv) Lieberman (17).

P. S.); *Sonoma Co.*: 2 km ENE Glen Ellen, 150 m (Ward, P. S.); 3 km NW Camp Meeker, 120 m (Ward, P. S.); 8 km NNW Cazadero, 300 m (Ward, P. S.); Annadel State Pk., 360 m (Ward, P. S.); Mt. Hood, 820 m (Ward, P. S.); Sugarloaf Ridge St. Pk., 640 m (Ward, P. S.); *Stanislaus Co.*: Del Puerto Canyon, 18 km WSW Patterson, 300 m (Ward, P. S.); *Sutter Co.*: 1 km W North Butte, Sutter Buttes, 200 m (Ward, P. S.); *Tehama Co.*: 26 km WSW Red Bluff, 240 m (Ward, P. S.); *Tulare Co.*: 15 km NE Three Rivers, 900 m (Ward, P. S.); 9 mi S Fairview (Rude, P.); Ash Mountain, Kaweah Power Station #3 (Hannel, M.); Ash Mtn., Kaweah Power Sta. #3 (Bezark, L. G.); Ash Mtn., Kaweah Power Sta. #3 (Burdick, D. J.); Ash Mtn., Kaweah Power Sta. #3 (Halstead, J. A.); Ash Mtn., Sequoia Natl. Pk., 915 m (Fitton, M. G.); Ash Mtn., Three Rivers (Haines, R. D.); Horse Creek Rd. (Brawner, O. L.); Strathmore (Snelling, R. R.); Three Rivers (Pierce, D.); Tulare (Snelling, R. R.); Visalia (Mankins, E. O.); *Tuolomne Co.*: Sonora (Addiego); *Ventura Co.*: Big Sycamore Cyn., Pt. Mugu St. Park (Nagano, C.); Matilija Crk., T5N, R24W, s. 22, 500 m (Longino, J.); Saticoy (Barrett, R. E.); *Yolo Co.*: 13 km W Rumsey, 650 m (Fisher, B. L.); 3 km NE Guinda, 410 m (Ward, P. S.); 4 km NW Rumsey, 150 m (Ward, P. S.); 6 km WNW Rumsey, 190 m (Ward, P. S.); Guinda, 150 m (Ward, P. S.); ***New Mexico***: *Dona Ana Co.*: La Cueva, Organ Mts. (c.u.); *Hidalgo Co.*: Deer Creek, Diamond A Ranch, 1,500 m (Andersen, A. N.); ***Texas***:

Downloaded from https://academic.oup.com/isd/article/6/1/4/6514767 by ThULB Jena user on 27 January 2022

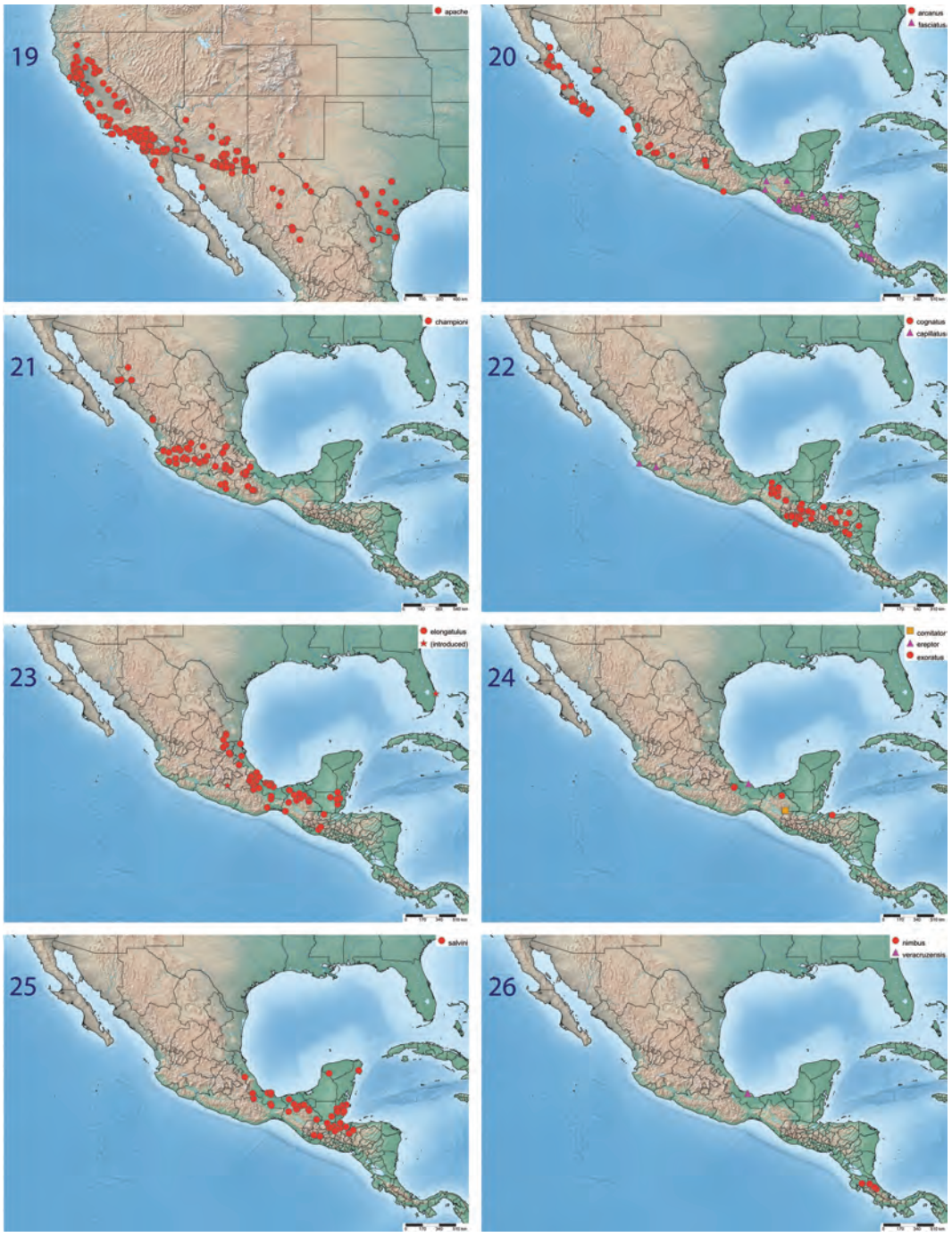

Fig. 19–26. *Pseudomyrmex elongatulus* group: distribution maps. 19, *P. apache*; 20, *P. arcanus* (circles), *P. fasciatus* (triangles); 21, *P. championi*; 22, *P. capillatus* (triangles), *P. cognatus* (circles); 23, *P. elongatulus* (circles), probable introduced populations (stars); 24, *P. comitator* (square), *P. ereptor* (triangle), *P. exoratus* (circles); 25, *P. salvini*; 26, *P. nimbus* (circles), *P. veracruzensis* (triangle).

Bexar Co.: San Antonio, 230 m (Ward, P. S.); San Antonio (Ward, P. S.); *Cameron Co.*: Esprza Rch., Brownsville (c.u.); *Duval Co.*: Freer (Rogers, R. R.); San Diego (c.u.); *Goliad Co.*: [no specific locality] (Mitchell, J. D.); *Hidalgo Co.*: Monte Alto, 20 m (Creighton, W. S.); *La Salle Co.*: Fowlerton, 90 m (Creighton, W. S.); *Maverick Co.*: El Indio [as 'El Indigo'] (Bixby, D. H.); *Presidio Co.*: Arsaca Canyon, Chinati Mtns., 1,465 m (Creighton, W. S.); Big Bend Ranch SP, Las Cruces Amarillas (Ubick, D.); *Real Co.*: Camp Wood (Ward, C. R.); *Starr Co.*: [no specific locality] (Knull, D. J.; Knull, J. N.); *Travis Co.*: Austin, 150 m (Ward, P. S.); Austin (Ward, P. S.); Austin, Zilker Park, Rollingwood Drive, 155 m (Wild, A. L.); *Uvalde Co.*: [no specific locality] (Knull, D. J.; Knull, J. N.); Uvalde (Bradley, J. C.).

Worker measurements (n = 17). HW 0.88–1.00, HL 1.08–1.21, MFC 0.039–0.066, LHT 0.77–0.87, CI 0.80–0.84, FCI 0.042–0.070, REL 0.40–0.44, REL2 0.48–0.53, FI 0.38–0.44, PLI 0.55–0.61, PWI 0.50–0.57, MSC 3–8.

Downloaded from https://academic.oup.com/isd/article/6/1/4/6514767 by ThULB Jena user on 27 January 2022

Worker Diagnosis. Medium-sized species (HW 0.88–1.00) with moderately elongate head (CI 0.80–0.84) (Fig. 4) and relatively short eyes (see REL and REL2 values); frontal carinae separated by about basal scape width or slightly less; metanotal groove present but weakly impressed; in profile, dorsal face of propodeum almost flat and more or less differentiated from declivitous face, rounding into the latter, and the two faces subequal in length; petiole relatively short and high (PLI 0.55–0.61, PL/HL 0.48–0.54), with a slight anterior peduncle; profemur slender; hind leg relatively short (LHT/HL 0.69–0.73). Head subopaque, densely punctulate-coriarious. Standing pilosity sparse, absent from propodeum and (nearly always) the mesonotum (MSC 3–8). Uniformly light yellow- to orange-brown, the tip of gaster usually infuscated.

Comments. *P. apache* is closely related to *P. championi*, and our UCE phylogeny recovers it nested phylogenetically within that species (Fig. 1). The main distinction between the two taxa rests on body color: workers of *P. apache* are concolorous yellow- or orange-brown, whereas those of *P. championi* are bicolored with at least the gaster and hind leg dark brown and contrasting with the lighter orange-brown mesosoma (other body parts are usually dark brown but in some individuals they are concolorous with the mesosoma). The distinction is a slight one, but where the two species are geographically adjacent to one another in Sonora and Chihuahua (Figs. 19 and 21) the color differences appear to be sustained. For the moment, we treat *P. apache* as a distinct species, presumably recently derived from *P. championi*, in a daughter and parent relationship that renders *P. championi* paraphyletic at most loci. Nevertheless, further study of populations in northwest Mexico is desirable; it might reveal evidence of gene flow between the two taxa. *P. apache* can also be confused with *P. arcanus*, a more distantly related species in the *P. elongatulus* group, whose workers are similarly colored (light yellow- to orange-brown) but have more elongate eyes and a more gently rounded propodeum and petiole (see under *P. arcanus* for more discussion).

Distribution and Biology. *Pseudomyrmex apache* occurs widely across the southwestern United States from northern California to east Texas, and south into adjacent northern Mexico (Fig. 19). This species inhabits a variety of xeric habitats, including chaparral, coastal sage scrub, mesquite scrub, oak woodland, and oak-pine-juniper woodland, nesting in dead branches of various woody plants, especially *Arctostaphylos*, *Baccharis*, *Prosopis*, and *Quercus*. Colonies are polydomous—occupying multiple dead branches within a tree or shrub—and they contain one to several inseminated queens (Ward 1985). For locality records with elevation, the range is 20 m to 2,020 m (mean 905 m; $n = 145$). In addition to the examined material listed above, we have seen one old worker labeled as coming from Washington, DC. (24 Aug 1919, leg. B. P. Currie) (USNM). We judge this to be either mislabeled or representing an accidental introduction.

Pseudomyrmex arcanus sp. nov.

Figs. 5 and 20

Zoobank LSID: urn:lsid:zoobank.org:act:5CA6B80D-C6DA-47A1-82AD-1721A990214F

Pseudomyrmex apache; Ward 1985: 231 (part).

Pseudomyrmex psw053; Chomicki et al. 2015: 4. Placement in molecular phylogeny.

Holotype Worker. MEXICO Michoacán: 20 km S Uruapán, 880 m, 19° 14′ N 102° 03′ W, 28 Dec 1987, ex dead twig of vine, tropical dry forest, P. S. Ward PSW09293 (UNAM) (CASENT0863536). Paratypes: series of workers, same data as holotype (CASC, CZUG, IEXA, MCZC, PSWC, UCDC, USNM).

Other material examined (CASC, JTLC, LACM, MCZC, PSWC, RAJC, SEMC, UCDC, USNM).

Mexico, ***Baja California***: 19 km E El Arco, 400 m (Suarez, A. V.); 25 mi N El Arco (Ewart, W. H.); Palm Cyn., Angel de la Guardia Is. (Van Duzee, E. P.); ***Baja California Sur***: 1 km NE La Burrera, 500 m (Ward, P. S.); 12 mi S Guillermo Prieto (Wasbauer, M.); 13 mi SW Guillermo Prieto (Phelps, B.; Phelps, M.); 19 mi SE El Cien (Andrews, F.; Faulkner, D.); 2 km WSW Todos Santos, 5 m (Ward, P. S.); 2.5 mi S Hwy.1 on rd. to Pta Agua Verde, 325 m (Johnson, R. A.); 2.7 mi SE Valle Perdido (c.u. [Snelling?]); 28–29 km N Todos Santos, 275 m (Fisher, E.; Westcott, R.); 4.8 km N San Ignacio (Savary, W. E.; Mullinex, C. L.); 59 mi SE Guerrero Negro (Andrews, F.; Faulkner, D.); 7 mi NW Santa Rosalia, 260 m (Snelling, R. R.); 72 mi NW La Paz, 30 m (Snelling, R. R.); Bahia de Los Frailes (Ira LaRivers); Las Barracas (DeBach, P.); Playa Los Cerritos (Andrews, F.; Faulkner, D.); San Domingo (Ross; Bohart); San Jose del Cabo (c.u.); Triunfo (Michelbacher; Ross); Venancio (Michelbacher; Ross); ***Colima***: 13 mi NE Comala, El Jabali (Ballmer, G.); 16 km NNE Comala, 1,280 m (Ward, P. S.); ***Jalisco***: 20 mi W of Tecolotlán (Lipovsky, L. J.); 39 km N Colima, 970 m (MacKay, W. P.); Est. Biología Chamela, 100 m (Ward, P. S.); Mun. Zapotiltic, 24 km S Cd. Guzman, 1,095 m (MacDougal, J.); Tecolotlan (Villegas, B.); ***Michoacán***: 20 km S Uruapán, 880 m (Ward, P. S.); ***Morelos***: 7.3 mi S Yautepec, 1,066 m (Carney, L. B.); ***Nayarit***: 13.9 mi E San Blas (Janzen, D. H.); 19.3 km S Rosamorada, 30 m (MacKay, W. P.); Isla Tres Marias, Maria Madre Id. Village (Keifer, H. H.); ***Oaxaca***: Juquila, San Juan Mixtepec, 36 km W Puerto Escondido, 23 m (Kautz, S.); ***Puebla***: 3 km SW El Salado, 850 m (da Silva, P.G.; Eager, T.); ***Sinaloa***: 1 km NNE Chupaderos, Hwy 40, 400 m (Ward, P. S.); 23.5 mi SW El Palmito, mi 1704.8 (Janzen, D. H.); 4.2 mi S Villa Union on Hwy. 15 (Janzen, D. H.); 5 km E Concordia, 50 m (Ward, P. S.); ***Sonora***: Rancho El Palmarito, 23 km E Alamos, 470 m (Irwin, M. E.); La Quintera (Timberlake).

Worker measurements (n = 17). HW 0.82–0.97, HL 0.99–1.19, MFC 0.030–0.052, LHT 0.69–0.85, CI 0.80–0.85, FCI 0.036–0.055, REL 0.42–0.47, REL2 0.52–0.58, FI 0.42–0.46, PLI 0.49–0.57, PWI 0.45–0.55, MSC 2–5.

Worker Diagnosis. Small to medium-sized species (HW 0.82–0.97) with moderately elongate head (CI 0.80–0.85) and eyes (see REL and REL2 values); frontal carinae separated by less than basal scape width; metanotal groove present but weakly impressed; in profile, dorsal face of propodeum rounding obtusely into declivitous face, the two faces subequal in length; petiole relatively slender (PLI 0.49–0.57, PL/HL 0.50–0.56), in profile the convex anterodorsal face of petiole ascending gradually to summit in the posterior half of node, then rounding into more rapidly descending posterior face (Fig. 5); profemur slender; hind leg relatively short (LHT/HL 0.68–0.72). Head sublucid, densely punctulate-coriarious to coriarious-imbricate. Standing pilosity sparse, absent from propodeum and mesonotum (MSC 2–5). Uniformly light yellow-brown to orange-brown.

Comments. This species is characterized by a combination of light yellow-orange coloration, without additional maculation; moderately elongate eyes; weakly impressed metanotal groove (in the

Downloaded from https://academic.oup.com/isd/article/6/1/4/6514767 by ThULB Jena user on 27 January 2022

worker); and slender petiole. The workers of *P. arcanus* can be distinguished from those of other orange-yellow species in the *P. elongatulus* group as follows. *Pseudomyrmex elongatulus* has a better-developed metanotal groove, more elongate eyes (REL 0.47–0.53), petiole (PL/HL 0.57–0.61) and legs (LHT/HL 0.74–0.79), and some degree of infuscation on the gaster. *Pseudomyrmex exoratus* has a much more elongate head (CI 0.67–0.69) and a robust profemur (FI 0.46–0.49). *Pseudomyrmex fasciatus* essentially lacks a metanotal groove (as seen in in profile) and has conspicuous transverse maculation on the gaster. *Pseudomyrmex apache* has shorter eyes (on average), a more angular propodeum, and a more robust petiole, and the tip of the gaster is frequently darkened. Although they are not one another's closest relatives (Fig. 1), *P. apache* and *P. arcanus* can be difficult to distinguish, the differences in propodeal and petiole shape being rather subtle. Bivariate plots of some measurements reveal two separate clouds of points (Fig. 3), but increased samples sizes might show some overlap.

In our UCE phylogeny there is an early diverging sample of *P. arcanus* (D1228) that is sister to all others (Fig. 1; Supp Fig. 4 [online only]). This is a southern outlier, from Oaxaca (Supp Table 2 [online only]), but we do not treat this as a separate species because 1) it is phenotypically similar to other samples of *P. arcanus*, 2) it is allopatric to the other populations, and 3) there are geographically intermediate populations from southern Mexico (Fig. 20) which we did not have an opportunity to sequence. More intensive sampling of such southern populations could be expected to reveal a paraphyletic series at the base of the *P. arcanus* tree, for which excisement of D1228 would be arbitrary and ill-founded.

Distribution and Biology. This species is found at low to medium elevations in western Mexico, from Baja California to Oaxaca. Recorded elevations vary from 5 m to 1,280 m (mean 474 m; n = 19). Habitats in which *P. arcanus* has been collected include coastal sand dunes, pasture, tropical dry forest, and mixed tropical/temperate mesic forest. Nests have been taken in a dead stalk of a woody Asteraceae (*?Viguiera*), dead stem of *Cassia*, dead twig of thorny vine, dead twig of vine, and dead twigs of unidentified woody plants. The records of '*Pseudomyrmex apache*' cited in Ward (1985: 231) from Baja California refer to this species.

***Pseudomyrmex capillatus* sp. nov.**
Figs. 13 and 22
Zoobank LSID: urn:lsid:zoobank.org:act:B01C7CB2-8ACA-47D3-AE4D-E4C4F4997F13

Pseudomyrmex undescribed species (*elongatulus* group); Ward 2017: 528. In key.

Holotype Worker. MEXICO Jalisco: Est. Biología Chamela, 100 m, 19° 30′ N 105° 02′ W, 18 Dec 1987, ex dead twig of thorny vine, tropical dry forest, P. S. Ward PSW09248 (UNAM) (CASENT0863535). Paratypes: series of workers, same data as holotype (CASC, CZUG, IEXA, MCZC, PSWC, UCDC, USNM).

Other material examined (EBCC, LACM, PSWC, UCDC).
Mexico: *Colima*: Rio Tuxpan, 18 mi E Colima, 365 m (Dixon, J.; Heyer, R.); ***Jalisco***: Chamela (Rodríguez, A.); Est. Biol. Chamela [as 'Búho'] (c.u.); Est. Biol. UNAM 'Chamela' (Feener, D. H.); Est. Biología Chamela, 100 m (Ward, P. S.).

Worker measurements (n = 6). HW 0.99–1.07, HL 1.18–1.32, MFC 0.040–0.058, LHT 0.83–0.92, CI 0.81–0.84, FCI 0.040–0.054, REL 0.44–0.46, REL2 0.54–0.55, FI 0.41–0.46, PLI 0.54–0.57, PWI 0.47–0.51, MSC 25–39.

Worker Diagnosis. Medium-sized species (HW 0.99–1.07) with moderately elongate head (CI 0.81–0.84) and eyes (see REL and REL2 values); frontal carinae separated by slightly less than basal scape width; metanotal groove distinctly impressed; dorsal face of propodeum flat, elevated anteriorly above level of mesonotum, rounding into declivitous face, the two faces subequal in length; petiole relatively slender (PLI 0.54–0.57, PL/HL 0.54–0.56), in profile petiole with a slight anterior peduncle and with flat to convex anterodorsal face, ascending gradually to summit in the posterior half of node, then rounding into more rapidly descending posterior face; profemur slender; hind leg relatively short (LHT/HL 0.70–0.72). Head opaque, densely coriarious to coriarious-imbricate, punctulae very fine and inconspicuous. Standing pilosity common on head, mesosoma (including mesonotum and propodeum), petiole, postpetiole, and gaster (MSC 25–39, HTC 0, MTC 1–2). Body rather uniformly dark-brown, except scapes, mandibles, anterior quarter of head capsule, protibia, and protarsus, which are a contrasting light yellowish-brown.

Comments. This species is notable for the conspicuous standing pilosity that covers the entire mesosoma dorsum (Fig. 13). Such pilosity is generally restricted to 1–3 pairs of setae on the worker pronotum in other members of the *P. elongatulus* group. Other salient features of the *P. capillatus* worker are the densely sculptured and opaque head, raised dorsal face of the propodeum, and unique color pattern (see Worker Diagnosis). Surprisingly, our UCE analyses show *P. capillatus* to be embedded phylogenetically within *P. arcanus* (Fig. 1), although the two are superficially quite different in appearance. Both species occur sympatrically at Estación Biología Chamela, the type locality of *P. capillatus*, but the Chamela sample of *P. arcanus* (D1651) is not sister to the two *P. capillatus* samples. This suggests that *P. arcanus*, the more widespread of the two species, is in the process of achieving allelic monophyly relative to *P. capillatus*, but that this has not yet gone to completion.

Distribution and Biology. Pseudomyrmex capillatus is thus far known only from Jalisco and Colima in western Mexico. In tropical dry forest at Estación Biología Chamela two nest series were collected by P.S.W., both in dead twigs of vines (the vines were 1 m apart, so the nests were likely part of a single colony), and a worker was collected foraging on low vegetation. Recorded elevations are 100 m and 365 m.

***Pseudomyrmex championi* (Forel)**
Figs. 6 and 21

Pseudomyrma championi Forel 1899: 96. Syntype worker, Amula, 6000 ft., Guerrero, Mexico (H. H. Smith) (BMNH) [examined].
Pseudomyrma leonhardi Stitz 1937: 132. Two syntype workers, Guerrero, Mexico (L. Schultze) (ZMHB) [examined]. Synonymy by Kempf 1961: 391.
Pseudomyrmex championi (Forel); Wheeler and Wheeler 1956: 382. Combination in *Pseudomyrmex*.
Pseudomyrmex championi (Forel); Kempf 1961: 391-393 (in part).

Other material examined (AMNH, CASC, CUIC, CZUG, EMEC, IEXA, JTLC, KWJC, LACM, MCZC, MHNG, MNHN, MSNG, MZSP, OSAC, PSWC, SEMC, UCDC, UCRC, USNM).
Mexico: *Chihuahua*: 6.5 km NW Batopilas, 1,550 m (Ward, P. S.); Mpio. Ocampo, 16 k E Basaseachic (Mackay, W.; Mackay, E.);

Downloaded from https://academic.oup.com/isd/article/6/1/4/6514767 by ThULB Jena user on 27 January 2022

Ciudad de México: Cd. de México, Jardín Botánico UNAM, 2,344 m (Dubovikoff); ***Colima***: 16 km NNE Comala, 1,280 m (Ward, P. S.); ***Guanajuato***: 5 mi S Salvatierra (Schlinger, E. I.); Guanajuato [as 'Guanaxuato'] (Dugès, E.); ***Guerrero***: Xucumanatlan, 2,135 m (Smith, H. H.); ***Hidalgo***: 11 mi W Jct. 45 & 85, 1,980 m (Scullen; Bolinger); 8 mi NE Jacala (Fisher, E. M.); 8 mi SW Jacala, 1,645 m (Snelling, R. R.); ***Jalisco***: [no specific locality] (Krauss, N. L. H.); 1 km S El Fresnito (Rifkind, J.); 10 km S Autlán, 1,600 m (Ward, P. S.); 4 mi W Mazamitla, 2,070 m (Smith, R. F.); 7 mi S Manzamitla (Leech, H. B.); Guadalajara (c.u.); Lagos de Moreno, Sta. Rosa, 1,900 m (Vásquez, M.); Mascota, El Atajo, km. 15 camino a San Sebastian del O., 1,200 m (Vásquez, M.); Mixtlán, Cerro Chato, Carr. Ameca-Mascota, km. 48, 1,780 m (Vásquez, M.); Mun. Autlán de Navarro, SSE Autlán, 1,435 m (MacDougal, J.); San Ignacio, Cerro Gordo, 2,200 m (Navarrete, J. L.); Tepatitlán, carretera a Arandas, 1,950 m (Vásquez, M.); Tequila, Volcán de Tequila, 1,435 m (Pérez, D.); Zapopan, Santa Lucia, 1,642 m (Vásquez, M.); ***México***: Valle de Bravo (Parker, F. D.); ***Michoacán***: 12.3 mi E Morelia, 2,165 m (Snelling, R. R.); 15–20 mi W Jiquilpan (Leech, H. B.); 3 mi E Carapan (Parker, F. D.; Stange, L. A.); 8 km E Quiroga, 2,285 m (Evans, H. E.); Cotija (Villegas, B.); Morelia (Krauss, N. L. H.); Pátzcuaro [as 'Patzquero'] (Lipovsky, L. J.); ***Morelos***: Chamilpa, 1,850 m (Quiroz, L.); Cuernavaca (Krauss, N. L. H.); Cuernavaca (Lipovsky, L. J.); Sto. Domingo, 1,900 m (Quiroz, L.); Tepotzlán (Olson, D. M.); Tlacotepec, Mpio. Zacualpan (Alemán, G.); Tlalnepantla, 2,030 m (Alemán, G.); Tres Marias [as 'Tres Maria'] (Pereira, P.); Zacualpan, 1,730 m (Alemán, G.); ***Oaxaca***: 12 mi SE Oaxaca, 1,630 m (Scullen; Bolinger); 5 mi SE Oaxaca, 1,875 m (Scullen; Bolinger); 9 mi SE Nochistlan (Janzen, D. H.); Monte Alban (Malkin, B.); Monte Alban (Vaurie, P.; Vaurie, C.); Oaxaca (Malkin, B.); ***Puebla***: Cacaloapan (Parker, F. D.); km. 275, Hwy. 150, NE of Chapulco (Cornell Univ. Mexico Field Party); Tehuacán (Janzen, D. H.); ***Sinaloa***: 1.6 km NNE El Palmito, 2,130 m (Ward, P. S.); 6 mi NE Potrerillos (Parker, F. D.; Stange, L. A.); Potrerillos (Schlinger, E.); ***Sonora***: La Quintera (Timberlake); Santa Barbara, near Alamos, 1,450 m (Franklin, K. A.); ***Veracruz***: Acultzingo nr. Orizaba (Janzen, D. H.); Huatusco (Quiroz, L.).

Worker measurements (n = 13). HW 0.82–1.05, HL 1.02–1.28, MFC 0.033–0.069, LHT 0.71–0.91, CI 0.80–0.87, FCI 0.040–0.071, REL 0.38–0.44, REL2 0.46–0.55, FI 0.39–0.44, PLI 0.49–0.57, PWI 0.46–0.54, MSC 4–8.

Worker Diagnosis. Small to medium-sized species (HW 0.82–1.05) with moderately elongate head (CI 0.80–0.87) (Fig. 6) and relatively short eyes (see REL and REL2 values); frontal carinae separated by about basal scape width or less; metanotal groove present but weakly impressed; in profile, dorsal face of propodeum generally flat and more or less differentiated from declivitous face, rounding into the latter, and the two faces subequal in length; petiole moderately slender (PLI 0.49–0.57, PL/HL 0.52–0.56); in profile petiole with slight or no anterior peduncle, the anterodorsal face flat to convex, ascending gradually to summit in posterior half of node, then rounding into more steeply descending posterior face; profemur slender; hind leg relatively short (LHT/HL 0.69–0.75). Head opaque to subopaque, densely punctulate-coriarious, the punctulae on vertex usually separated by less than their diameters (but separated by more than their diameters in some populations, and the vertex correspondingly shinier). Standing pilosity sparse, absent from propodeum and mesonotum (MSC 4–8). Gaster, metacoxa, metafemur and metatibia dark brown, contrasting with light orange-brown mesosoma; head, first and second pairs of legs, petiole, and postpetiole varying from dark brown (usually) to much lighter and concolorous with mesosoma.

Comments. The worker of this species is characterized by having a light-colored (orange-brown) mesosoma and contrasting dark gaster and hind leg. The head, other legs, petiole, and postpetiole also tend to be strongly infuscated, but in some samples (from Colima, Jalisco, and Chihuahua) they are lighter colored and even concolorous with the mesosoma. Workers of the closely related *P. apache* are uniformly orange-brown in color; see further discussion under that species. *Pseudomyrmex championi* has been confused with dark brown workers of a more distantly related species, *P. cognatus*, which occurs from southern Mexico to Nicaragua. The supposed descriptions of the larva (Wheeler and Bailey 1920, Wheeler and Wheeler 1956) and queen (Kempf 1961) of *P. championi* actually refer to *P. cognatus*. Workers of the two taxa can be distinguished as follows: *P. championi* is conspicuously bicolored, the dark gaster contrasting with the light orange-brown mesosoma, whereas *P. cognatus* is more uniformly dark brownish-black, with the mesosoma at most moderately lighter (and often dark on top); the metanotal groove is better developed (but still slight) in *P. championi* compared to *P. cognatus*; and the eye is generally shorter in *P. championi* than *P. cognatus* (REL 0.38–0.44 vs 0.43–0.48). The geographical distributions of *P. championi* and *P. cognatus* do not overlap (Figs. 21 and 22) but because they belong to different species complexes in the *P. elongatulus* group (Fig. 1), they cannot be treated as allopatric variants of the same species. Their similarities must reflect convergence or shared ancestral features.

Distribution and Biology. *Pseudomyrmex championi* occurs in the Sierra Madre Occidental, Sierra Madre del Sur, and the intervening Transmexican Volcanic Belt (Fig. 21). Collection labels with habitat and/or elevation information document the occurrence of this species in oak woodland, oak-pine forest, old field/pasture, mixed tropical/temperate mesic forest, mid-montane dry forest, and yucca desert, at elevations ranging from 1,200 m to 2,344 m (mean 1,828 m; *n* = 28). Four nests of *P. championi* encountered by one of us (P.S.W.) were all from dead twigs of woody shrubs (one Asteraceae, one Verbenaceae, and two unidentified plants).

Pseudomyrmex cognatus sp. nov.

Figs. 7, 8 and 22

Zoobank LSID: urn:lsid:zoobank.org:act:A7ABFF2F-818B-4FE9-B143-380786E61C48

Pseudomyrma championi; Wheeler and Bailey 1920: 260. Description of larva (misidentified as *P. championi*).

Pseudomyrmex championi; Wheeler and Wheeler 1956: 382. Description of larva (misidentified as *P. championi*).

Pseudomyrmex championi; Kempf 1961: 392. Description of queen (misidentified as *P. championi*).

Pseudomyrmex championi; Chomicki et al. 2015: 4. Placement in molecular phylogeny (misidentified as *P. championi*).

Pseudomyrmex psw159; Ward 2017: 533. Comparison with *Pseudomyrmex feralis*.

Holotype Worker. MEXICO Chiapas: Tziscao, Lagos de Montebello, 1,500 m, 16° 05′ N 91° 41′ W, 21 Dec 1991, ex dead twig of vine, mixed tropical/temperate mesic forest, P. S. Ward PSW11560 (UNAM) (CASENT0863537). Paratypes: series of workers, 1 dealate queen, same data as holotype (CASC, CZUG, IEXA, JTLC, MCZC, PSWC, UCDC, USNM).

Downloaded from https://academic.oup.com/isd/article/6/1/4/6514767 by ThULB Jena user on 27 January 2022

Other material examined (AMNH, CASC, CEET, CNCC, CSCA, FSCA, JTLC, LACM, MCZC, MZLU, MZSP, PSWC, SEAN, SMPC, UCDC, USNM, UTIC, UVGC).

El Salvador: ***Santa Ana***: Monte Cristo (Cartwright, O. L.); **Guatemala**: ***Alta Verapaz***: 1 km NE Santa Cruz Verapaz, 1,400 m (Ward, P. S.); 7 km SW Cobán, 1,460 m (Ward, P. S.); airport near Cobán, 1,320 m (Janzen, D. H.); Tactic, Finca Xilicá (Andrade, L.); Tactic, Finca Xilicá (Haeussler, A.); ***Baja Verapaz***: 1 km SSW La Cumbre, 1,480 m (Ward, P. S.); 2 km N La Unión Barrios, 1,620 m (Ward, P. S.); 3 km ESE Purulhá, 1,620 m (Ward, P. S.); 4 km WSW Purulhá, 1,700 m (Ward, P. S.); ***Chimaltenango***: km. 143 a Chimalte (Perez, R.); ***Escuintla***: ex San José (in quarantine San Francisco, USA) (c.u.); ***Guatemala***: ex Guatemala City (in quarantine San Francisco, USA) (c.u.); Guatemala City (Bloem, K.; Bloem, S.); ***Retalhuleu***: Puente Samala, 3.8 mi NE San Felipe, Quezal-Retal. Rd. (Janzen, D. H.); ***Sacatepéquez***: Antigua, 2,000 m (Ekis, G.); Antigua (Bloem, S.); Antigua (Krauss, N. L. H.); Parque Florencia, nr. San Miguel Milpas Altas, 1,900 m (Ward, P. S.); ***Santa Rosa***: Barberena, El Naranjito (Perez, R.); ***Sololá***: 1 km N San Andrés Semetabaj, 1,840 m (Ward, P. S.); 2 km ESE San Lucas Tolimán, 1,780 m (Wild, A. L.); 7 km SSE San Lucas Tolimán, 1,140 m (Ward, P. S.); Lake Atitlan (Wheeler, W. M.); Panajachel, 1,573 m (Stange, L. A.); San Lucas Toliman (Wheeler, W. M.); Tsanjuyo (c.u.); ***unknown***: ex 'Guatemala' (in quarantine San Francisco, CA, USA) (c.u.); ***Zacapa***: 2 km SE La Unión, 1,550 m (LLAMA); San Lorenzo, 1,800 m (LeSage, L.); **Honduras**: ***Comayagua***: 10 km E Comayagua, 1,730 m (LLAMA); 10 km E Comayagua, 2,000 m (Boudinot, B.); 9 km E Comayagua, 1,730 m (LLAMA); ***Cortés***: P.N. Cusuco, 5 km N Buenos Aires (Hansson, C.); PN Cusuco, 1,220 m (LLAMA); ***Francisco Morazán***: Cerro Uyuca, 2,000 m (Gupta, V.; Gupta, S.); Montañita [as 'Montañito'] (Hubbell, T. H.); ***Olancho***: 9 km N Catacamas, 1,270 m (LLAMA); 9 km N Catacamas, 1,330 m (LLAMA); 9 km N Catacamas, 1,340 m (LLAMA); 9 km NNW La Unión, 1,460 m (Ward, P. S.); 9 km NNW La Unión, 1,470 m (Ward, P. S.); Parq. Nac. La Muralla, 1,450 m (Ward, P. S.); Parq. Nac. La Muralla, 1,470 m (Ward, P. S.); PN La Muralla, 1,440 m (LLAMA); PN La Muralla, 1,450 m (LLAMA); PN La Muralla, 1,460 m (LLAMA); PN La Muralla, 1,480 m (LLAMA); PN La Muralla, 1,490 m (LLAMA); **Mexico**: ***Chiapas***: 1 km E Tulanca (Pérez, L.); 2 km SE Custepec, 1,520 m (LLAMA); 3 km E San Cristóbal (Jones, R. W.); 36 mi N inters. Hwy. 190 × Tux.Gut.-Vil.Her. Rd., km 58 (Janzen, D. H.); 5 km E Rayón, 1,700 m (Ward, P. S.); km 44 Tuxtla Gutierrez to San Cristobal, near Chiapa de Corzo (Whitacre, D. F.); Laguna Montebello, 1,430 m (O'Brien, C. W.; O'Brien, L.; Marshall); Río Yashanal (Girón, M.); San Miguel, Mpio. El Bosque, 1,105 m (Philpott, S. M.); Tziscao, Lagos de Montebello, 1,500 m (Ward, P. S.); Tzuluwitz, Mpio. San Juan Cancuc, 1,310 m (Philpott, S. M.); Yevalchen, Mpio. Tumbala, 1,350 m (Philpott, S. M.); Zinacantan, 1,900 m (Ekis, G.); **Nicaragua**: ***Jinotega***: 5 km [from] Jinotega, Los Pinares (Maes; Pineda); PN Cerro Saslaya, 1,110 m (LLAMA); Santa Maria de Ostuma (Maes; Pineda); ***Matagalpa***: Fuente Pura (Maes, J. M.; et al.); Hotel Selva Negra, km 139 N of Matagalpa, 1,200 m (Kugler, C.; Hahn, J.); Reserva Miraflor, 1,369 m (MacKay, W.); Santa Martha, 8 km N Matagalpa, 1,219 m (Ross, E. S.); Selva Negra, 1,285 m (MacKay, W.); ***Nueva Segovia***: 9 km NW Jalapa, 1,410 m (LLAMA); 9 km NW Jalapa, 1,470 m (LLAMA).

Worker measurements (n = 14). HW 0.93–1.06, HL 1.07–1.22, MFC 0.040–0.057, LHT 0.82–0.94, CI 0.82–0.88, FCI 0.039–0.058, REL 0.45–0.48, REL2 0.52–0.56, FI 0.40–0.44, PLI 0.49–0.57, PWI 0.44–0.52, MSC 2–5.

Worker Diagnosis. Medium-sized species (HW 0.93–1.06) with moderately elongate head (CI 0.82–0.88) (Fig. 7) and relatively large eyes (see REL and REL2 values); frontal carinae separated by less than basal scape width; metanotal groove weakly impressed, in profile barely discernable; dorsal face of propodeum flat and more or less differentiated from declivitous face, rounding into the latter, and the two faces subequal in length; petiole moderately slender (PLI 0.49–0.57, PL/HL 0.53–0.59); in profile petiole with slight or no anterior peduncle, the anterodorsal face flat to convex, ascending gradually to summit in posterior half of node, then rounding into more steeply descending posterior face; profemur slender; hind leg relatively short (LHT/HL 0.71–0.77). Head subopaque, densely punctulate-coriarious, the punctulae on vertex usually separated by less than their diameters. Standing pilosity sparse, absent from propodeum and mesonotum (MSC 2–5). Head, postpetiole, gaster and legs dark brown, mesosoma and petiole varying from concolorous to lighter medium-brown, not strongly contrasting, however, with rest of body (mesosoma sometimes darkened dorsally); mandibles, antennae, and distal portions of legs tending to be a lighter medium-brown to yellowish-brown.

Comments. This is a widespread and rather common Mesoamerican species that was previously confused with *P. championi*, although the two are not sister taxa—in fact, UCE data demonstrate that they belong to different complexes within the *P. elongatulus* group (Fig. 1). *Pseudomyrmex cognatus* can be recognized by the combination of dark brown coloration of most of the body (mesosoma often lighter but not contrastingly so); densely punctulate-coriarious head; relatively large eyes (worker REL 0.45–0.48, queen REL 0.42–0.46); and weakly developed metanotal groove (in the worker). For distinctions between *P. cognatus* and *P. championi*, see under the latter species.

Workers from a single nest collection from Parque Florencia, Sacatepéquez, Guatemala (PSW15039) have more widely separated frontal carinae (MFC 0.065–0.070; *n* = 3), shorter eyes (REL 0.43–0.45), and a broader and shorter petiole (PWI 0.56–0.58, PL/HL 0.50–0.53). In the UCE phylogeny this sample is sister to all others of *P. cognatus* (Fig. 1). We have no other *P. cognatus* workers from this site, i.e., no sympatric association with more 'typical' *P. cognatus* that would confirm PSW15039 as a distinct species. Hence there is some ambiguity about the status of these divergent individuals. For the moment we treat them as conspecific with *P. cognatus*, while noting that further study might support their treatment as a different species.

Distribution and Biology. *Pseudomyrmex cognatus* ranges from Chiapas, Mexico to Nicaragua, and has been recorded from mixed tropical/temperate mesic forest, montane rainforest, montane rainforest edge, oak-pine forest, mixed pine-mesophyll forest, oak cloud forest, roadside, and old field/pasture, at elevations ranging from 1,105 m to 2,000 m (mean 1,507 m; *n* = 47). Nests have been collected from dead twigs of various woody plants, including Asteraceae, Fabaceae, Orchidaceae, and *Pinus*; one was collected from a dead sedge culm.

***Pseudomyrmex comitator* sp. nov.**

Figs. 9 and 24

LSID: urn:lsid:zoobank.org:act:4BAA462E-31A4-4799-BEF6-D7BC23B346F0

P. championi nr; Chomicki et al. 2015: 4. Placement in molecular phylogeny.

Downloaded from https://academic.oup.com/isd/article/6/1/4/6514767 by ThULB Jena user on 27 January 2022

Holotype dealate queen, MEXICO Chiapas: 29 km E La Trinitaria, 1,520 m, 16° 06′ N 91° 46′ W, 21 Jul 2007, ex nest of *P. cognatus* in dead stick, pine oak scrubby forest, J. Longino JTL6094 (UNAM) (JTLC000010310). Paratype dealate queen, MEXICO Chiapas: Lagos de Montebello, 1,520 m, 16° 08′ N 91° 44′ W, 21 Jul 2007, on ground, pine oak *Liquidambar* forest, J. Longino JTL6093-s (UCDC) (JTLC000010349).

Other material examined. Known only from the type material.

Queen measurements (n = 2, with holotype measurement given first). HW 0.81, 0.77; HL 1.01, 1.00; MFC 0.038, 0.046; LHT 0.70, 0.69; CI 0.80, 0.77; FCI 0.047, 0.060; REL 0.40, 0.42; REL2 0.51, 0.54; FI 0.40, 0.43; PLI 0.67, 0.83; PWI 0.56, 0.80; MSC 4, 7.

Queen Diagnosis. Small species (see HW, HL, and LHT measurements), with elongate head (CI 0.77–0.80); upper surface of mandible finely reticulate with scattered punctures, lacking striae; eyes relatively short (REL 0.40–0.42, REL2 0.51–0.54); frontal carinae separated by slightly less than basal scape width; petiole stout and short, the height and width of petiole about 0.8× the length (less so in the paratype); in profile, petiole with flat to convex anterodorsal face, ascending to summit in posterior quarter of node, then rounding into more steeply descending posterior face; profemur slender; hind leg relatively short (LHT/HL 0.69). Head sublucid, densely punctulate-coriarious. Standing pilosity sparse and short on most of body (MSC 4–7). Dark brown to brownish-black, head and gaster darker than rest of body.

Comments. This species, known only from two dealate queens, bears some resemblance to *P. cognatus*, but differs in ways that suggest it represents a workerless inquiline (see also notes on Distribution and Biology below). The *P. comitator* queens are notably smaller than those of *P. cognatus* (HW 0.77–0.81, HL 1.00–1.01, vs HW 0.99–1.11, HL 1.28–1.42 in queens of *P. cognatus*), lack striae on the mandibles, have reduced mesosomal pilosity (MSC 4–7 vs 15–22 in *P. cognatus* queens), and possess an oddly swollen and foreshortened petiole (PLI 0.67–0.83, vs 0.45–0.53 in *P. cognatus* queens) (Figs. 8 and 9). The two specimens of *P. comitator* do not show the same degree of modification of the petiole (compare PLI and PWI values), with the holotype being more extreme, indicating some instability in the expression of this character. Both individuals of *P. comitator* were sequenced; they are sister taxa in our UCE tree and embedded phylogenetically within the putative host species (Fig. 1). They are more closely related to *P. cognatus* populations from Honduras and Nicaragua, however, than to samples from Chiapas.

Distribution and Biology. Pseudomyrmex comitator is an apparent workerless social parasite of *P. cognatus*, and is currently known only from two adjacent sites in high-elevation forest (1,520 m) of Chiapas, Mexico. The holotype was collected by Jack Longino in a nest of *P. cognatus* that contained workers, alate males, alate queens, and brood (larvae, prepupae) of the presumed host. Only a single dealate queen of *P. comitator* was found in the nest. The paratype queen was encountered as a stray on the ground, in a nearby locality.

Pseudomyrmex elongatulus **(Dalle Torre)**

Figs. 10, 11 and 23

Pseudomyrma elongata F. Smith 1877: 67. Syntype worker, Mexico (BMNH) [examined]. Junior primary homonym of *Pseudomyrma elongata* Mayr 1870: 413.

Pseudomyrma elongatula Dalle Torre, 1892: 89. Replacement name.

Pseudomyrma decipiens Forel 1899: 95. Syntype workers, queens, Teapa, Mexico (H. H. Smith) (BMNH, MHNG) [examined]. Synonymy by Kempf 1967: 6.

Pseudomyrmex decipiens (Forel); Creighton 1953: 132. Combination in *Pseudomyrmex*.

Pseudomyrmex elongatulus (Dalle Torre); Kempf 1967: 6. Combination in *Pseudomyrmex*.

Pseudomyrmex elongatulus (Dalle Torre); Ward and Downie 2005: 314, 316. Placement in morphological and molecular phylogenies.

Pseudomyrmex elongatulus (Dalle Torre); Chomicki et al. 2015: 4. Placement in molecular phylogeny.

Other material examined (AMNH, BMNH, CASC, CEET, CHAH, CSCA, CUIC, CZUG, FSCA, IEXA, JTLC, LACM, MCZC, MNHN, MZSP, PSWC, SEMC, SMPC, UCDC, UCRC, USNM, UTEP, UWEM).

Belize: ***Cayo***: Belmopan (Krauss, N. L. H.); Chiabul Forest, 5 km SE Millionario (Beard, J.); Chiabul Forest, San Pastor (Beard, J.); El Cayo (Krauss, N. L. H.); Las Cuevas, 5 km SE Millionario (Beard, J.); Las Cuevas, 5 km SE Millionario (Lyal, C.; Hollis, D.); ***Orange Walk***: Rio Bravo Conserv. Area, La Milpa Res. Stn. (Davis, L. R.); **Guatemala**: ***Escuintla***: 6.6 mi NE Escuintla (Janzen, D. H.); ***Guatemala***: ex Guatemala City (in quarantine San Francisco, USA) (c.u.); Peten: Tikal Mayan ruins, 183 m (Ross, E. S.); Petén: Tikal (Hubbell, T. H.); ***unknown***: ex 'Guatemala' (in quarantine San Francisco, CA, USA) (c.u.); **Mexico**: ***Chiapas***: 8 km SE Salto de Agua, 100 m (LLAMA); 8 km SE Salto de Agua, 60 m (LLAMA); 8 km SE Salto de Agua, 70 m (LLAMA); Lago Metzabok, 560 m (LLAMA); Lago Metzabok, 570 m (LLAMA); Lago Metzabok, 575 m (LLAMA); Laguna Bélgica (Girón, M.); Nahá, 860 m (LLAMA); Nahá, 950 m (LLAMA); Palenque ruins, 170 m (Cox, D. J.); Simojovel to Santo Domingo (Chemsak, J. A.); Tonalá [as 'Tonola'] (Petrunkewitch); Yevalchen, Mpio. Tumbala, 1,335 m (Philpott, S. M.); ***Morelos***: Huautla (Quiroz, L.); ***Oaxaca***: 11–17 mi W Tehuantepec (Janzen, D. H.); 22 mi S Jesus Carranza (Graber, J. W.); 5 mi E Temascal (Janzen, D. H.); Café Carlota, 950 m (Gray, K. W.); Temascal (Janzen, D. H.); Uluapan, 4 km NE Ayautla, 410 m (Longino, J.); Uluapan, 4 km NE San Bartolomé Ayautla, 420 m (ADMAC); Uluapan, 4 km NE San Bartolomé Ayautla, 470 m (ADMAC); Uluapan, 4 km NE San Bartolomé Ayautla, 500 m (ADMAC); Uluapan, 4 km NE San Bartolomé Ayautla, 510 m (ADMAC); Uluapan, 4 km NE San Bartolomé Ayautla, 620 m (ADMAC); ***Puebla***: Villa Juarez (intercepted at Brownsville, Texas) (Heinrich; Jackson); ***San Luis Potosí***: 13 km N Tamazunchale, 290 m (MacKay, W.); 84 km W Cd. Valle, 645 m (MacKay, W.); Ciudad Valles, Carr. al Naranjo, Salto Micos, 168 m (Vásquez, M.); El Salto, 520 m (Carney, L.); Tamasopo, Cascadas El Paraiso, 400 m (Vásquez, M.); Tamazunchale, 120 m (Creighton, W. S.); Tamazunchale, 245 m (Creighton, W. S.); Tamazunchale (Ross, W. S.); Tamazunchale (intercepted at Brownsville, Texas) (Heinrich); Tamazunchale (intercepted at Laredo, Texas) (c.u.); Tamazunchale (POE: Brownsville, Texas) (Arsego); Xilitla, Arroyo La Conchita, 431 m (Vásquez, M.); ***Tabasco***: 13 km W border Chis., Rt. 186 (MacKay, W.); 3 mi W Cardenas (Janzen, D. H.); Cardenas (Janzen, D. H.); Teapa (Shenefelt, R. D.); Teapa (Smith, H. H.); ***Tamaulipas***: 10 km W El Encino, 510 m (Ward, P. S.); Gomez Farias (MacKay, W.); Tampico (Locke); ***Veracruz***: 10 mi E Conejos (Janzen, D. H.); 10 mi W Veracruz (Bohart, G. E.); 11 km NNE Sontecomapan, 175 m (Ward, P. S.); 15 km SW Paso del Toro, 50 m (Ward, P. S.); 29.5 mi NW Tuxpam (Janzen, D. H.); 3 km NW La Tinaja, 50 m (MacKay, W.); 6 km NW Tecolapán, 55 m (Kautz, S.; Eilmus, S.); 8 km NNE Soteapan, 1,010 m (Ward, P. S.); 8 km NNE Soteapan, 970 m (Ward, P. S.); 9 km NE San

Downloaded from https://academic.oup.com/isd/article/6/1/4/6514767 by ThULB Jena user on 27 January 2022

Andrés Tuxtla, 965 m (Ward, P. S.); 9 km NNW Sontecomapan, 20 m (Ward, P. S.); Apazapan, 347 m (Quiroz, L.); Apazapan (Sivinski, J.); Camaron (Skwarra, E.); Catemaco Hills, 8 mi S Angel (Janzen, D. H.); Cordoba (Bohart, G. E.); Córdoba, Cuauhtémoc (Navarrete, J. L.); Cotaxtla Exp. Stn., Cotaxtla (Janzen, D. H.); Est. Biol. 'Los Tuxtlas', nr. San Andres Tuxtla (Ibarra M., G.); Est. Biol. de Los Tuxtlas (Hespenheide, H. A.); Est. Biol. La Mancha, 20 m (ADMAC); Est. Biol. Los Tuxtlas, 110 m (ADMAC); Est. Biol. Los Tuxtlas, 140 m (ADMAC); Est. Biol. Los Tuxtlas, 160 m (ADMAC); Est. Biol. Los Tuxtlas, 170 m (ADMAC); Est. Biol. Los Tuxtlas, 180 m (ADMAC); Est. Biol. Los Tuxtlas, 450 m (ADMAC); Estación de Biología Los Tuxtlas, 115 m (Ward, P. S.); Estación de Biología Los Tuxtlas, 150 m (Ward, P. S.); Estación de Biología Los Tuxtlas, 170 m (Ward, P. S.); Estación de Biología Los Tuxtlas, 450 m (Ward, P. S.); Fortin, 950 m (Ward, P. S.); Fortín de las Flores (Edwards, G. B.); Fortín de las Flores - Sumidero, Planta de la Cerveceria, 840 m (Weems, Jr., H. V.); La Mancha (c.u.); Las Hamacas, 17 km N Santiago Tuxtla (Wilson, E. O.); Los Tuxtlas, 140 m (Kautz, S.; Heil, M.); Los Tuxtlas (Jeanne, R. L.); Los Tuxtlas, 10 km NNW Sontecomapan, 200 m (Ward, P. S.); Los Tuxtlas, 10 km NNW Sontecomapan, 500 m (Ward, P. S.); Mirador (Skwarra); Pueblo Nuevo, nr. Tetzonapa (Cornell Univ. Mexico Field Party); Pueblo Nuevo, nr. Tetzonapa (Wilson, E. O.); Rio Tonto (Janzen, D. H.); Ruiz Cortínez, 12 km NE San Andrés Tuxtla, 1,050 m (ADMAC); Sa. Teoviscocla, nr. Cuichapa (Cornell Univ. Mexico Field Party); San Andrés Tuxtla (Janzen, D. H.); St. Lucrecia (Knab, F.); St. Lucrecia (Mann, W. M.); Tuxpango-Orizaba (Gillogly, A. R.); Vera Cruz (Townsend); Veracruz (Krauss, N. L. H.); ***unknown***: 'Mexico' (c.u.); 'Mexique' (Smith, H. H.); **United States**: ***Florida***: Palm Beach Co.: MacArthur Beach SP (Deyrup, M.).

Worker measurements (n = 14). HW 0.93–1.09, HL 1.03–1.32, MFC 0.034–0.045, LHT 0.80–0.97, CI 0.81–0.90, FCI 0.033–0.046, REL 0.47–0.53, REL2 0.54–0.61, FI 0.43–0.47, PLI 0.44–0.52, PWI 0.41–0.48, MSC 2–4.

Worker Diagnosis. Medium-sized species (HW 0.93–1.06, LHT 0.80–0.97); head only moderately elongate (CI 0.81–0.90) and with rounded posterolateral corners in full-face view (Fig. 10); eyes relatively large (see REL and REL2 values); frontal carinae separated by less than basal scape width; metanotal groove strongly impressed, conspicuous in profile; dorsal face of propodeum flat, rounding into declivitous face, the two subequal in length; petiole slender, elongate-triangular in profile (PLI 0.47–0.53, PL/HL 0.57–0.61, PL/LHT 0.75–0.80); petiole with slight anterior peduncle, in profile the anterodorsal face flat to convex, ascending gradually to summit in posterior quarter of node, then rounding into steeply descending posterior face; profemur moderately robust (FI 0.43–0.47); hind leg moderately long (LHT/HL 0.74–0.79). Head subopaque to sublucid, densely punctulate-coriarious, the punctures becoming less dense on vertex (separated by their diameters or more). Standing pilosity sparse, absent from propodeum and mesonotum (MSC 2–4). Typically light yellow-brown to orange-brown, with darker brown anterolateral patches on abdominal tergite 4 (first gastric tergite) and brown transverse bands on abdominal tergites 5–7 (gastric tergites 2–4); in some samples from Guatemala and Belize head and mesosoma more infuscated, and gaster tending to be more uniformly medium brown.

Comments. Distinctive features of this species are the moderately elongate head with rounded posterolateral corners, large eyes (worker REL 0.47–0.53, queen REL 0.44–0.46), conspicuous metanotal groove in the worker (Fig. 10), and slender elongate-triangular petiole (worker PLI 0.44–0.52, queen PLI 0.45–0.51). *Pseudomyrmex elongatulus* is typically light yellow-brown to orange-brown with darker transverse maculation on the gaster, but some specimens from Guatemala and Belize are darker brown overall. Leaving aside *P. ereptor* (see *Pseudomyrmex ereptor* sp. nov.), the closest relative of *P. elongatulus* is *P. exoratus* (Fig. 1), easily told apart by its much more elongate head (worker CI 0.67–0.69, vs 0.81–0.90 in *P. elongatulus*).

Distribution and Biology. This species is widely distributed in eastern Mexico, from Tamaulipas to Chiapas, with outlying populations in Guatemala and Belize. The record from Morelos needs to be confirmed since it lies outside the expected range of this species. It may represent a transient introduction. There are records of *P. elongatulus* being intercepted at U.S. ports of entry in Texas and California, from shipments originating in Puebla, San Luis Potosí, and Guatemala (see list of material examined, above), indicating that this species has a propensity to be transported by human commerce. A single worker collected recently by Mark Deyrup in a natural setting in south Florida evidently represents an accidental introduction. It is unclear if *P. elongatulus* is established in that state; a second visit to the site failed to locate additional workers (Deyrup, personal communication). *P. elongatulus* has been recorded from lowland rainforest, rainforest edge, second-growth rainforest, mixed tropical/temperate mesic forest, shaded coffee, tropical dry forest, and roadside habitats, at elevations ranging from 20 m to 1355 m (mean 417 m; n = 53). Nests are found in dead twigs of various plants. Specific nest site records include dead stalk of grass, dead twig of liana, and dead twigs/stems of *Cecropia*, *Heliocarpus appendiculatus*, *Gliricidia sepium*, *Mimosa*, Orchidaceae, woody Asteraceae, and unidentified woody plants.

***Pseudomyrmex ereptor* sp. nov.**

Figs. 12 and 24

Zoobank LSID: urn:lsid:zoobank.org:act:3F4584C3-EB0C-4C74-B067-01CBEDC8F4EB

Holotype alate queen, MEXICO Veracruz: Los Tuxtlas, 10 km NNW Sontecomapan, 500 m, 18° 35′ N, 95° 05′ W, 21 Mar 1985, ex dead twig of liana [in nest of *P. elongatulus*], rainforest, P. S. Ward PSW07360A (UNAM) (CASENT0863524).

Other material examined. Known only from the holotype.

Queen measurements (*n* = 1). HW 0.98, HL 1.25, MFC 0.058, LHT 0.76, CI 0.78, FCI 0.059, REL 0.44, REL2 0.56, FI 0.46, PLI 0.61, PWI 0.75, MSC 11.

Queen Diagnosis. Small species (see HW, HL, and LHT measurements), with moderately elongate head (CI 0.78); upper surface of mandible smooth and shiny, with scattered punctures; eyes of moderate length (REL 0.44, REL2 0.56); frontal carinae separated by basal scape width; petiole relatively short (PLI 0.61, PL/HL 0.52) and broad (PWI 0.75, DPW/LHT 0.64), with stout, recurved anteroventral tooth; in profile, petiole with convex anterodorsal face ascending gradually to summit in posterior quarter of node, then rounding into steep posterior face; postpetiole very broad, ovorectangular in dorsal view (PPW/LHT 1.01); profemur robust (FI 0.46); hind leg short (LHT/HL 0.61). Head sublucid, densely but finely punctulate, the punctures separated by one to several diameters, the interspaces smooth and shiny, or (towards vertex) finely coriarious. Standing pilosity scattered on head, mesosoma (MSC

Downloaded from https://academic.oup.com/isd/article/6/1/4/6514767 by ThULB Jena user on 27 January 2022

11), and gaster, short and sparse on petiole, postpetiole, and fourth abdominal (first gastric) tergite. Uniformly light orange-brown.

Comments. The small size (HL 1.25, LHT 0.76), smooth and shiny mandibles, and very broad (ovorectangular) postpetiole (PPW/LHT 1.01) are distinctive features of *P. ereptor* that set it apart from the queen of its apparent host species, *P. elongatulus*, and from other species in the *P. elongatulus* group. Queens of *P. elongatulus* are larger (HL 1.37–1.42, LHT 0.90–0.94), with striate mandibles, and a slender, pyriform postpetiole as seen in dorsal view (PPW/LHT 0.78–0.83). Our UCE phylogeny shows that *P. ereptor* is sister to the entire assemblage of *P. elongatulus* samples (Fig. 1). It is well separated from an alate queen of *P. elongatulus* (D1985) collected in the same nest, thus confirming its status as a different species.

Distribution and Biology. The only known specimen of *P. ereptor*—an alate queen—was collected in a nest of *P. elongatulus* in a dead twig attached to a liana, on Vereda Cima, Estación de Biología 'Los Tuxtlas', Veracruz. The nest (collection code PSW07360) contained numerous workers, alate queens, males, and brood of *P. elongatulus*. *Pseudomyrmex ereptor* apparently represents a workerless, inquiline parasite of *P. elongatulus*. The fact that only a single alate queen of *P. ereptor* was found in the nest suggests that she was a recent arrival. The absence of a dealate queen of *P. elongatulus* should not be over-interpreted; it could simply indicate that this was part of a larger polydomous colony. *Pseudomyrmex* colonies are often comprised of disjunct nests occupying several dead twigs on a plant.

***Pseudomyrmex exoratus* sp. nov.**
Figs. 14 and 24
Zoobank LSID: urn:lsid:zoobank.org:act:8D3D17CF-131E-4E3F-9C67-B9B67E475B1D

Pseudomyrmex psw041; Chomicki et al. 2015: 4. Placement in molecular phylogeny.

Holotype Worker. MEXICO Oaxaca: Temascal, 25 m, 2 Feb 1964, at house, D. H. Janzen (UNAM) (CASENT0863539). Paratypes: series of workers, same data as holotype (CASC, CZUG, IEXA, JTLC, LACM, MCZC, PSWC, UCDC, USNM).

Other material examined (LACM, MZLU, PSWC, UCDC).
Honduras: ***Atlántida***: Lancetilla, Tela (Cave, R.); **Mexico**: ***Chiapas***: Palenque ruins, 170 m (Cox, D. J.); ***Oaxaca***: 5 mi E Temascal (Janzen, D. H.); Temascal, 25 m (Janzen, D. H.); Temascal (Janzen, D. H.).

Worker measurements (n = 6). HW 0.83–0.86, HL 1.19–1.28, MFC 0.043–0.049, LHT 0.78–0.84, CI 0.67–0.69, FCI 0.050–0.058, REL 0.42–0.45, REL2 0.62–0.66, FI 0.46–0.49, PLI 0.52–0.56, PWI 0.49–0.55, MSC 3–4.

Worker Diagnosis. Medium-sized species (LHT 0.78–0.84), with notably elongate head (CI 0.67–0.69) and eyes (see REL and REL2 values); frontal carinae separated by basal scape width or slightly less; ocelli prominent (Fig. 14); metanotal groove conspicuously impressed; dorsal face of propodeum rounding insensibly into declivitous face, the two subequal in length; petiole relatively slender (PLI 0.52–0.56, PL/HL 0.51–0.52), in profile the weakly convex anterodorsal face of petiole ascending gradually to summit in the posterior half of node, then rounding into steeper posterior face; profemur relatively robust (FI 0.46–0.49); hind leg short, relative to head length (LHT/HL 0.65–0.67). Head sublucid, anterior half densely punctulate with shiny interspaces, becoming sparsely punctulate-coriarious on vertex. Standing pilosity sparse, absent from propodeum and mesonotum (MSC 3–4). Light orange-brown, with dark brown anterolateral patches on abdominal tergite 4 (first gastric tergite) and a transverse band on abdominal tergite 6 (gastric tergite 3); distal half of anterior face of metafemur weakly infuscated.

Comments. This light orange-brown species is easily recognized by its exceptionally elongate head (worker CI 0.67–0.69, queen CI 0.55–0.59), which is unlike that of any other species in the *P. elongatulus* group. *Pseudomyrmex exoratus* also has a rather robust profemur (worker FI 0.46–0.49, queen FI 0.47–0.49) and distinctive maculation on the gaster: dark anterolateral patches on abdominal tergite 4 and a transverse band on abdominal tergite 6. Our UCE phylogeny shows *P. exoratus* to be closely related to the more common and widespread species, *P. elongatulus* (Fig. 1). Both species occur sympatrically at the type locality of *P. exoratus*.

Distribution and Biology. Pseudomyrmex exoratus is known from only three low-elevation localities in southern Mexico (in Oaxaca and Chiapas) and one collection from Honduras. Janzen collected two series at Temascal, Oaxaca, labeled 2.ii.1964 II and 2.ii.1964 IV (the latter including alate queens and males), plus a single queen on 10 Jan 1964, for which the label states 'flew into car, at house'. Little is known about the biology of this species although it is presumed to nest in dead twigs, like most other members of the *P. elongatulus* group. The robust profemur suggests that it might occupy rather hard dead wood.

***Pseudomyrmex fasciatus* sp. nov.**
Figs. 15 and 20
Zoobank LSID: urn:lsid:zoobank.org:act:52CB59B3-D99C-4E09-8A83-522B3E21714F

Holotype Worker. COSTA RICA Puntarenas: 2 km SSE Monteverde, 1,230 m, 10.28906 –84.80304 ± 3 m, 5 Jan 2018, ex dead twig of vine, montane rainforest edge, P. S. Ward PSW18011 (MUCR) (CASENT0863540). Paratypes: series of workers, 1 dealate queen, same data as holotype (CASC, JTLC, LACM, MCZC, PSWC, UCDC, UNAM, USNM).

Other material examined (AMNH, INBC, JTLC, LACM, MCZC, MIZA, MUCR, PSWC, SMPC, UCDC, USNM).
Costa Rica: ***Alajuela***: Rio Peñas Blancas, 950 m (Longino, J.); Zarcero, 1,600 m (Solis, A.); ***Cartago***: Agua Caliente, nr. Cartago (Wheeler, W. M.); Nombre Dulce, vivero Linda Vista, 1,300 m (Hanson, P.); ***Heredia***: Monte Allegro, Sto. Domingo de Heredia (Perfecto, I.); ***Puntarenas***: 2 km SSE Monteverde, 1,230 m (Ward, P. S.); 2 km SSW Monteverde, 1,245 m (Ward, P. S.); 3 km SE Monteverde, 1,200 m (Longino, J.); 3 km SSE Monteverde, 1,100 m (Longino, J.); Monteverde, 1,100 m (Ward, P. S.); Monteverde, 1,200 m (Cover, S.); Monteverde, 1,200 m (Ward, P. S.); Monteverde, 1,400 m (Longino, J.); Monteverde (Daly, H.); San Luis de Monteverde, 1,100 m (LaPierre, L.); San Luis Valley, 1,090 m (Sumnicht, T. P.; Longino, J. T.); Sta. Elena, 1,300 m (Longino, J.); vic. Alto San Luis, 1,100 m (Hovore, F. T.); ***San José***: San Pedro de Montes de Oca (Ballou, C. H.); **El Salvador**: ***La Libertad***: Ecoparque El Espino (Mendoza, E.); **Guatemala**: ***Chimaltenango***: El Amparo (c.u.); ***Escuintla***: 6.6 mi NE Escuintla (Janzen, D. H.); ***Guatemala***: ex Guatemala City (in quarantine San Francisco, USA) (c.u.); ***Santa***

Downloaded from https://academic.oup.com/isd/article/6/1/4/6514767 by ThULB Jena user on 27 January 2022

Rosa: El Piño (Sivinski, J.); ***unknown***: ex 'Guatemala' (intercepted at Hoboken, NJ, USA) (c.u.); **Honduras**: ***Atlántida***: 9 km S Yaruca, 950 m (Ward, P. S.); ***Cortés***: Lago Yojoa, N end (Brown, W. L.); PN Cusuco, 1,210 m (LLAMA); PN Cusuco, 1,330 m (LLAMA); **Mexico**: ***Chiapas***: 15 mi NW Ocozocoautla, 790 m (Newton, A.); Finca Hamburgo, Río Tepuzapa, 1,030 m (Andresen, D.); Finca Irlanda, 975 m (Philpott, S. M.); Nahá, 860 m (LLAMA); Nahá, 950 m (LLAMA); Sierra Morena, 1,380 m (LLAMA); **Nicaragua**: ***Matagalpa***: RN Cerro Musún, 1,090 m (LLAMA); RN Cerro Musún, 750 m (LLAMA); RN Cerro Musún, 880 m (LLAMA); RN Cerro Musún, 900 m (LLAMA).

Worker measurements (n = 12). HW 0.84–0.94, HL 1.05–1.15, MFC 0.019–0.042, LHT 0.74–0.83, CI 0.79–0.86, FCI 0.023–0.045, REL 0.45–0.48, REL2 0.54–0.59, FI 0.41–0.47, PLI 0.46–0.58, PWI 0.42–0.50, MSC 2–5.

Worker Diagnosis. Small to medium-sized species (HW 0.84–0.94) with moderately elongate head (CI 0.79–0.86) (Fig. 15) and relatively large eyes (REL 0.45–0.48); frontal carinae separated by less than basal scape width; metanotal groove weakly impressed, in profile barely discernable; dorsal face of propodeum flat, rounding into declivitous face, and the two subequal in length; petiole relatively slender (PLI 0.46–0.58, PL/HL 0.54–0.60); in profile, anterodorsal face of petiole flat to convex, ascending gradually to summit in posterior half of node, then rounding into more steeply descending posterior face; profemur generally slender (FI 0.41–0.47); hind leg relatively short (LHT/HL 0.67-0.76). Head subopaque to sublucid, densely punctulate-coriarious, the punctulae on vertex separated by less than their diameters. Standing pilosity sparse, absent from propodeum and mesonotum (MSC 2–5). Light yellow- to orange-brown, with dark brown anterolateral patches on abdominal tergite 4 (first gastric tergite), sometimes joined medially, and conspicuous transverse bands on abdominal tergites 5 and 6 (gastric tergites 2 and 3); distal half of metafemur weakly (and variably) infuscated.

Comments. Among species in the *P. elongatulus* group that are predominantly yellow-orange to light orange-brown in color, this species can be recognized by the combination of relatively large eyes (worker REL 0.45–0.48, queen REL 0.45–0.46), moderately elongate head (worker CI 0.79–0.86, queen CI 0.72–0.76), weakly developed metanotal groove in the worker, and conspicuous transverse maculation on abdominal tergites 4–6 (gastric tergites 1–3). Our phylogenomic data reveal that *P. fasciatus* is sister to *P. cognatus* (including its phylogenetically embedded inquiline, *P. comitator*) (Fig. 1). *Pseudomyrmex fasciatus* and *P. cognatus* are broadly sympatric and quite different in appearance, with workers and queens of *P. cognatus* being brown to brownish-black in color.

Distribution and Biology. Pseudomyrmex fasciatus occurs from Chiapas, Mexico to Costa Rica. Recorded habitats include montane rainforest edge, montane wet forest, montane moist forest, and second-growth forest edge, at elevations ranging from 750 m to 1,600 m (mean 1,115 m; *n* = 28). Nests have been collected in dead twigs of various woody plants, including vines and orchids. Two series of specimens intercepted in quarantine at San Francisco, from Guatemala, are labeled 'ex *Oncidium wentworthianum*' and 'ex *Epidendrum atropurpurium*', respectively. A third interception, at Hoboken, New Jersey was from an *Oncidium* stem.

***Pseudomyrmex nimbus* sp. nov.**
Figs. 16 and 26
Zoobank LSID: urn:lsid:zoobank.org:act:A03034A9-FADF-4AD5-9990-6E13516BD6A2

Pseudomyrmex psw003; Chomicki et al. 2015: 4. Placement in molecular phylogeny.

Holotype Worker. COSTA RICA Alajuela: Río Peñas Blancas, 800 m, 10° 19′ N, 84° 43′ W, 22–25 May 1990, ex live stems *Inga* sapling, wet forest clearing, J. Longino JTL2694 (MUCR) (CASENT0863541). Paratypes: series of workers, same data as holotype (CASC, JTLC, LACM, MCZC, PSWC, UCDC, UNAM, USNM).

Other material examined (ANSP, BMNH, GCSC, JTLC, LACM, PSWC, UCDC).
Costa Rica: ***Alajuela***: Peñas Blancas, 940 m (Longino, J.); Rio Peñas Blancas, 800 m (Longino, J. T.); Rio Peñas Blancas, 950 m (Longino, J.); ***Cartago***: 4 km E Moravia, 1,200 m (Longino, J.); La Fuente, e. slope of volcano of Turrialba, 1,200 m (Alfaro, A.); Turrialba, km. 22, to Limón (King, A. B. S.); ***Heredia***: Rara Avis, 730 m (Rifkind; Gum).

Worker measurements (n = 8). HW 1.03–1.20, HL 1.18–1.41, MFC 0.034–0.053, LHT 0.96–1.09, CI 0.85–0.89, FCI 0.031–0.047, REL 0.48–0.51, REL2 0.55–0.59, FI 0.41–0.45, PLI 0.44–0.53, PWI 0.42–0.50, MSC 2–5.

Worker Diagnosis. Relatively large species (HW 1.03–1.20, LHT 0.96–1.09); head only moderately elongate (CI 0.85–0.89) and with rounded posterolateral corners in full-face view (Fig. 16); eyes relatively large (REL 0.48–0.51); frontal carinae separated by less than basal scape width; metanotal groove strongly impressed, conspicuous in profile; dorsal face of propodeum generally convex in profile, rounding into declivitous face, the two subequal in length; petiole slender, elongate-triangular in profile (PLI 0.44-0.53, PL/HL 0.58–0.60, PL/LHT 0.71–0.79); petiole with slight anterior peduncle, in profile the anterodorsal face flat to convex, ascending gradually to summit in posterior third of node, then rounding into more steeply descending posterior face; profemur relatively slender (FI 0.41–0.45); hind leg relatively long (LHT/HL 0.76–0.82). Head subopaque, densely punctulate-coriarious, the punctures becoming less dense on vertex (separated by their diameters or more). Standing pilosity sparse, absent from propodeum and mesonotum (MSC 2–5). Head, dorsum of propodeum, metafemur, and gaster dark brown, other parts of body with variably lighter coloration (medium brown to yellow-brown).

Comments. *Pseudomyrmex nimbus* can be recognized by the combination of large size (worker HW 1.03–1.20; queen HW 1.15–1.18), well-developed metanotal groove (in worker), and predominantly dark coloration. The relatively long legs (worker LHT/HL 0.76–0.82, queen LHT/HL 0.70–0.72) and elongate eyes (worker REL 0.48–0.51; queen REL 0.48) are also notable. This species is in the *P. elongatulus* complex (within the *P. elongatulus* group), and is a distant sister to the trio of *P. exoratus*, *P. elongatulus*, and *P. ereptor* (Fig. 1).

Distribution and Biology. Pseudomyrmex nimbus is known only from several cloud forest sites in Costa Rica, at elevations of 730 m to 1,200 m. The following are Jack Longino's field notes on the type

Downloaded from https://academic.oup.com/isd/article/6/1/4/6514767 by ThULB Jena user on 27 January 2022

series (JTL2694): 'Workers abundant on small *Inga* sapling. I dissected the entire tree, finding 3 nests excavated in live stems (there was also stem-borer damage here and there, so the ants could have been invading pre-existing cavities). I never found reproductives. Either the queen was little different from workers and escaped, or the colony was queenless, or there was more of the colony off the *Inga* tree.' Another nest series (JTL/5Jul84/1017) was collected 'inside branch of still live but recently felled *Inga*' and included workers, alate queens, and a male. A third collection by Longino (JTL0900) was taken in a live *Cecropia insignis* sapling. Thus, the available data suggests that this species is a live-stem nester, a habit not seen in the majority of *Pseudomyrmex* species (Ward 1991). There is no evidence that *P. nimbus* keeps trophobionts (hemipterans) in these nests.

***Pseudomyrmex salvini* (Forel)**
Figs. 17 and 25

Pseudomyrma salvini Forel 1899: 94. Syntype workers, queens, males, Teapa, Tabasco, Mexico (H. H. Smith) (BMNH, MHNG) [examined].
Pseudomyrmex salvini (Forel); Kempf, 1960: 30. Combination in *Pseudomyrmex*. Description of worker and queen.
Pseudomyrmex salvini (Forel); Chomicki et al. 2015: 4. Placement in molecular phylogeny.

Other material examined (AMNH, CASC, CEET, CHAH, CSCA, EMEC, GKMC, IEXA, JTLC, LACM, MCZC, MNHN, MSNG, MZLU, MZSP, NHMW, PSWC, SMPC, STDC, UCDC, UCRC, USNM, UVGC).
Belize: ***Belize***: Belize (c.u.); Big Falls Road (Mosser, G. K.); Monkey Bay W.S. (Mosser, G. K.); ***Cayo***: El Cayo (Krauss, N. L. H.); nr. Macal River, 10 mi S Augustine (Reiskind, J.); nr. Teakettle Bank, Pooks Hill, 85 m (Bartlett, C. R.); Pine Mtn. Ridge, Rubber Camp, Mecal River, 415 m (Alpert, G. D.); ***Stann Creek***: Cockscomb Basin Jaguar Preserve, 414 m (Alpert, G. D.); Mama Noots, Bocawina, 16 km W Dangriga, 83 m (Keller, M. F.); **Guatemala**: ***Alta Verapaz***: Cacao, Trece Aguas (Barber; Schwarz); Region of Sebal, headwtrs Rio Pasión. (Hubbs; van der Schalie); ***Guatemala***: Mixco (Mann, W. M.); ***Izabal***: 16 km ESE Morales, 440 m (LLAMA); 16 km ESE Morales, 530 m (LLAMA); Bobos [as 'Bobas'] (Mann, W. M.); Lago Izabal, 1.5 km NE El Estor (Janzen, D. H.); Livingston (Barber; Schwarz); Los Amates (Kellerman); Parque Arqueológico, 84 m (Mackay, W.; Mackay, E.); Polochic R. (Barber; Schwarz); ***Petén***: 13 km NW Machaquilá, 375 m (LLAMA); ***Sololá***: Tsanjuyo (c.u.); ***Zacapa***: Gualán, Finca La Cartuchera (Vasquez, J.); **Honduras**: ***Comayagua***: PN Cerro Azul Meambar, 750 m (LLAMA); PN Cerro Azul Meambar, 770 m (LLAMA); ***Cortés***: Lago de Yojoa, 625 m (Krauss, N. L. H.); P.N. Cusuco, 5 km N Buenos Aires (Hansson, C.); ***Yoro***: Pico Pijol, 2,200 m (Hansson, C.); **Mexico**: ***Chiapas***: 21 km SW Salto de Agua, 180 m (LLAMA); 4 mi S Simojovel (Schlinger, E. I.); 4 mi SW Simojovel (Bechtel, R. C.; Schlinger, E. I.); Lago Metzabok, 560 m (LLAMA); Laguna Bélgica (Girón, M.); Nahá, 860 m (LLAMA); Palenque Ruins (Goodnight, C. J.); Plan Paredon, Mpio. Simojovel, 990 m (Philpott, S. M.); Playón de la Gloria, 160 m (LLAMA); Playón de la Gloria, 170 m (Cox, D. J.); Playón de la Gloria, 180 m (LLAMA); ***Oaxaca***: Uluapan, 4 km NE San Bartolomé Ayautla, 400 m (ADMAC); Uluapan, 4 km NE San Bartolomé Ayautla, 420 m (ADMAC); ***Puebla***: Cascada Las Hamacas, 8 km ENE Cuetzalan, 290 m (ADMAC); ***Quintana Roo***: Rives Caraibes, entre Puerto Juares et Touloum (Carayon, J.); ***Tabasco***: 3 mi W Cardenas (Janzen, D. H.); Teapa (Smith, H. H.); ***Veracruz***: 10 km N Sontecomapan, 10 m (Ward, P. S.); 4 mi N Catemaco (Fisher, E. M.); 6 mi NE Catemaco, 455 m (Newton, A.); 8 mi NW Sontecomapan, 150 m (Newton, A.); Est. Biol. de Los Tuxtlas (Hespenheide, H. A.); Est. Biol. Los Tuxtlas, 110 m (ADMAC); Est. Biol. Los Tuxtlas, 120 m (ADMAC); Est. Biol. Los Tuxtlas, 140 m (ADMAC); Est. Biol. Los Tuxtlas, 150 m (ADMAC); Est. Biol. Los Tuxtlas, 160 m (ADMAC); Est. Biol. Los Tuxtlas, 170 m (ADMAC); Est. Biol. Los Tuxtlas, 180 m (ADMAC); Est. Los Tuxtlas (Quiroz, L.); Estación de Biología Los Tuxtlas, 115 m (Ward, P. S.); Estación de Biología Los Tuxtlas, 150 m (Ward, P. S.); La Buenaventura (Petrunkewitch); Lago Catemaco (Gillogly, A. R.); Las Hamacas, 17 km N Santiago Tuxtla (Wilson, E. O.); Los Tuxtlas, 160 m (Kautz, S.; Heil, M.); Los Tuxtlas (Jeanne, R. L.); Los Tuxtlas Res. Stn. (Sivinski, J.); Los Tuxtlas, 10 km NNW Sontecomapan, 200 m (Ward, P. S.); Playa Escondita, nr. San Andreas Tuxtlas (Meyer, D.); Pueblo Nuevo, nr. Tetzonapa (Wilson, E. O.); St. Lucrecia (Mann, W. M.); ***Yucatán***: env. Uxmal (Carayon, J.).

Worker measurements (n = 10). HW 1.12–1.21, HL 1.19–1.35, FCI 0.038–0.055, LHT 0.96–1.12, CI 0.90–0.96, FCI 0.032–0.047, REL 0.54–0.59, REL2 0.59–0.62, FI 0.37–0.41, PLI 0.43–0.49, PWI 0.43–0.49, MSC 2–4.

Worker Diagnosis. Relatively large species (HW 1.12–1.21, LHT 0.96–1.12) with broad head and large eyes (see REL and REL2 values); frontal carinae separated by less than basal scape width; pronotum laterally submarginate, flattened, and with a weak longitudinal median depression; metanotal groove obsolete to absent; in profile propodeum short and high, the dorsal face shorter than, and rounding insensibly into, the declivitous face; petiole elongate and gracile, with a well differentiated anterior peduncle (Fig. 17) (PLI 0.43–0.49, PL/HL 0.64–0.69); profemur slender; hind leg relatively long (LHT/HL 0.80–0.84). Head varying from sublucid to (in more southern populations) subopaque; anterior half of head between eyes densely punctulate-coriarious, punctures becoming sparser on posterior half (separated by more than their diameters), and with intervening reticulate-coriarious sculpture of varying reflectance. Standing pilosity sparse, confined on the mesosoma dorsum to the pronotum (MSC 2-4). Head dark blackish-brown, remainder of body varying from contrastingly yellow-orange (except for transverse infuscated bands on abdominal tergites 4–6) to medium brown, appendages generally lighter.

Comments. *Pseudomyrmex salvini* is a distinctive species, sister to all other members of the *P. elongatulus* group (Fig. 1). It is easily recognized by its large size, elongate eyes (more than one-half head length), broad head (worker CI 0.90–0.96, queen CI 0.81–0.84), short high propodeum (in the worker), and elongate petiole with well-developed anterior peduncle (Fig. 17). In populations from Veracruz the head contrasts strikingly with the lighter colored remainder of the body; farther southward and eastward the mesosoma and metasoma become increasingly infuscated and the contrast is muted.

Distribution and Biology. This species is confined to southeastern Mexico, Guatemala, Belize, and Honduras, where it occurs in or at the edge of mesic forest, at elevations ranging from 10 m to 990 m (mean 316 m; *n* = 35). One worker, from Pico Pijol, Honduras (leg. C. Hansson) (MZLU), has the elevation given as '2200 m', but this is likely to be an error. Habitats recorded on specimen labels include littoral vegetation, rainforest, rainforest edge, mesophil forest, and

Downloaded from https://academic.oup.com/isd/article/6/1/4/6514767 by ThULB Jena user on 27 January 2022

roadside. Among the material examined by us, there were only four explicit nest series: 'ex dead twig of liana', 'ex dead weed stalk', 'ex dead twig', and 'nest in twig'. Most collections consist of workers or dealate queens foraging on low vegetation. At Los Tuxtlas, Veracruz one of us (P.S.W.) observed a salticid spider, apparently the dark-cephalic morph of *Synemosyna decipiens* (Cambridge) (see Cutler 1985: 87), mimicking workers of *P. salvini*.

***Pseudomyrmex veracruzensis* sp. nov.**
Figs. 18 and 26
Zoobank LSID: urn:lsid:zoobank.org:act:BB9D186E-1313-44F6-A9A6-F63AB60653B2

Holotype Worker. MEXICO Veracruz: Ruiz Cortínez, 13 km NE San Andrés Tuxtla, 1,055 m, 18.53387–95.13839 ± 4 m, 5 Jun 2016, ex dead twig of *Heliocarpus*, montane rainforest edge, P. S. Ward PSW17618 (UNAM) (CASENT0863542). Paratypes: series of workers, same data as holotype (CASC, CZUG, IEXA, JTLC, MCZC, PSWC, UCDC, USNM).

Other material examined (PSWC, UCDC).
Mexico: ***Veracruz***: 10 km NNE San Andrés Tuxtla, 1,010 m (Ward, P. S.); Ruiz Cortínez, 13 km NE San Andrés Tuxtla, 1,050 m (Ward, P. S.); Ruiz Cortínez, 13 km NE San Andrés Tuxtla, 1,055 m (Ward, P. S.).

Worker measurements (n = 8). HW 0.97–1.07, HL 1.13–1.30, MFC 0.035–0.050, LHT 0.84–0.94, CI 0.81–0.86, FCI 0.034–0.048, REL 0.46–0.48, REL2 0.55–0.58, FI 0.42–0.45, PLI 0.44–0.49, PWI 0.43–0.48, MSC 2-5.

Worker Diagnosis. Medium-sized species (HW 0.97–1.07) with moderately elongate head (CI 0.81–0.86) and eyes (REL 0.46–0.48); frontal carinae separated by less than basal scape width; metanotal groove moderately impressed, evident in profile; dorsal face of propodeum more or less flat, rounding into declivitous face, the two subequal in length; petiole slender, elongate (PLI 0.44–0.49, PL/HL 0.57–0.60, PL/LHT 0.76–0.82); petiole with slight anterior peduncle, in profile the anterodorsal face flat to convex, ascending gradually to summit in posterior half of node, then rounding into more steeply descending posterior face; profemur relatively slender (FI 0.42–0.45); hind leg relatively short (LHT/HL 0.71–0.76). Head subopaque, densely punctulate-coriarious, the punctures becoming less dense on vertex (separated by their diameters or more). Standing pilosity sparse, absent from propodeum and mesonotum (MSC 2–5). Medium ferrugineus-brown, with darker and rather diffuse transverse bands on anterior half of abdominal tergites 4–6 (gastric tergites 1–3); metafemur and, to a lesser extent, mesofemur infuscated.

Comments. Key features of this species are the ferrugineus-brown body, with darker transverse bands on the gaster; relatively large size (worker HW 0.97–1.07); and low, elongate petiole (worker PL 0.65–0.77, worker PLI 0.44–0.49). Workers of *P. veracruzensis* are superficially similar to those of the Costa Rican species, *P. nimbus*, but can be distinguished by their shorter legs (LHT 0.84–0.94 and LHT/HL 0.71–0.76 vs LHT 0.96–1.09 and LHT/HL 0.76–0.82 in *P. nimbus*), smaller eyes (REL 0.46–0.48 vs 0.48–0.51 in *P. nimbus*), less strongly impressed metanotal groove, differently shaped petiole (compare Figs. 16 and 18), and lighter coloration. An index combining PL, LHT and HW also separates the two species: (PL/LHT)/HW 0.74–0.80 versus 0.62–0.71 in *Pseudomyrmex nimbus*. *P. veracruzensis* is somewhat isolated phylogenetically, as sister to (*P. nimbus*, (*P. exoratus* (*P. ereptor*, *P. elongatulus*))) (Fig. 1).

Distribution and Biology. Pseudomyrmex veracruzensis is known only from two adjacent sites in the Sierra de los Tuxtlas, Veracruz. Collections include two nest series from dead twigs of *Heliocarpus*, and isolated workers foraging on low vegetation, all at the edge of montane rainforest (1,010 m–1,055 m).

Discussion

In this study of a Mesoamerican ant clade we recognize thirteen species, of which nine were previously undescribed. This is not an inflated number: we have been careful to allow for geographical variation within species, and to seek instances of sympatry to confirm species distinctness. Our findings reflect, therefore, the incomplete state of taxonomic knowledge of Neotropical ants, a situation demonstrated by other recent studies (e.g., Lattke 2011, Branstetter 2013, Ladino and Feitosa 2020, Longino and Branstetter 2021, Prebus 2021b). In investigating the *P. elongatulus* group we adopted an iterative strategy, involving scrutiny of morphological variation in a large series of (mostly worker) specimens, provisional recognition of species, UCE sequencing of a carefully chosen subset of specimens, inference of phylogenetic relationships, and then further scrutiny, delimitation, and sequencing, guided by the findings of each round of phylogenetic analysis. The postulated species boundaries are the outcome of several such cycles. Throughout this process the geographical distribution of putative species was given prominent attention, and an attempt was made to distinguish between variation within species—manifested as continuous changes in color, size, shape, and pilosity among individuals and among populations—from interspecific variation, evidenced by more abrupt morphological shifts. Such gaps were considered most compelling when observed among sympatric taxa. With the exception of *P. apache*, all of the species recognized in this study overlap geographically with one or more other species in the *P. elongatulus* group, often a sister species or close relative.

Some areas of taxonomic uncertainty remain. The relationship between *P. championi* and its phylogenetically embedded, parapatric sibling, *P. apache*, deserves greater study. More intensive sampling and genetic analysis of populations in northwestern Mexico might reveal some degree of gene flow and blurring of the morphological differences between these two. There is also ambiguity about the status of a morphologically and genetically divergent population of *P. cognatus* (D1983) from Guatemala: UCE data place it as sister to all other *P. cognatus* samples (Fig. 1), whereas the mitogenome sequences indicate that it is more closely related to the sister species, *P. fasciatus* (Supp Figs. 6-7 [online only]). This discordance raises the possibility of occasional hybridization between different species in the *P. elongatulus* group, as has been inferred for other ant taxa (Feldhaar et al. 2008, Butler et al. 2018, Cordonnier et al. 2020), with greater introgression of mitochondrial than nuclear DNA.

Nevertheless, most species in the *P. elongatulus* group are delimited by mutually supportive morphological and genetic differences, and these differences are maintained where the species occur in sympatry with close congeners. The relationships among these species, and among deeper branches of the tree, are robustly resolved under different analytical treatments of our UCE data (Fig. 1; Supp Figs. 1-3 [online only]). We infer that the origin and diversification of the *P. elongatulus* group occurred relatively recently, in the late Miocene, Pliocene, and Pleistocene (10 Ma–1 Ma), initially in Mexico and/or northern Central America, but later expanding to include southern

Downloaded from https://academic.oup.com/isd/article/6/1/4/6514767 by ThULB Jena user on 27 January 2022

Mesoamerica and the southwestern Nearctic region (Fig. 2). At this time the Mesoamerican lowlands would have been well populated by arboreal ants such as *Camponotus*, *Cephalotes*, *Crematogaster*, and other *Pseudomyrmex* (Blaimer 2012, Price et al. 2014, Chomicki et al. 2015), a situation that could have favored retreat to higher elevations—and escape from competition—in some members of the *P. elongatulus* group. Our ancestral state reconstructions suggest, however, that some lineages were able to persist in or recolonize low-elevation environments (Fig. 2). It is perhaps significant that the species with the widest elevational range, *P. apache*, occurs in a region with almost no other congeners (Ward 1985).

In our UCE phylogeny there are three instances of monophyletic/paraphyletic species pairs, involving a geographically restricted or peripheral 'daughter' species and a widely distributed 'parental' species, in which there has been evidentally insufficient time for allelic coalescence. We treat the pairs of taxa as different species because in each instance the daughter species occurs sympatrically with, or geographically adjacent to, the parent species, while maintaining its phenotypic and genetic distinctness. Two examples involve free-living species in which the daughter species presumably originated allopatrically. In contrast, the workerless social parasite, *P. comitator*, is apparently dependent on the presence of its host species, *P. cognatus*, within which it is embedded phylogenetically. Assuming that no host switching has occurred, this points to an origin of the parasite via sympatric speciation, as inferred for some other ants (Rabeling et al. 2014, Leppänen et al. 2015). The *P. ereptor*/*P. elongatulus* parasite/host pair arguably represents a later stage in this process, since *P. ereptor* is sister to, rather than phylogenetically contained within, its host (Fig. 1).

The molecular species delimitation methods that we employed (SODA, bPTP, BPP) gave markedly inflated estimates of the number of species, when applied to a range of data matrices: UCE unphased, UCE phased, mitogenome, and COI barcode (Fig. 1). Comparable results were obtained with all approaches, including the more computationally intensive, and arguably more accurate, BPP method (Luo et al. 2018). It is also noteworthy that the phased data delimited more species than the unphased data, a result that contradicts recent conclusions that phasing UCE alignments produces better estimates of species boundaries (Andermann et al. 2019). Overall, the most obvious explanation for the inflated species estimates is that such procedures do not adequately account for geographical variation within species, and hence conflate species boundaries with intraspecific population structure (Jackson et al. 2017, Sukumaran and Knowles 2017, Sukumaran et al. 2021). If such algorithmic approaches to species delimitation are to be broadlly useful then more biologically realistic models are needed, especially those that distinguish between the formation of species and the establishment of population lineages within species (Sukumaran et al. 2021).

The species estimates from our taxonomic revision are lower because we allowed for population divergence within species, assessed the geographic relationships of differentiated forms (whether sympatric, parapatric, or allopatric), and took into account the nature of phenotypic differences between taxa (such as socially parasitic traits, which indicate non-conspecificity with the host species). Our delineation of *P. fasciatus* illustrates these points. This taxon occurs from southern Mexico to Costa Rica, and shows relative morphological and ecological homogeneity across this range: the workers have a distinctive and consistent color pattern (Fig. 15), and populations are restricted to cloud forest. Any variation among populations is well below the sympatry threshhold (Tobias et al. 2010), i.e., the degree of phenotypic difference seen among closely related sympatric species, including *P. fasciatus* and its sister species, *P. cognatus*. What we circumscribe as *P. fasciatus*, then, is a series of phenotypically similar, allopatric samples, from about 35 localities, broadly distributed across Central America (see species account). Given the morphological coherence of these populations we have no reason to expect them to be reproductively isolated from one another. The UCE phylogeny, based on a sampling of five of these localities, yields a pattern of geographic structure (Fig. 1) consistent with an isolation-by-distance model (Wright 1943). Yet application of bPTP, SODA, and BPP to the UCE data and the mitochondrial data resulted in estimates of 3-5 species (Fig. 1), with most populations being assigned to different species. Similar over-splitting of taxa has occurred in other molecular species delimitation studies, in which no allowance is made for population structure within species (Barley et al. 2018, Chambers and Hillis 2020, Sukumaran et al. 2021).

In summary, our study of these Mesoamerican ants demonstrates the utility of phylogenomic data—and to a lesser extent single-locus data, such as mitochondrial DNA sequences—for evaluating species hypotheses based on phenotype and geography, but it also emphasizes that such data can mislead when used in isolation from other lines of evidence (see also Prebus 2021a), and when analyzed with methods that assume species-wide panmixia. As a final point, we note that in insect systematics an investigator typically has available for morphological examination hundreds to thousands of specimens, many more than the set of exemplars targeted for molecular phylogenetic analysis. That is certainly the situation in this study: 46 ingroup specimens were UCE-sequenced but ~2,930 specimens were examined for the taxonomic revision. Under these circumstances, phylogenomics can provide an invaluable framework—and of course illuminate evolutionary history in a way not possible with morphological data or with a small number of genetic markers—but an integrative accounting of the remaining (un-sequenced) specimens, their morphological features, and their associated ecological and geographical attributes, remains indispensable for developing a comprehensive picture of insect biodiversity.

Supplementary Data

Supplementary data are available at *Insect Systematics and Diversity* online.

Table S1. Detailed collection data of specimens examined for taxonomic study.

Table S2. List of sequenced samples and voucher specimens. Full collection data for all voucher specimens can be obtained by searching on the specimen code in AntWeb (www.antweb.org).

Table S3. Species distributions and elevation occurrences.

Table S4. Sequencing and assembly statistics for UCE samples.

Table S5. UCE matrix statistics.

Table S6. BioGeoBEARS model comparison results.

Table S7. Ancestral state reconstruction results for elevation.

Table S8. NCBI accession numbers for UCE samples.

Acknowledgments

We are grateful to the following individuals for access to material in the indicated collections: D. Agosti (AMNH); S. O. Shattuck (ANIC); J. Newlin (ANSP); B. Bolton (BMNH); W. Pulawski and B. L. Fisher (CASC); J. Longino (CEET); H. A. Hespenheide (CHAH); J. Denis (CNCC); M. Wasbauer (CSCA); M. Vásquez Bolaños (CZUG); R. Ayala (EBCC); Z. Prusak (FSCA); G. C. Snelling (GCSC); G. K. Mosser (GKMC); L. N. Quiroz Robledo (IEXA); A. Solis (INBC); J. Longino (JTLC); K. W. Jaffé

Downloaded from https://academic.oup.com/isd/article/6/1/4/6514767 by ThULB Jena user on 27 January 2022

(KWJC); R. R. Snelling (LACM; also old loans to D. H. Janzen from CMNH, CUIC, EMEC, UCRC and UWEM that were acquired by LACM and later returned by P.S.W. to their original owners); W. L. Brown, M. Moffett, C. Vogt and S. Cover (MCZC); C. Besuchet, I. Löbl and B. Merz (MHNG); J. Lattke (MIZA); J. Casevitz-Weulersse (MNHN); R. Poggi and V. Raineri (MSNG); P. Hanson (MUCR); R. Danielsson (MZLU); C. R. F. Brandão and R. Probst (MZSP); M. Fischer and Stefan Schödl (NHMW); D. C. Darling (OSAC); R. A. Johnson (RAJC); J. M. Maes (SEAN); R. W. Brooks (SEMC); S. M. Philpott (SMPC); S. T. Dash (STDC); D. Yanega (UCRC); D. R. Smith and T. R. Schultz (USNM); W. P. Mackay (UTEP); A. L. Wild (UTIC); J. C. Schuster (UVGC); and F. Koch (ZMHB). Additional useful specimens were received from Alan Andersen, Kim Franklin, Juergen Gadau, Stephanie Kautz, Dave Olson, Andy Suarez, Mark Trepanier, Robin Waugaman, and Dave Whitacre. P.S.W. thanks Alejandro Estrada, Rosamond Coates-Estrada, and Ricardo Ayala for facilitating visits to Estación de Biología 'Los Tuxtlas' and Estación Biología Chamela in 1985 and 1987, respectively. More recent fieldwork in Mexico and Central America was conducted partly under the auspices of Projects LLAMA and ADMAC, ably spearheaded and coordinated by Jack Longino (University of Utah). For assistance with lab work, UCE sequencing, and imaging we thank Matt Prebus, Marek Borowiec, Jill Oberski, Zach Griebenow and Ziv Lieberman. AntWeb (www.antweb.org) was a source of pre-existing images for several species. We appreciate the input of the editor and three anonymous reviewers, whose comments helped to improve the manuscript. This research was supported by a series of U. S. National Science Foundation grants to P.S.W., most recently DEB-1354996 (Project ADMAC) and DEB-1932405 (Ants of the World Project).

Author Contributions

P.S.W.: Conceptualization; Data curation; Formal analysis; Funding acquisition; Investigation; Methodology; Resources; Visualization; Writing—original draft; Writing—review & editing. M.G.B.: Conceptualization; Data curation; Formal analysis; Methodology; Visualization; Writing—original draft; Writing—review & editing.

Data Availability

Detailed collection data for all examined specimens is available in Supp Table S1 (online only). Raw Illumina reads and contigs representing UCE loci have been deposited at the NCBI Sequence Read Archive and GenBank, respectively (BioProject# PRJNA776900). All COI sequences have been deposited at GenBank (OL416051–OL416095). A complete list of relevant NCBI accession numbers are available in Supp Table S8 (online only). All UCE and mtDNA matrices, all SPAdes contigs, all tree files, unfiltered UCE alignments, and additional data analysis files have been deposited at Dryad (https://doi.org/10.5061/dryad.280gb5mr3). The Phyluce package and associated programs can be downloaded from github (github.com/faircloth-lab/phyluce). The ant-specific baits used to enrich UCE loci can be purchased from Arbor Biosciences (https://arborbiosci.com/%20genomics/targeted-sequencing/mybaits/mybaits-expert/mybaits-expert-uce/) and the UCE bait sequence file is available at figshare (https://figshare.com/authors/brant-faircloth/97201).

References Cited

Allio, R., A. Schomaker-Bastos, J. Romiguier, F. Prosdocimi, B. Nabholz, and F. Delsuc. 2020. MitoFinder: efficient automated large-scale extraction of mitogenomic data in target enrichment phylogenomics. Mol. Ecol. Resour. 20: 892–905.

Andermann, T., A. M. Fernandes, U. Olsson, M. Töpel, B. Pfeil, B. Oxelman, A. Aleixo, B. C. Faircloth, and A. Antonelli. 2019. Allele phasing greatly improves the phylogenetic utility of ultraconserved elements. Syst. Biol. 68: 32–46.

Avise, J. C. 2000. Phylogeography. The history and formation of species. Harvard University Press, Cambridge, Mass.

Bankevich, A., S. Nurk, D. Antipov, A. A. Gurevich, M. Dvorkin, A. S. Kulikov, V. M. Lesin, S. I. Nikolenko, S. Pham, A. D. Prjibelski, et al. 2012. SPAdes: a new genome assembly algorithm and its applications to single-cell sequencing. J. Comput. Biol. 19: 455–477.

Barley, A. J., J. M. Brown, and R. C. Thomson. 2018. Impact of model violations on the inference of species boundaries under the multispecies coalescent. Syst. Biol. 67: 269–284.

Beza-Beza, C. F., L. Jiménez-Ferbans, and D. D. McKenna. 2021. Historical biogeography of New World passalid beetles (Coleoptera, Passalidae) reveals Mesoamerican tropical forests as a centre of origin and taxonomic diversification. J. Biogeogr. 48: 2037–2052.

Blaimer, B. B. 2012. Acrobat ants go global – origin, evolution and systematics of the genus *Crematogaster* (Hymenoptera: Formicidae). Mol. Phylogenet. Evol. 65: 421–436.

Blumenstiel, B., K. Cibulskis, S. Fisher, M. DeFelice, A. Barry, T. Fennell, J. Abreu, B. Minie, M. Costello, G. Young, J. Maquire, A. Kernytsky, A. Melnikov, P. Rogov, A. Gnirke, and S. Gabriel. 2010. Targeted exon sequencing by in-solution hybrid selection. Curr. Protoc. Hum. Genet. 66: 18.14.11–18.14.24.

Bolger, A. M., M. Lohse, and B. Usadel. 2014. Trimmomatic: a flexible trimmer for Illumina sequence data. Bioinformatics. 30: 2114–2120.

Borowiec, M. 2019. Spruceup: fast and flexible identification, visualization, and removal of outliers from large multiple sequence alignments. J. Open Source Softw. 4: 1635.

Bouckaert, R., J. Heled, D. Kühnert, T. Vaughan, C. H. Wu, D. Xie, M. A. Suchard, A. Rambaut, and A. J. Drummond. 2014. BEAST 2: a software platform for Bayesian evolutionary analysis. PLoS Comput. Biol. 10: e1003537.

Branstetter, M. G. 2013. Revision of the Middle American clade of the ant genus *Stenamma* Westwood (Hymenoptera, Formicidae, Myrmicinae). ZooKeys. 295: 1–277.

Branstetter, M. G., J. T. Longino, P. S. Ward, and B. C. Faircloth. 2017. Enriching the ant tree of life: enhanced UCE bait set for genome-scale phylogenetics of ants and other Hymenoptera. Method. Ecol. Evol. 8: 768–776.

Bushnell, B. 2014. BBTools software package. URL http://sourceforge.net/projects/bbmap. Computer program, version by Bushnell, B.

Butler, I. A., M. K. Peters, and D. J. C. Kronauer. 2018. Low levels of hybridization in two species of African driver ants. J. Evol. Biol. 31: 556–571.

Caudell, A. N. 1907. On some earwigs (Forficulidae) collected in Guatemala by Messrs. Schwarz and Barber. Proc. U. S. Natl. Mus. 33: 169–176.

Chambers, E. A., and D. M. Hillis. 2020. The multispecies coalescent oversplits species in the case of geographically widespread taxa. Syst. Biol. 69: 184–193.

Chomicki, G., P. S. Ward, and S. Renner. 2015. Macroevolutionary assembly of ant/plant symbioses: *Pseudomyrmex* ants and their ant-housing plants in the Neotropics. Proc. R. Soc. B. 282: 20152200.

Cordonnier, M., G. Escarguel, A. Dumet, and B. Kaufmann. 2020. Multiple mating in the context of interspecific hybridization between two *Tetramorium* ant species. Heredity (Edinb). 124: 675–684.

Coyne, J. A., and H. A. Orr. 2004. Speciation. Sinauer Associates, Sunderland, Mass.

Creighton, W. S. 1953. *Pseudomyrmex apache*, a new species from the southwestern United States (Hymenoptera: Formicidae). Psyche (Cambridge). 59: 131–142.

Creighton, W. S. 1954. Additional studies on *Pseudomyrmex apache* (Hymenoptera: Formicidae). Psyche (Cambridge). 61: 9–15.

Cutler, B. 1985. Taxonomic notes on Neotropical species in the genus *Synemosyna* (Araneae: Salticidae), Stud. Neotrop. Fauna Environ. 20: 83–91.

Dalla Torre, K. W. 1892. Hymenopterologische Notizen. Wien. Entomol. Ztg. 11: 89–93.

Davison, I., J. N. F. Hull, and J. Pindell (eds). 2021. The basins, orogens and evolution of the southern Gulf of Mexico and northern Caribbean. Geol. Soc. Lond. Special Publ. 504: 1–560.

Edwards, D. P., J. B. Socolar, S. C. Mills, Z. Burivalova, L. P. Koh, and D. S. Wilcove. 2019. Conservation of Tropical Forests in the Anthropocene. Curr. Biol. 29: R1008–R1020.

Downloaded from https://academic.oup.com/isd/article/6/1/4/6514767 by ThULB Jena user on 27 January 2022

Fairchild, D. 1912. Seeds and plants imported during the period from April 1 to June 30, 1911: inventory No. 27; nos. 30462 to 31370. Bull. Bur. Plant Ind. 242: 1–99.

Faircloth, B. 2013. Illumiprocessor: a trimmomatic wrapper for parallel adapter and quality trimming. Available at: https://doi.org/10.6079/J9ILL

Faircloth, B. C. 2016. PHYLUCE is a software package for the analysis of conserved genomic loci. Bioinformatics. 32: 786–788.

Feldhaar, H., S. Foitzik, and J. Heinze. 2008. Lifelong commitment to the wrong partner: hybridization in ants. Philos. Trans. R. Soc. Lond. B Biol. Sci. 363: 2891–2899.

Fitz-Díaz, E., T. F. Lawton, E. Juárez-Arriaga, and G. Chávez-Cabello. 2018. The Cretaceous-Paleogene Mexican orogen: structure, basin development, magmatism and tectonics. Earth-Sci. Rev. 183: 56–84.

Flouri, T., X. Jiao, B. Rannala, and Z. Yang. 2018. Species tree inference with BPP using genomic sequences and the multispecies coalescent. Mol. Biol. Evol. 35: 2585–2593.

Foottit, R. G., and P. H. Adler (eds.). 2017. Insect biodiversity. Science and society, 2nd ed., vol. 1. Wiley-Blackwell, Oxford.

Forel, A. 1899. Formicidae. [part]. Biol. Cent.-Am. Hym. 3: 81–104.

Fujita, M. K., A. D. Leaché, F. T. Burbrink, J. A. McGuire, and C. Moritz. 2012. Coalescent-based species delimitation in an integrative taxonomy. Trends Ecol. Evol. 27: 480–488.

Funk, D. J., and K. E. Omland. 2003. Species-level paraphyly and polyphyly: frequency, causes, and consequences, with insights from animal mitochondrial DNA. Annu. Rev. Ecol. Evol. Syst. 34: 397–423.

García Cubas, A. 1891. *Diccionario geográfico, histórico y biográfico de los Estados Unidos Mexicanos*. Tomo V. Oficina Tipográfica de la Secretaría de Fomento, México.

Glenn, T. C., R. A. Nilsen, T. J. Kieran, J. G. Sanders, N. J. Bayona-Vásquez, J. W. Finger, T. W. Pierson, K. E. Bentley, S. L. Hoffberg, S. Louha, et al. 2019. Adapterama I: universal stubs and primers for 384 unique dual-indexed or 147,456 combinatorially-indexed Illumina libraries (iTru & iNext). PeerJ. 7: e7755.

Goodrich, C., and H. van der Schalie. 1937. Mollusca of Petén and north Alta Vera Paz, Guatemala. Univ. Mich. Mus. Zool. Misc. Publ. 34: 1–50.

Grab, H., M. G. Branstetter, N. Amon, K. R. Urban-Mead, M. G. Park, J. Gibbs, E. J. Blitzer, K. Poveda, G. Loeb, and B. N. Danforth. 2019. Agriculturally dominated landscapes reduce bee phylogenetic diversity and pollination services. Science. 363: 282–284.

Graham, A. 2010. Late Cretaceous and Cenozoic history of Latin American vegetation and terrestrial environments. Missouri Botanical Garden Press, St. Louis, Missouri.

Guindon, S., J. F. Dufayard, V. Lefort, M. Anisimova, W. Hordijk, and O. Gascuel. 2010. New algorithms and methods to estimate maximum-likelihood phylogenies: assessing the performance of PhyML 3.0. Syst. Biol. 59: 307–321.

Gutiérrez-García, T. A., and E. Vázquez-Domínguez. 2013. Consensus between genes and stones in the biogeographic and evolutionary history of Central America. Quat. Res. 79: 311–324.

Halffter, G. 1987. Biogeography of the montane entomofauna of Mexico and Central America. Annu. Rev. Entomol. 32: 95–114.

Halffter, G., and J. J. Morrone. 2017. An analytical review of Halffter's Mexican transition zone, and its relevance for evolutionary biogeography, ecology and biogeographical regionalization. Zootaxa. 4226: 1–46.

Hansen, M. C., P. V. Potapov, R. Moore, M. Hancher, S. A. Turubanova, A. Tyukavina, D. Thau, S. V. Stehman, S. J. Goetz, T. R. Loveland, et al. 2013. High-resolution global maps of 21st-century forest cover change. Science. 342: 850–853.

Harris, R. A. 1979. A glossary of surface sculpturing. Calif. Dep. Food Agric. Lab. Serv. Entomol. Occas. Pap. 28: 1–31.

Harris, R. S. 2007. Improved pairwise alignment of genomic DNA. Pennsylvania State University, University Park, Penn.

Hoang, D. T., O. Chernomor, A. von Haeseler, B. Q. Minh, and L. S. Vinh. 2018. UFBoot2: improving the ultrafast bootstrap approximation. Mol. Biol. Evol. 35: 518–522.

Jackson, N. D., B. C. Carstens, A. E. Morales, and B. C. O'Meara. 2017. Species delimitation with gene flow. Syst. Biol. 66: 799–812.

Janzen, D. H. 1967. Interaction of the bull's-horn acacia (*Acacia cornigera* L.) with an ant inhabitant (*Pseudomyrmex ferruginea* F. Smith) in eastern Mexico. Univ. Kans. Sci. Bull. 47: 315–558.

Junier, T., and E. M. Zdobnov. 2010. The Newick utilities: high-throughput phylogenetic tree processing in the UNIX shell. Bioinformatics. 26: 1669–1670.

Kalyaanamoorthy, S., B. Q. Minh, T. K. F. Wong, A. von Haeseler, and L. S. Jermiin. 2017. ModelFinder: fast model selection for accurate phylogenetic estimates. Nat. Methods. 14: 587–589.

Katoh, K., and D. M. Standley. 2013. MAFFT multiple sequence alignment software version 7: improvements in performance and usability. Mol. Biol. Evol. 30: 772–780.

Kempf, W. W. 1960. Estudo sôbre *Pseudomyrmex* I. (Hymenoptera: Formicidae). Rev. Bras. Entomol. 9: 5–32.

Kempf, W. W. 1961. Estudos sôbre *Pseudomyrmex*. III. (Hymenoptera: Formicidae). Stud. Entomol. 4: 369–408.

Kempf, W. W. 1967. Estudos sôbre *Pseudomyrmex*. IV (Hymenoptera: Formicidae). Rev. Bras. Entomol. 12: 1–12.

Kim, J., and M. J. Sanderson. 2008. Penalized likelihood phylogenetic inference: bridging the parsimony-likelihood gap. Syst. Biol. 57: 665–674.

Ladino, N., and R. M. Feitosa. 2020. Taxonomic revision of the genus *Prionopelta* Mayr, 1866 (Formicidae: Amblyoponinae) for the Neotropical region. Zootaxa. 4821: 201–249.

Landis, M. J., N. J. Matzke, B. R. Moore, and J. P. Huelsenbeck. 2013. Bayesian analysis of biogeography when the number of areas is large. Syst. Biol. 62: 789–804.

Lattke, J. E. 2011. Revision of the New World species of the genus *Leptogenys* Roger (Insecta: Hymenoptera: Formicidae: Ponerinae). Arthr. Syst. Phylogeny. 69: 127–264.

Leppänen, J., P. Seppä, K. Vepsäläinen, and R. Savolainen. 2015. Genetic divergence between the sympatric queen morphs of the ant *Myrmica rubra*. Mol. Ecol. 24: 2463–2476.

Lomolino, M. V., B. R. Riddle, and R. J. Whittaker. 2017. Biogeography: biological diversity across space and time, 5th ed. Sinauer Associates, Sunderland, Mass.

Longino, J. T., and M. G. Branstetter. 2021. Integrating UCE phylogenomics with traditional taxonomy reveals a trove of New World *Syscia* species (Formicidae: Dorylinae). Insect Syst. Divers. 5: 2.

Luo, A., C. Ling, S. Y. W. Ho, and C. D. Zhu. 2018. Comparison of methods for molecular species delimitation across a range of speciation scenarios. Syst. Biol. 67: 830–846.

Marshall, C. J., and J. K. Liebherr. 2001. Cladistic biogeography of the Mexican transition zone. J. Biogeogr. 27: 203–216.

Matzke, N. J. 2013. BioGeoBEARS: BioGeography with Bayesian (and Likelihood) Evolutionary Analysis in R Scripts. R package, version 1.1.2 computer program, version by Matzke, N. J.

Mayr, G. 1870. Formicidae novogranadenses. Sitzungsber. Kais. Akad. Wiss. Wien. Math.-Naturwiss. Cl. Abt. I 61: 370–417.

Mayr, E. 1942. Systematics and the origin of species, from the viewpoint of a zoologist. Columbia University Press, New York.

Minh, B. Q., H. A. Schmidt, O. Chernomor, D. Schrempf, M. D. Woodhams, A. von Haeseler, and R. Lanfear. 2020. IQ-TREE 2: new models and efficient methods for phylogenetic inference in the genomic era. Mol. Biol. Evol. 37: 1530–1534.

Misof, B., S. Liu, K. Meusemann, R. S. Peters, A. Donath, C. Mayer, P. B. Frandsen, J. Ware, T. Flouri, R. G. Beutel, et al. 2014. Phylogenomics resolves the timing and pattern of insect evolution. Science. 346: 763–767.

Palacios Roji García, A., and P. Palacios Roji García. 2006. Por las carreteras de México, 2007. Guia Roji, Mexico City.

Pante, E., C. Schoelinck, and N. Puillandre. 2015. From integrative taxonomy to species description: one step beyond. Syst. Biol. 64: 152–160.

Paradis, E. 2013. Molecular dating of phylogenies by likelihood methods: a comparison of models and a new information criterion. Mol. Phylogenet. Evol. 67: 436–444.

Paradis, E., J. Claude, and K. Strimmer. 2004. APE: analyses of phylogenetics and evolution in R language. Bioinformatics. 20: 289–290.

Petrunkevitch, A. 1909. A trip to southern Mexico for spiders. Am. Mus. J. 9: 249–256.

Downloaded from https://academic.oup.com/isd/article/6/1/4/6514767 by ThULB Jena user on 27 January 2022

Prebus, M. M. 2021a. Phylogenomic species delimitation in the ants of the *Temnothorax salvini* group (Hymenoptera: Formicidae): an integrative approach. Syst. Entomol. 46: 307–326.

Prebus, M. M. 2021b. Taxonomic revision of the *Temnothorax salvini* clade (Hymenoptera: Formicidae), with a key to the clades of New World *Temnothorax*. PeerJ 9: e11514.

Price, S. L., S. Powell, D. J. Kronauer, L. A. Tran, N. E. Pierce, and R. K. Wayne. 2014. Renewed diversification is associated with new ecological opportunity in the Neotropical turtle ants. J. Evol. Biol. 27: 242–258.

Rabeling, C., T. R. Schultz, N. E. Pierce, and M. Bacci, Jr. 2014. A social parasite evolved reproductive isolation from its fungus-growing ant host in sympatry. Curr. Biol. 24: 2047–2052.

Rabiee, M., and S. Mirarab. 2021. SODA: multi-locus species delimitation using quartet frequencies. Bioinformatics. 36: 5623–5631.

Rambaut, A., A. J. Drummond, D. Xie, G. Baele, and M. A. Suchard. 2018. Posterior Summarization in Bayesian phylogenetics using tracer 1.7. Syst. Biol. 67: 901–904.

Rannala, B., and Z. Yang. 2013. Improved reversible jump algorithms for Bayesian species delimitation. Genetics. 194: 245–253.

R Core Team. 2021. R: a language and environment for statistical computing. R Foundation for Statistical Computing, Vienna, Austria. https://www.r-project.org/

Ree, R. H., and I. Sanmartín. 2018. Conceptual and statistical problems with the DEC+J model of founder-event speciation and its comparison with DEC via model selection. J. Biogeogr. 45: 741–749.

Ree, R. H., and S. A. Smith. 2008. Maximum likelihood inference of geographic range evolution by dispersal, local extinction, and cladogenesis. Syst. Biol. 57: 4–14.

Ree, R. H., B. R. Moore, C. O. Webb, and M. J. Donoghue. 2005. A likelihood framework for inferring the evolution of geographic range on phylogenetic trees. Evolution. 59: 2299–2311.

Ritchie, A. M., N. Lo, and S. Y. Ho. 2017. The impact of the tree prior on molecular dating of data sets containing a mixture of inter-and intraspecies sampling. Syst. Biol. 66: 413–425.

Ronquist, F. 1997. Dispersal-vicariance analysis: a new approach to the quantification of historical biogeography. Syst. Biol. 46: 195–203.

Ross, H. A. 2014. The incidence of species-level paraphyly in animals: a re-assessment. Mol. Phylogenet. Evol. 76: 10–17.

Sánchez-González, L. A., J. J. Morrone, and A. G. Navarro-Sigüenza. 2008. Distributional patterns of the Neotropical humid montane forest avifaunas. Biol. J. Linn. Soc. 94: 175–194.

Savage, J. M. 1966. The origins and history of the Central American herpetofauna. Copeia. 1966: 719–766.

Schultze-Jena, L. 1938. Indiana. Band III. Bei den Azteken, Mixteken und Tlapaneken der Sierra Madre del Sur von Mexiko. G. Fischer, Jena.

Selander, R. B., and P. Vaurie. 1962. A gazetteer to accompany the "Insecta" volumes of the "Biologia Centrali-Americana". Am. Mus. Novit. 2099: 1–70.

Skwarra, E. 1934. Ökologische Studien über Ameisen und Ameisenpflanzen in Mexiko. Published by author (printer: R. Leupold), Königsberg.

Slevin, J. R. 1923. Expedition of the California Academy of Sciences to the Gulf of California in 1921. General Account. Proc. Calif. Acad. Sci. 12: 55–72.

Smith, F. 1877. Descriptions of new species of the genera *Pseudomyrma* and *Tetraponera*, belonging to the family Myrmicidae. Trans. Entomol. Soc. Lond. 1877: 57–72.

Smith, J. B. 1899. Some new species of *Hadena*. Can. Entomol. 31: 257–265.

Stitz, H. 1937. Einige Ameisen aus Mexiko. Sitzungsber. Ges. Naturforsch. Freunde Berl. 1937: 132–136.

Ströher, P. R., E. Zarza, W. L. E. Tsai, J. E. McCormack, R. M. Feitosa, and M. R. Pie. 2016. The mitochondrial genome of *Octostruma stenognatha* and its phylogenetic implications. Insectes Soc. 64: 149–154.

Sukumaran, J., and L. L. Knowles. 2017. Multispecies coalescent delimits structure, not species. Proc. Natl. Acad. Sci. U. S. A. 114: 1607–1612.

Sukumaran, J., M. T. Holder, and L. L. Knowles. 2021. Incorporating the speciation process into species delimitation. PLoS Comput. Biol. 17: e1008924.

Syring, J., K. Farrell, R. Businský, R. Cronn, and A. Liston. 2007. Widespread genealogical nonmonophyly in species of Pinus subgenus Strobus. Syst. Biol. 56: 163–181.

Tagliacollo, V. A., and R. Lanfear. 2018. Estimating improved partitioning schemes for ultraconserved elements. Mol. Biol. Evol. 35: 1798–1811.

Talavera, G., and J. Castresana. 2007. Improvement of phylogenies after removing divergent and ambiguously aligned blocks from protein sequence alignments. Syst. Biol. 56: 564–577.

Tobias, J. A., N. Seddon, C. N. Spottiswoode, J. D. Pilgrim, L. D. C. Fishpool, and N. J. Collar. 2010. Quantitative criteria for species delimitation. Ibis. 152: 724–746.

Ward, P. S. 1985. The Nearctic species of the genus *Pseudomyrmex* (Hymenoptera: Formicidae). Quaest. Entomol. 21: 209–246.

Ward, P. S. 1989. Systematic studies on pseudomyrmecine ants: revision of the *Pseudomyrmex oculatus* and *P. subtilissimus* species groups, with taxonomic comments on other species. Quaest. Entomol. 25: 393–468.

Ward, P. S. 1991. Phylogenetic analysis of pseudomyrmecine ants associated with domatia-bearing plants, pp. 335–352. *In* D. F. Cutler, and C. R. Huxley. (eds.), Ant/plant interactions. Oxford Univ. Press, Oxford.

Ward, P. S. 2014. The phylogeny and evolution of ants. Annu. Rev. Ecol. Evol. Syst. 45: 23–43.

Ward, P. S. 2017. A review of the *Pseudomyrmex ferrugineus* and *Pseudomyrmex goeldii* species groups: acacia-ants and their relatives (Hymenoptera: Formicidae). Zootaxa. 4227: 524–542.

Ward, P. S. 2019. Capítulo 33. Subfamilia Pseudomyrmecinae, pp. 1089–1113. *In* F. Fernández, R. J. Guerrero, and T. Delsinne (eds.), Hormigas de Colombia. Universidad Nacional de Colombia, Bogotá.

Ward, P. S., and D. A. Downie. 2005. The ant subfamily Pseudomyrmecinae (Hymenoptera: Formicidae): phylogeny and evolution of big-eyed arboreal ants. Syst. Entomol. 30: 310–335.

Wheeler, W. M. 1936. A singular *Crematogaster* from Guatemala. Psyche (Cambridge). 43: 40–48.

Wheeler, W. M., and I. W. Bailey. 1920. The feeding habits of pseudomyrmine and other ants. Trans. Am. Philos. Soc. 22: 235–279.

Wheeler, G. C., and J. Wheeler. 1956. The ant larvae of the subfamily Pseudomyrmecinae (Hymenoptera: Formicidae). Ann. Entomol. Soc. Am. 49: 374–398.

Wilson, E. O. 1955. A monographic revision of the ant genus *Lasius*. Bull. Mus. Comp. Zool. 113: 1–201.

Wolf, C., T. Levi, W. J. Ripple, D. A. Zárrate-Charry, and M. G. Betts. 2021. A forest loss report card for the world's protected areas. Nat. Ecol. Evol. 5: 520–529.

Wright, S. 1943. Isolation by distance. Genetics. 28: 114–138.

Yeates, D. K., A. Seago, L. Nelson, S. L. Cameron, L. Joseph, and J. W. H Trueman. 2011. Integrative taxonomy, or iterative taxonomy? Syst. Entomol. 36: 209–217.

Yang, Z., and B. Rannala. 2010. Bayesian species delimitation using multilocus sequence data. Proc. Natl. Acad. Sci. U. S. A. 107: 9264–9269.

Zhang, J., P. Kapli, P. Pavlidis, and A. Stamatakis. 2013. A general species delimitation method with applications to phylogenetic placements. Bioinformatics. 29: 2869–2876.

Zhang, C., E. Sayyari, and S. Mirarab. 2017. ASTRAL-III: increased scalability and impacts of contracting low support branches, pp. 53–75. *In* J. Meidanis, and L. Nakleh (eds.), Comparative Genomics. RECOMB-CG 2017. Lecture Notes in Computer Science, vol. 10562. Springer, Cham.

Downloaded from https://academic.oup.com/isd/article/6/1/4/6514767 by ThULB Jena user on 27 January 2022